Nanosized Particles in North American Snow: Physicochemical Properties of Efficient Ice Nucleating Particles

Rodrigo Rangel-Alvarado

Department of Chemistry
McGill University
Montreal, Quebec, Canada

June 28, 2018

A thesis submitted to McGill University in partial fulfillment of the requirements of the degree of Doctor of Philosophy

Acknowledge

I thank my supervisor, Prof. Parisa A. Ariya for all the advice and support she provided to me during my studies. I would like to thank all group members, past and current: Nermin Eltouny, Zhenzhong Hu, Ali Moridnejad, Yevgen Nazarenko, Jim Ghoshdastidar, Uday Kurien, Andrea Rocha, Devendra Pal, Ryan Hall and Bryan Lee for the help in the lab and discussion about research. I thank the Chemistry department and staff, especially Chantal Marotte, Rick Rossi, Weihua Wang, and Jean-Philippe Guay for all their help through out these years. I thank FQRNT and NSERC CREATE Mine of Knowledge for providing the financial assistance during my studies. I also thank my beloved family for their understanding and continuous support throughout my studies.

Table of Contents

List of Figures vi

List of Tables x

List of Abbreviations xi

Abstract xii

1. Introduction 1

  1.1. Types of Aerosols and Their Source 1

    1.1.1. Organic Aerosols 1

    1.1.2. Inorganic Aerosols 3

  1.2. Deposition of Aerosols and Snow 7

  1.3. Homogeneous Ice Nucleation 7

  1.4. Heterogeneous Ice Nucleation 10

    1.4.1. Evaluation of Ice Nucleation Ability 12

  1.5. Aerosols Properties and their Effect on Ice Nucleation 14

    1.5.1. Ice Nucleation of Different Aerosols 15

    1.5.2. Ice Nucleation by Nanoparticles and Nanosized Particles 17

  1.6. Measurement of Aerosols 18

    1.6.1. Electron Microscopy Techniques 18

    1.6.2. Optical Sizing Techniques 19

    1.6.3. Chemical Characterisation of Aerosols 20

  1.7. Research Objectives 22

  1.8. Structure of the Thesis 23

2. Novel Aerosol Analysis Approach for Characterization of Nanoparticulate Matter in Snow 33

  2.1. Introduction 35

  2.2. Materials and Methods 37

    2.2.1. Sampling and Storage 37

    2.2.2. Processing of Melted Snow 39

    2.2.3. Chemical Analysis of Melted Snow 40

    2.2.4. Nanoparticle Tracking Analysis of Melted Snow 40

    2.2.5. Generation of Melted Snow Aerosol 40

    2.2.6. Collection of Samples for Electron Microscopy 43

    2.2.7. Transmission Electron Microscopy 44

    2.2.8. Aerosol Size Distribution Analysis 45

2.3. Results and Discussion 45
2.3.1. Direct Characterization of Liquid Melted Snow Samples 46
2.3.2. Aerosol-Mediated Characterization of Melted Snow Samples 55
2.3.3. Verification of the Aerosol-Mediated Characterization Technique 59
2.4. Concluding Remarks and Future Work 62
3. Snow-Borne Nanosized Particles: Abundance, Distribution, Composition, and Significance in Ice Nucleation Processes 67
3.1. Introduction 69
3.2. Experimental and Methods 73
3.2.1. Sampling 73
3.2.2. Aerosol Size Distributions 75
3.2.3. Hydrodynamic Diameter Distribution 77
3.2.4. Matrix-Assisted Laser Desorption/Ionization Time-Of-Flight Mass Spectrometry (MALDI-TOF-MS/MS) 77
3.2.5. Electrospray Ionization Mass Spectrometry (ESI/MS) 78
3.2.6. Total Organic Carbon (TOC) 78
3.2.7. High-Resolution Transmission Electron Microscopy with Energy Dispersive X-Ray Spectroscopy (HR-TEM-EDS) 79
3.2.8. Drop-Freezing Assays 79
3.2.9. Ion Chromatography 80
3.2.10. Materials and Supplies 80
3.3. Results and Discussion 81
3.3.1. Nanosized Particle Size Distributions 81
3.3.2. Chemical Composition of the Observed Nanosized Materials and Particles 84
3.3.3. Nanosized Ice Nuclei 88
3.3.4. Microbiological Diversity in Snow 93
3.3.5. Why do Nanosized Compounds Act as Efficient Ice Nuclei? 94
3.4. Concluding Remarks and Future Work 95
4. Athabasca Oil Sand Snow Contains Efficient Ice Nucleating Particles 102
4.1. Introduction 105
4.2. Experimental section 107
4.2.1. Sample collection and storage 107
4.2.2. Particle Size Distributions 108

4.2.3. High-resolution scanning transmission electron microscopy with energy dispersive X-ray spectroscopy (HR-STEM-EDS) and Scanning Electron Microscopy (SEM) 108

4.2.4. Analysis of metal concentrations by ICP-(QQQ)-MS/MS 109

4.2.5. Brunauer–Emmett–Teller Specific surface area of particles 109

4.2.6. X-ray Powder Diffraction (XRD) patterns of particles 110

4.2.7. Ice nucleation experiments on snow-borne particles 110

4.3. Results and Discussion 111

4.3.1. Snow-borne particle composition, size and morphology: AORS vs. Urban Montreal 111

4.3.2. Comparison of ice nucleation efficiency between AOSR and Montreal snow-borne particles 116

4.3.3. Relationship between snow-borne particle size and ice nucleation efficiency 116

4.3.4. The effect of Hg halide coverage on the ice nucleation on model mineral particles 118

4.3.5. Surface studies of iron oxide (BET & XRD): Hg halides alter iron oxide surfaces 120

Acknowledgements 122

5. Conclusions and Future Work 127

5.1. Summary 127

5.2. Original Contribution to Knowledge 128

5.3. Future Work 128

A. Chapter 2 Supplementary Information 130

A.1. Supplementary Methods 130

A.1.1. Analysis of Total Organic Carbon in Melted Snow 130

A.1.2. Ion Chromatography Analysis of Melted Snow 130

A.2. Supplementary Figures 131

B. Chapter 3 Supplementary Information 135

B.1. Supplementary Figures 136

C. Chapter 3 Supplementary Information 138

List of Figures

Figure 1.1 Chemical composition of mineral dust particles from four source regions in the global dust belt. Data taken from Krueger et al., 2004.[29] 5

Figure 1.2 Free energy as a function of the order parameter. Image taken from Kalikmanov, 2013 (Chapter 3)[49]. Reproduced with the permission of Springer. 8

Figure 1.3 Change in free energy of the system as a function of the ice embryo's radius. The energy of the bulk is represented by the bottom curve and the energy of the surface of the ice embryo is represented by the upper curve. The inflection point corresponds to the critical radius where the contribution from the bulk is equal to the contribution from the surface. Image taken from Ragone, 1994 (Chapter 1).[58] Reproduced with the permission of John Wiley & Sons. Inc. 9

Figure 1.4 Heterogeneous ice nucleation modes. 11

Figure 2.1 Setup for collection of samples for electron microscopy through the aerosol phase. HEPA Filter high-efficiency particulate air filter, SMPS scanning mobility particle sizer, OPS optical particle sizer. 41

Figure 2.2 Snow processing procedures and analyses. 46

Figure 2.3 Hydrodynamic particle size distributions of snow samples from (a, b) Montreal 2006, (c, d) Alert, and (e, f) Barrow. All samples were analyzed both unprocessed and filtered using a syringe filter with pores of 0.22 mm in diameter. a, c, e. Adapted with permission from Supporting Information for (Rangel-Alvarado et al. 2015). Error bars indicate ±1 standard error of the mean. 48

Figure 2.4 Representative high- and mid-resolution TEM images of aerosolized particles. a–c With prior dialysis and d–i without any prior processing. a–f. Stained with uranyl formate and g–i stained with uranyl acetate 54

Figure 2.5 Aerosol particle size distributions of the aerosolized snow samples measured using the NanoScan scanning mobility particle sizer (SMPS) and the optical particle sizer (OPS). 57

Figure 2.6 High-resolution aerosol nanoparticle size distributions of the aerosolized snow samples measured with the NanoScan scanning mobility particle sizer (SMPS). 58

Figure 2.7 Aerosol particle size distributions measured using the NanoScan scanning mobility particle sizer (SMPS) and the optical particle sizer (OPS) of the aerosolized TiO_2 colloid solutions with or without added solutes: oxalic acid and different concentrations of NaCl. Oxalic acid concentration is 630 mg/L. 60

Figure 3.1 A simplified schematic of nanoparticle cycling in the atmosphere and snow-air interfaces. For simplicity, the splitting effects for clusters and the splintering effect of cloud microphysics are not shown. 70
Figure 3.2 Size distributions of snow-borne particles. (a) Measured concentrations of particles as a function of particle size (logarithmic scale) using both nanoparticle tracking analysis (NTA) and aerosolization techniques in Montréal, Alert and Barrow. (b-d) Particle abundance as a function of hydrodynamic diameter for several snow samples from Montréal, Alert and Barrow sites; different colors represent different samples. 82
Figure 3.3 Examples of a) MALDI-TOF MS mass spectra depicting patterns related to bioorganic materials with suggested structures; b) ESI/MS spectra showing relatively high molecular mass with suggested structures in case the analyzed molecules are in fact peptides; c) EDS showing elements such as silicon and iron, which are usually found in ice nucleating mineral dust particles. 86
Figure 3.4 Electron microscopy images of filtered snow samples depicting filaments and vesicles likely of organic origin, and the probable presence of some inorganic compounds. 87
Figure 3.5 Comparison of the cumulative nucleus spectra (Log10, Ice Nuclei/Liter) of the top layers (3 cm) of surface snow samples. (a) All sampled sites; b) Alert, Nunavut; c) Barrow, Alaska; and d) Montréal, Québec. Same symbol shapes represent the same sample types in all regions. The mean freezing temperatures of unprocessed snow are for Barrow -12.52 °C (Standard Deviation (Σ): 8.58); Alert -11.48 °C (Σ: 2.94); and Montréal -12.82 °C (Σ: 2.60). The mean freezing temperatures of filtered snow are for Barrow -17.3 °C (Σ: 7.8); Alert -17.1 °C (Σ: 6.3); and Montréal -15.0 °C (Σ: 1.7). 89
Figure 3.6 Cumulative nucleus spectrum of centrifuged snow samples. From Alert, Nunavut (●); Barrow, Alaska (▲); and Montréal, Québec (■). Green curves represent samples from the top 1 cm layer of centrifuged samples, and red curves represent samples from the bottom 1 cm layer of a 1.5 mL conical vial. The blue line is the average of samples from the top layer, whereas the black line is the average of samples from the bottom layer. 90
Figure 3.7 Cumulative nucleus spectrum of snow samples from Montréal, Québec, collected at different depths. Lower layer (■), 5 cm close to the ground, intermediate layer (▲), and top 3 cm of snow (●). Green curves represent samples containing particles with sizes smaller than 0.22 mm, and red curves represent unfiltered samples. Grey circles represent Milli-Q water for comparison. 92
Figure 3.8 Electron microscopy images of snow samples. (a-b) Scanning Electron Microscopy (SEM) images of some microorganisms in different types of

snow. (C-H) Transmission Electron Microscopy (TEM) images of filtered snow samples using a filter with a pore diameter of 0.22 mm. 94
Figure 4.1 Electron microscopy images of particles found in snow from AOSR: (A) particles containing anthropogenic structures, (B) close-up of A showing a nanotube structure, (C) EDS analysis of A, (D) cluster of nanoparticles, (E-F) EDS analysis of (D). 113
Figure 4.2 Particle number density of aerosolized melted snow from Montreal and near AOSR as electrical mobility diameter (EMD) in the size range of 10 – 100, 100-200, 200-500, 500-1000, 1000-2000, and 2000-5000. 115
Figure 4.3 Cumulative INP concentration of: (A) snow collected near AOSR compared to snow collected at Mont Royal park, Montreal, (B) filtered AOSR snow containing particles <200 nm compared to particles >200 nm, and (C) filtered Montreal snow containing mostly particles <200 nm compared to particles >200 nm. For Montreal data, different symbols represent samples from different years: ▲ 2014, ■ 2015, and ● 2017. For AOSR data different symbols represent the different sampling sites: ▲ (0 Km), ■ (7 Km), and ● (25 Km). 117
Figure 4.4 Freezing average temperatures of HgCl2 and HgBr2 compared to a-Fe2O3, Fe3O4, kaolinite, montmorillonite, and their respective mixtures with Hg halides. 119
Figure 4.5 X-ray powder diffraction patterns of Fe3O4 in the presence of HgCl2 and HgBr2.. 121
Figure A.1 Particle size distribution of samples from Alert: (a) unprocessed; (b) dialyzed; (c) filtered; and (d) filtered and dialyzed. 131
Figure A.2 EDS Spectrum of a particle in snow from Montreal, Quebec, collected in 2006. Peaks for Cu around 8 and 9 keV are caused by copper in the sample substrate (TEM-grids)... 132
Figure A.3 EDS Spectrum of a particle in snow from Alert, Nunavut. Peaks for Cu around 8 and 9 keV are caused by copper in the sample substrate (TEM-grids).. 132
Figure A.4 EDS Spectrum of a particle in snow from Barrow, Alaska. Peaks for Cu around 8 and 9 keV are cause by copper in the sample substrate (TEM-grids).. 133
Figure A.5 Effect of dilution of select melted snow samples on aerosol size distribution: high resolution for the 10 – 100 nm region and complete for the total measured region of 10 – 10,000 nm. 134
Figure B.1 Particle size distributions as a function of hydrodynamic diameter. Particle size distributions of individual samples (black line). Each sample was tested 5 times. The red bars represent the weighed standard deviation of the 5 runs at each single diameter... 136
Figure B.2 MALDI- TOF spectrum of the blank. This spectrum shows the contamination (if any) of the matrix used for the analysis of snow

samples. The peaks in this figure do not match the peaks of the sample shown in the main text. 137

Figure C.1 Sampling sites in the AOSR. Sampling location (A) is located < 1 Km from the two of the largest upgrading facilities. Sampling location (B) is 7 Km southeast from location (A), and sampling location (C) is 25 Km ways from location (A). 139

Figure C.2 Back-trajectory analysis for the 4th, 7th, 11th, and 14th of March 2015 calculated for the 0 km site. Calculations were done for 72 hours every 6 hours with 12 trajectories each. Most trajectories show that air masses come from the north. 140

Figure C.3 Electron microscopy images of particles > 2.5 micron. 141

Figure C.4 Cumulative ice nucleating particle concentration of particles separated by centrifugation. Different symbols represent the different sampling sites: ▲ (0 Km), ■ (7 Km), and ● (25 Km). 142

List of Tables

Table 1.1 Annual estimated emissions of different aerosols. 3
Table 1.2 Comparison of the freezing temperatures of common ice nucleating particles. 17
Table 1.3 Size and composition of particles that can be analysed by common techniques used in the study of aerosols. Taken from Georgakopoulos et al., 2009.[125] 22
Table 2.1 Comparison of ion content in the original and dialyzed snow. 50
Table 2.2 Total organic carbon in snow samples. 52
Table 2.3 Comparison of the mode diameters and concentrations for different locations of snow sampling. The concentrations are at corresponding primary and secondary mode particle diameter and expressed as dN/dlogDp, where dN is the number-based concentration of particles in the particle size range delimited by the upper and lower particle size boundaries of the corresponding measurement bin. Dp is the difference between these upper and lower instrument measurement bin boundaries... 56
Table 3.1 Total Organic Carbon (TOC) and ion concentrations (ppm) in 2 snow samples from the 3 sampling sites (σ: standard deviation of at least 3 repeats; detection limit: 0.1 ppm). Data for different snow samples from Barrow, Alaska, USA; Alert, Nunavut and Montréal, Québec, Canada. ... 84
Table 4.1 Elemental concentrations in melted snow from Montreal and AOSR. ND signifies non-detectable, and DL the detection limit. An (F) next to the element symbol means that the sample was filtered using a 0.2 mm filter. Montreal samples are denoted as MTL followed by the year they were sampled (2014, 2015, and 2017). 113

List of Abbreviations

AOSR	Athabasca oil sands region
BET	Brunauer–Emmett–Teller specific surface area
CCN	cloud condensation nuclei
DOC	dissolved organic carbon
EDS	energy-dispersive X-ray spectroscopy
ESI-MS	electrospray ionization mass spectrometry
HEPA filter	high efficiency particulate air filter
IC	ion chromatography
IN	ice nucleus
INP	ice nucleating particle
MALDI-TOF-MS	matrix-assisted laser desorption/ionization mass spectrometry
NTA	nanoparticle tracking analysis
OPS	optical particle sizer
SEM	scanning electron microscopy
SMPS	scanning mobility particle sizer
TEM	transmission electron microscopy
TOC	total organic carbon

Abstract

Aerosols interact with clouds and affect climate through absorption and scattering of radiation. However, aerosol-cloud interactions are complex, making radiative forcing predictions hard to calculate accurately. The most important uncertainty is the role of aerosols in the formation and dissipation of clouds, which are controlled by nucleation processes. In the lower troposphere, ice and mix-phase clouds are common. In these types of clouds, ice formation is primarily catalyzed by aerosols through heterogeneous ice nucleation. The conditions at which this process occurs depends on the properties of aerosols. Some aerosols are more efficient than other, but due to the complexity of aerosol-cloud interactions, models only focus on the contribution of aerosols that are efficient and abundant in the atmosphere. Even if an aerosol is very efficient, if its abundance in the atmosphere is low, its relevance as a global ice nucleating particle is minimal.

This thesis presents the particle size distributions in snow from four different locations as well as their physical and chemical properties to find which particles sizes are the most abundant. It also presents their ice nucleation behavior to determine their potential as relevant ice nucleating particles. Sampling was done in two remote locations, one urban, and one highly contaminated by oil sands activities. The remote locations were Barrow in Alaska, USA and Alert in Nunavut, Canada. The urban location was Montreal, Quebec, Canada and the highly polluted area was the Athabasca Oil Sands Region (AOSR) in Alberta, Canada.

The first part of the thesis presents the development of a system for the real-time measurement of aerosol size distributions in melted snow. This system brings particles suspended in melted snow into the airborne state. Collection of the generated particles onto electron microscopy grids is also possible. Samples are dialyzed before analysis to remove interferences from salts and other dissolved substances. Analysis of snow samples revealed that particles of 30 nm dominated the particle size distribution in Montreal snow and particles of 15 nm dominated the distribution in Alert and Barrow snow. Results suggest low particle size aggregation during the aerosolization process when compared to similar techniques. This developed technique had a high resolution of particle size in the range of 10-100 nm. Using this technique, it was also found that nanosized particles (<200 nm) are the most abundant (38-71 %) in the snow sampled from Alert, Barrow and Montreal. It was also found that nanoparticles represent 11-19% of all particles. Nanosized particles also exhibited high ice nucleation efficiencies, with average freezing temperatures of -19.6 ± 2.4 to -8.1 ± 2.6 °C. Chemical analysis of this size fraction revealed that these particles are composed by biological material such as amino acids and possibly cell debris as well as inorganic materials such as mineral dust.

In snow from the AOSR, nanosized particles dominated the size distributions as well, but their concentrations were as high as 2 orders of magnitude higher than Montreal. Additionally, these particles were much more efficient at nucleating ice with average freezing temperatures of -7.1 ± 1.8 °C. Analysis of these particles (even for samples collected 7-25 km away from major bitumen upgrading facilities) revealed the presence of anthropogenic nanostructures such as carbon nanotubes and trace metals with concentration up to 72 mg/L.

This thesis contributes to the understanding of the distribution of environmental particles and nanoparticles in northern locations and provided results that will help understand their effect on climate. With an increase in the release of chemicals by anthropogenic sources, understanding the properties of particles will help to predict atmospheric phenomena more accurately.

Résumé

Les aérosols interagissent avec les nuages et affectent le climat par l'absorption et la diffusion des rayonnements. Cependant, les interactions aérosols-nuages sont complexes, ce qui rend les prévisions de forçage radiatif difficiles à calculer. L'incertitude la plus importante est le rôle des aérosols dans la formation et la dissipation des nuages qui sont contrôlés par les processus de nucléation. Dans la basse troposphère, les nuages de glace et de phase mixte sont fréquents. Dans ce type de nuages, la formation de la glace est principalement catalysée par les aérosols grâce à la nucléation hétérogène de la glace. Les conditions dans lesquelles ce processus se produit dépendent des propriétés des aérosols. Certains aérosols sont plus efficaces que d'autres, mais en raison de la complexité des interactions aérosols-nuages, les modèles portent seulement sur les interactions pertinentes. Même si un aérosol est très efficace pour la nucléation de la glace, si son abondance dans l'atmosphère est faible, sa contribution sera minimale.

Cette thèse présente les distributions granulométriques dans des échantillons de neige provenant de quatre endroits différents ainsi que leurs propriétés physiques et chimiques qui servent à trouver les particules les plus abondantes. Elle présente également leur comportement de nucléation de la glace pour déterminer leur potentiel d’être des particules de nucléation de la glace pertinentes. L'échantillonnage a été effectué dans (1) deux sites de prélèvement éloignés: Barrow en Alaska, États-Unis et Alert au Nunavut, Canada; (2) un sites de prélèvement en milieu urbain: Montréal, Québec, Canada; (3) et le dernier dans un endroit hautement contaminé par les activités d'exploitation des sables bitumineux: La Région des Sables Bitumineux de l'Athabasca (AOSR) en Alberta, Canada.

Un système de mesure en temps réel des distributions de la taille des aérosols a été développé. Ce système amène les particules en suspension dans la neige fondue à l'état aéroporté. La collecte des particules générées sur des grilles de microscopie électronique est également possible comme une technique alternative. Les échantillons sont dialysés avant l'analyse pour éliminer les interférences des sels et autres substances dissoutes. L'analyse des échantillons de neige a révélé que les particules de 30 nm dominaient la distribution granulométrique dans la neige de Montréal et que les particules de 15 nm dominaient la distribution dans la neige Alert et Barrow. Les résultats suggèrent une faible agrégation de la taille des particules prélève du processus d'aérosolisation par rapport à des techniques similaires. Cette technique développée a eu une haute résolution de la taille des particules dans la gamme de 10-100 nm.

En utilisant cette technique, on a également constaté que les particules nanométriques (<200 nm) sont les plus abondantes (38-71%) dans la neige échantillonnée à Alert, Barrow et Montréal. C'était également constaté que les nanoparticules représentent 11-19% de toutes les particules. Les particules nanométriques présentaient également des propensions levées de nucléation de la glace, avec des moyennes de températures de germination entre 19,6 ± 2,4 - 8,1 ± 2,6 ° C. L'analyse chimique de cette fraction de taille a révélé que ces particules sont composées de matériaux biologiques tel que des acides aminés et probablement des débris cellulaires, ainsi que des matériaux inorganiques comme la poussière minérale.

Dans la neige de l'AOSR, les particules nanométriques dominaient aussi les distributions de taille, mais leurs concentrations atteignaient 2 ordres de grandeur plus levés que Montréal. En plus, ces particules étaient beaucoup plus efficaces pour la nucléation de la glace avec des moyennes de températures de germination de -7,1 ± 1,8 ° C. L'analyse de ces particules (même dans des échantillons prélevés à 7-25 km des principales installations de valorisation du bitume) a

révélé la présence de nanostructures d'origine anthropique telles que les nanotubes de carbone et de métaux traces avec des concentrations allant jusqu'à 72 mg / L.

Cette thèse contribue à la compréhension de la distribution des particules environnementales et des nanoparticules dans les régions du Nord et de leurs effets sur le climat. Avec une augmentation des rejets de substances chimiques par des sources anthropiques, la compréhension des propriétés des particules aidera à prévoir les phénomènes atmosphériques avec plus de précision.

Chapter 1

1. Introduction

Aerosols are particles suspended in air. Most of the aerosols in the atmosphere are in the solid phase,[1] but they can also be liquid.[2] In this work we focus on solid particles exclusively. Knowledge about the interactions of aerosol particles with clouds is limited and is considered a major research uncertainty by the International Panel on Climate Change (IPCC).[3-4] Atmospheric aerosols can affect the climate in 3 different ways: (1) by dictating the total radiation budget of Earth through absorption and scattering of incoming radiation, (2) by taking part in different surface reactions with various atmospheric chemical species, and (3) by inducing precipitation by catalysing the formation of water droplets and ice particles.[5-6] Additionally, the World Heath Organization considers aerosols a main cause of premature human mortality.[7-8]

1.1. Types of Aerosols and Their Source

Atmospheric aerosols can be divided into organic and inorganic aerosols, both varying widely in their properties, sources and abundance the atmosphere.

1.1.1. Organic Aerosols

Organic aerosols can be subdivided into primary organic aerosols (POA) and secondary organic aerosols (SOA).[9] POA can be released directly as aerosols from their source or condense from a gas to form an aerosol without undergoing any chemical reaction. SOA, on the other hand, are generated when organic compounds (generally volatile) in the gas phase undergo oxidation or other chemical reactions; they generate products with low enough vapour pressures to create a solid or liquid particle.[10] The resulting product can be semi-volatile or not volatile at all. PAO in general tend to be more hydrophobic.

Sources of POA can be anthropogenic or biogenic. The main source is combustion, which includes biomass burning (by natural fires and land-use practices) and vehicular exhaust (fossil fuels and biofuels) with estimated production of 33.2 Tg per year.[11] Table 1.1 contains a summary of annual emissions of different types of aerosols. Common particles generated from fuel combustion are monocarboxylic and dicarboxylic acids as well as polyaromatic hydrocarbons.[12]

Bioaerosols are another type of organic aerosol. These include whole microorganisms like bacteria, fungi and viruses, reproductive material like pollen, plant fragments, decaying matter, and others.[13] Sources of bioaerosols include forested areas around the globe; however, the major source of bioaerosols, many of which are aliphatic and humic-like substances, is the ocean.[14] The main process in which these aerosols are transferred from the ocean into the atmosphere is through bubble-bursting phenomena in the ocean surface layer.[15] It has been calculated that the production of bioaerosols, both marine and continental, is about 1000 Tg per year.[16]

Soot particles, also called black carbon, consist mostly of elemental carbon, but they can also contain some organic carbon.[17] This type of particle is very hydrophobic. Through oxidation processes, they can become less hydrophobic.[18] Their annual production has been estimated to be around 7.9 Tg.[12]

Generation of SOA commonly starts with the oxidation of volatile organic compounds (VOC) in the gas phase.[19] VOC can be anthropogenic or biogenic; nevertheless, biogenic sources dominate the production of atmospheric VOC by about 5.5 times.[20] Of all the biogenic VOC in the atmosphere, terpenes seem to be the dominant precursors of SOA.[21] Common atmospheric oxidants of terpenes are ozone, NO_x, and hydroxyl radicals.[12] It has been reported that the products of oxidation of terpenes by different oxidizing agents have varying nucleating properties. For example, reaction products of terpenes with NO_3 and hydroxyl radicals have lower nucleation efficiency than reaction products of terpenes with ozone.[22] SOA can also be generated through the oxidation of soot.[23] The products obtained contain oxygen-rich functional groups. This oxidation creates a more polar surface than the original soot particle.[24] Organic compounds can also be found as coatings of other aerosols. This type of aerosol can be seen as composites of organic and inorganic nature.

Table 1.1 Annual estimated emissions of different aerosols.

Primary Organic Aerosols (Tg/year)	
Organic carbon	33.2[11]
Bioaerosols	56[25]
Marine	1000[16]
Secondary Organic Aerosols (Tg/year)	
VOC	756-810[20]
Soot	7.9[11]
Inorganic Aerosols (Tg/year)	
Mineral dust	1921[26]
Sulphates	200[27]
Nitrates	18[27]

1.1.2. Inorganic Aerosols

Inorganic aerosols just as organic ones can be produced by anthropogenic and biogenic sources. These aerosols include salt particles and mineral dust among others. Mineral dust aerosols are one of the most important atmospheric aerosols because they are one of the largest contributors to the formation of precipitation.[28] They are generated by the effect of winds on the surfaces of the Earth. The main global source of mineral dust is the global dust belt expanding from the Saharan desert to deserts in the Arabian Peninsula and Oman and ending in the Gobi and Takla-Makan deserts in China.[29] Other important areas that contribute to atmospheric mineral dust production especially in the Southern Hemisphere include the Artesian Basin in Australia and Patagonian deserts in South America.[30] Nevertheless, regions in the Northern Hemisphere contribute more to atmospheric mineral dust at a global scale. Common components of mineral dust include calcite, quartz, dolomite, feldspar, iron oxides (such as magnetite, hematite and maghemite) and clay materials (such as kaolinite, illite and montmorillonite).[31] The chemical composition of mineral dust depends on the region it comes from (Figure 1.4). Particle sizes of mineral dust vary from a couple nanometers to several microns; however, submicron mineral dust particles are predominant in the atmosphere.[32] This is because for larger particles to become airborne, higher wind speeds are needed. Additionally, larger particles remain suspended in air for shorter periods of time. It has been reported that mineral dust particles between 0.1 and 5 microns can remain suspended long enough to travel 500 km in the atmosphere.[33] Anthropogenic sources are not the most important contributors of mineral dust, but they are still a source found throughout the globe. These include road constructions, factories, mining, etc.[34]

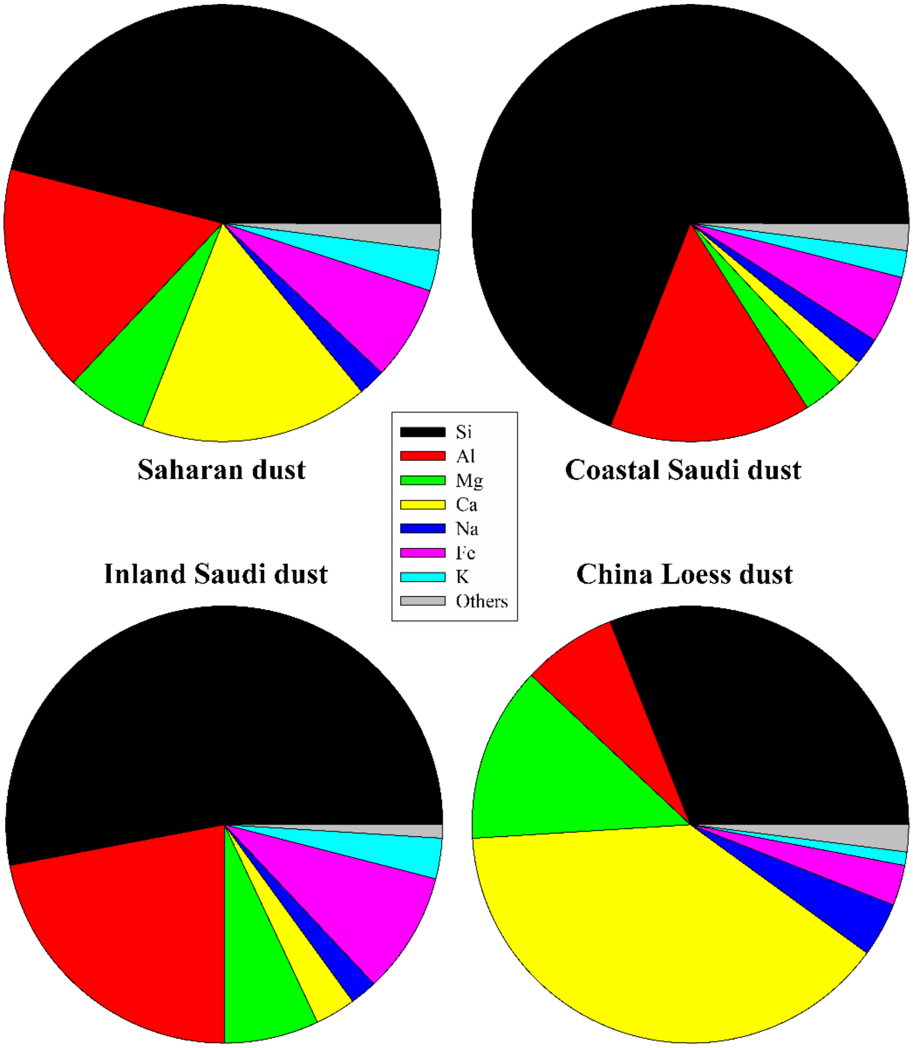

Figure 1.1 Chemical composition of mineral dust particles from four source regions in the global dust belt. Data taken from Krueger et al., 2004.[29]

Another type of inorganic aerosol includes salts of which the main source is the ocean. The main components are sodium and chloride, but other species like sulphate, potassium, magnesium and calcium are also generated. The way in which salt aerosols are generated is through bubble-bursting at the sea surface.[35] The sea spray generated may contain other species aside from salts including organic aerosols. These marine aerosols can travel large distances upwards as well as inland.[33]

Secondary aerosol formation can also occur with inorganic components. These include sulphur, nitrogen and inorganic carbon species. Sulphur aerosols are formed when sulphur-containing gases (like SO_2 and dimethyl sulphide) are oxidised to sulphuric acid. The oxidation processes can occur in the gas phase or in the liquid phase within water droplets.[25] If oxidation occurs in the gas phase, sulphuric acid rapidly condenses to form droplets of a sulphuric acid solution due to the low saturation vapour pressure of sulphuric acid itself.[33] Sulphuric acid can become the coating of other aerosols[36] or be neutralised by NH_3 and other species to form sulphate salts like $CaSO_4$ and Na_2SO_4.[37-38] Sources of sulphur gases include natural sources like volcanoes[39] and the ocean (dimethyl sulphide)[40], and anthropogenic sources like fossil fuel combustion, metal smelting, petroleum production and others. Nevertheless, anthropogenic sources dominate their release.[41]

Inorganic nitrogen aerosols just like sulphur aerosols are secondary in nature, formed from the reactions (mainly oxidation) of nitrogen-containing gases. The main products are salts of nitrate (NO_3^-) and ammonium (NH_4^+). Nitrate salts are formed when nitrogen oxide gases are further oxidised to nitric acid after release. Nitric acid can then form nitrate salts of sodium, calcium, etc. Nitric acid can be formed in the gas phase and in the liquid phase.[42] Furthermore, ammonia can react with nitric acid to form ammonium nitrate, but this molecule is not very stable and decomposes into its original compounds (HNO_3 and NH_3).[43] Sources of nitrogen oxides and ammonia include anthropogenic sources like combustion of fuels and biomass,[44] use of fertilizers[45] and biogenic sources like natural fires and emissions from plants and soils.[37]

Inorganic carbon aerosols are mainly composed of carbonate and bicarbonate salts (primarily of calcium and magnesium). These aerosols are mainly generated by suspension from the ground. Unlike sulphur and nitrogen aerosols, secondary production of carbonate aerosols does not exist because oxidation to H_2CO_3 leads to the generation of CO_2, which is mostly inert. Also, carbonate aerosols, especially soluble ones, can react with acids and generate CO_2.

1.2. Deposition of Aerosols and Snow

Removal of aerosols and gases from the atmosphere happens through wet and dry deposition processes. Particle size has a large effect on whether dry or wet deposition takes place. Larger particles > 10 μm cannot remain suspended long enough and generally settle down through dry deposition.[46] Smaller particles, on the other hand, can remain suspended in air for longer periods of time, therefore have higher chances of being deposited with precipitation (wet deposition).

Wet deposition can occur in 2 different ways: through nucleation processes and through scavenging (in-cloud and below-cloud).[47] Nucleation can lead to the formation of cloud droplets or ice crystals depending on the atmospheric conditions in which the aerosols are present. In arctic locations, ice crystal formation dominates wet deposition during wintertime in the form of falling snow. This process is called ice nucleation and it can occur homogenously (in the absence of particles) or heterogeneously (in the presence of particles). Because homogeneous ice nucleation is a simpler process, it will be reviewed before heterogeneous ice nucleation.

1.3. Homogeneous Ice Nucleation

Most of us have been told that water freezes at 0 °C at the standard pressure of 1 atm. When water is pure, however, it rarely freezes at 0 °C. The state in which water remains liquid below its melting point is called supercooled water.[48] This is a metastable state or a state at a local minimum of free energy (Figure 1.1). In contrast, a stable state (in this case ice) is a state at a global minimum of free energy.[49]

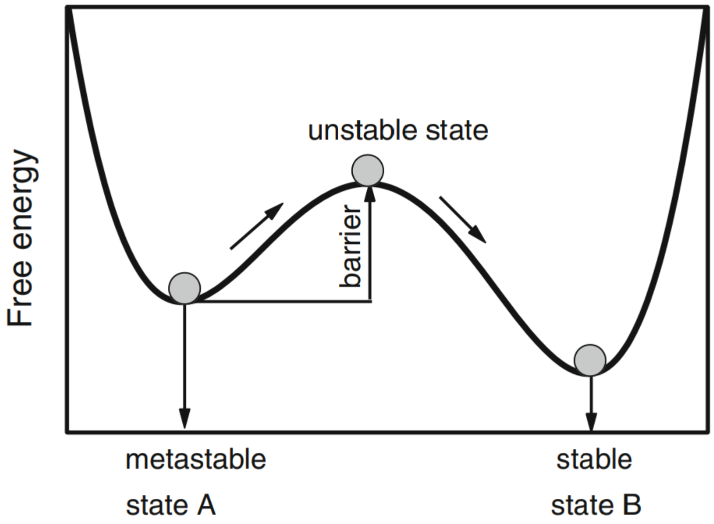

Figure 1.2 Free energy as a function of the order parameter. Image taken from Kalikmanov, 2013 (Chapter 3)[49]. Reproduced with the permission of Springer.

Metastable states can remain stable to small fluctuations in energy, but once the system transforms into the stable state, it cannot go back.[50] For supercooled water to freeze, it needs to cross the energy barrier characteristic of first-order phase transitions,[51] but in the absence of nucleating sites this rarely happens with decreasing probability at warmer temperatures. Supercooled water can easily remain liquid down to temperatures of around -38 °C.[52-55] At this or lower temperatures, small molecular clusters of the new phase start to form due to the random agglomeration of water molecules.[51] These clusters are called ice embryos and are characterised for having weak binding energies.[56] They will keep forming and disappearing randomly. The phase change will not happen until after an embryo grows to a critical size.[56] In terms of energy, the phase change will not occur until the energy barrier ΔG between the two phases (supercooled water and ice) is surpassed. In classical nucleation theory, ΔG as a function of the radius (r) of the ice embryo is calculated by[37]:

$$\Delta G(r) = n_i \frac{4\pi r^3}{3} \Delta\mu + 4\pi r^2 \gamma \qquad (1)$$

Where n_i is the number density of ice, $\Delta\mu$ is the change in chemical potential for the bulk liquid to ice phase transition, and γ is the interfacial free energy between the ice embryo and the bulk water. In equation (1) the first term corresponds to the energy of the bulk (negative) and the second term to the energy of the surface of the ice embryo (positive). At low values of r, the surface term dominates, and the phase change will not happen. Once the embryo surpasses its critical size, where the contribution of the bulk is equal to that of the surface, the phase change occurs (Figure 1.2).[51] This process is called homogeneous ice nucleation and according to the classical nucleation theory is a stochastic process.[57]

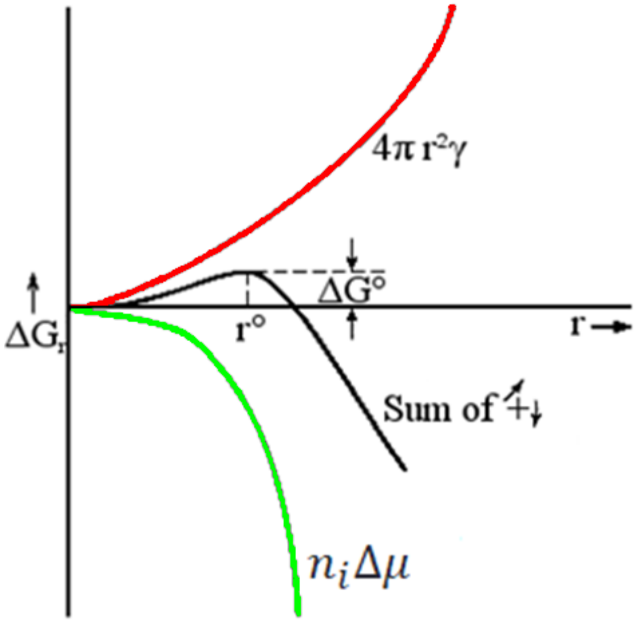

Figure 1.3 Change in free energy of the system as a function of the ice embryo’s radius. The energy of the bulk is represented by the green curve and the energy of the surface of the ice embryo is represented by the red curve. The inflection point corresponds to the critical radius where the contribution from the bulk is equal to the contribution from the surface. Image modified from Ragone, 1994 (Chapter 1).[58] Reproduced with the permission of John Wiley & Sons. Inc.

1.4. Heterogeneous Ice Nucleation

The presence of surfaces can lower the energy barrier by providing a more favourable interface with the ice embryo because the area of the interface between the ice embryo and the surrounding fluid is less than $4\pi r^2$. INP with good affinity for the ice embryo will deform it more resulting in a smaller contact angle (θ) between the INP and the ice embryo and therefore the area of the ice embryo exposed to supercooled water will be less than $4\pi r^2$. The contact angle (θ) is just a measurement of how well an INP interacts with the ice embryo and should not be confused with the contact angle used to measure the wettability of a particle (how well a material interacts with water) commonly used in material sciences. Equation (1) can be corrected by multiplying by a factor f(θ), which is a function of the contact angle (θ) between the surface and the ice embryo.[37]

$$f(\theta) = \frac{1}{4}(2 + cos\theta)(1 - cos\theta)^2 \qquad (2)$$

The process in which a surface catalyzes the phase change is called heterogeneous ice nucleation. When an aerosol catalyzes the formation of ice it is called an Ice Nucleus (IN) or Ice Nucleating Particle (INP) and when it does for a water droplet, it is called a Cloud Condensation Nucleus (CCN).[56] All aerosols can serve as CCN or INP depending on their properties. Heterogeneous ice nucleation can occur through 4 different pathways or modes (Figure 1.3):[59]

1. **Deposition**: Water vapour molecules deposit on the surface of the INP as a solid. This is the only one that happens directly from the gas phase.
2. **Condensation:** Water vapour molecules deposit on the surface of the INP as a liquid and then freeze. In other words, the INP acts as both a CCN and an INP.
3. **Contact:** A supercooled water droplet touches an INP and it freezes. The INP never goes inside the water droplet.

4. **Immersion**: An INP is already immersed in a supercooled water droplet. Freezing occurs only after the INP activates. A water droplet should have been formed through cloud condensation, but the CCN and the INP are not the same. Immersion nucleation is considered to be the dominant mode of ice nucleation in mixed-phase clouds (supercooled water and ice particles).[5] For immersion freezing, *in situ* measurements of clouds indicate that at temperatures below -15 °C, more than half the clouds contain ice particles while at higher temperatures, ice rarely forms.[1] In this work we'll focus on this mode of nucleation.

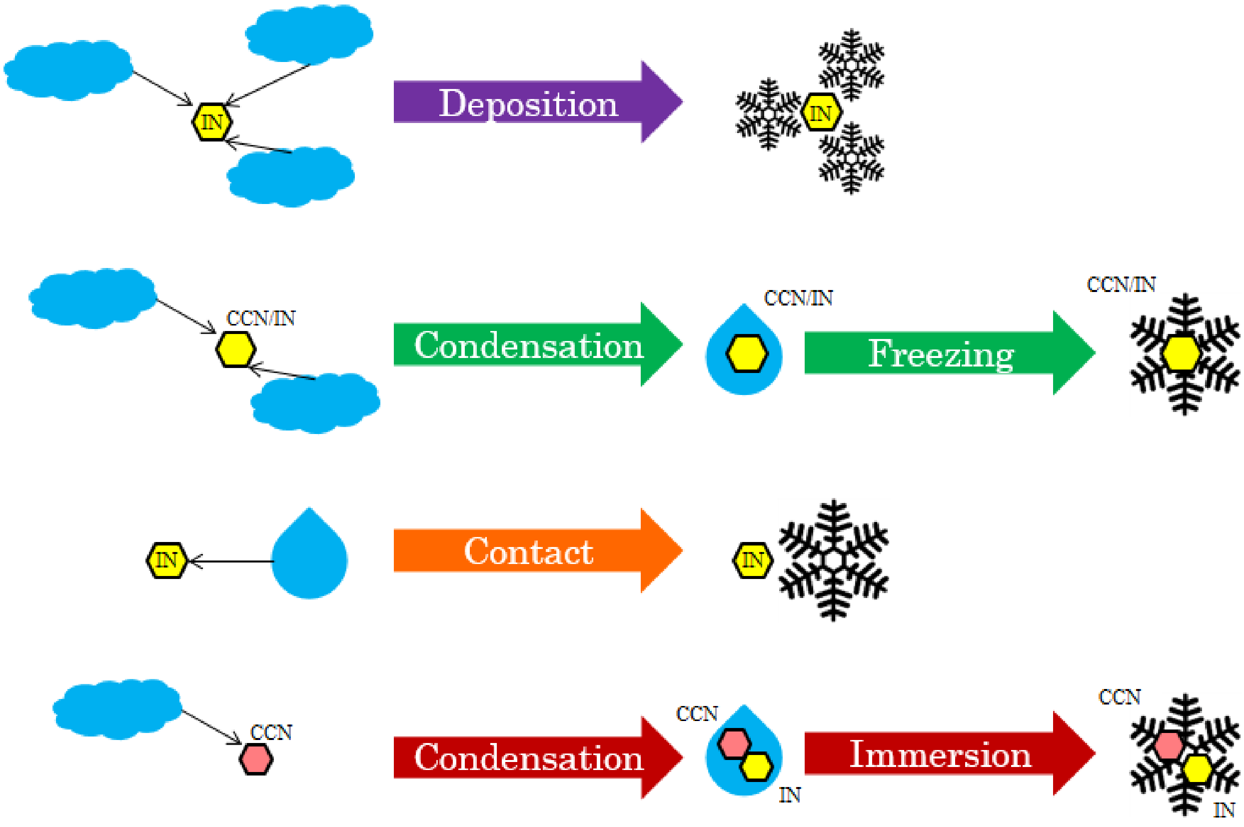

Figure 1.4 Heterogeneous ice nucleation modes.

Heterogeneous ice nucleation can be seen as either a stochastic process where nucleation takes place randomly[60] or as a process where nucleation occurs at singular surface sites at specific temperatures.[61] In the stochastic hypothesis, the INP are considered to have the same ability to nucleate ice given the chemical composition and size are the same.[62] This means they have the same probability of nucleating ice at the same temperature in the same time interval. Even if the temperature remains constant, nucleation will happen after certain time. Ice nucleation is time-dependent. In the singular hypothesis, nucleation occurs at specific sites or active sites on the surface of the INP.[62] Each site has a specific activation temperature. If the temperature remains constant, the probability for nucleating sites to activate and freeze water is very low.[63] In this case, nucleation is time-independent. There is an approach that combines the stochastic and singular nature of INP.[64] The idea is that the surface of an INP has several active sites and each site has different activation energies.[65] In this case a group of particles with similar physical and chemical properties will exhibit nucleation over a continuous range of temperatures.

1.4.1. Evaluation of Ice Nucleation Ability

A very important consideration when studying the ice nucleating properties of particles is the nucleation mode or mechanism. As stated before, there are 4 modes in which heterogeneous ice nucleation can take place. Different methodologies have been developed depending on the mode that one wants to study; scientists have even come up with different approaches to study the same mode. The conditions needed for ice nucleation to occur vary depending on the mode that is taking place. Even when studying the same mode, the results can vary. When studying the immersion mode of ice nucleation several methods and instruments exist; however, many of these methods revolve around drop freezing assays developed 50 years ago.[66] These experiments consist in breaking up a volume of water containing a specific type of INP into numerous small drops. The drops are then placed on an inert surface with a hydrophobic coating to minimize nucleation by the surface with the water droplets. The surface is cooled down at a constant rate and then is covered to minimise condensation from air. The temperature at which each droplet freezes is recorded.

Other experiments have been developed to better simulate the conditions found in the atmosphere. Latest instruments include some that recognize of the change in a droplet's brightness when it freezes to automate detection.[67] Another addition is the use of a nebulizer for generation of smaller droplets, the use of a microscope to detect freezing of smaller droplets with the end of studying single particles and the use of cameras. Other techniques involve the suspension of droplets in air to prevent any effect from surfaces where the droplets rest,[68] the use of an IR-thermometer to measure temperature changes indirectly and even the use of a Raman spectrometer coupled to a microscope. The implementation of these new methodologies is not as straight forward as it seems; nevertheless, the principle is still the same.[69]

One way to analyse the data of drop freezing assays is by calculating the mean freezing temperature of the droplets. But because each droplet contains many INP, freezing can span a long range of temperatures. Another way to study the distribution of active INP is by using the cumulative concentration of active IN at temperatures warmer than a specific sub-zero temperature in a unit volume. These experiments are based on the singular hypothesis of heterogenous ice nucleation. The cumulative nuclei concentration is derived from the differential nuclei concentration k(T) (in L^{-1}) which represents the concentration of active IN within an interval of temperature, n(T), per unit volume V.[66]

$$k(T) = n(T)/V \quad (4)$$

Rearranging this equation, we get

$$n(T) = k(T)V \qquad (5)$$

If we want to know the rate of change in the number of active IN in a very small change of temperature we can rewrite the equation as

$$n(T)dT = k(T)VdT \qquad (6)$$

A different way to see this is with N_0 being the initial number of droplets and N(T) the number of unfrozen droplets at temperature T. With a very small change in temperature, the number of droplets that may freeze is dN and the fraction of unfrozen droplets in this range of temperatures is dN/N(T). Therefore

$$\frac{dN}{N(T)} = k(T)VdT \quad (7)$$

Which can be integrated from the temperature at which a droplet freezes to 0°C to get the cumulative concentration of active INP, K(T) (in L^{-1})

$$K(T) = [lnN_0 - lnN(T)]/V \qquad (8)$$

Knowing the cumulative concentration of active INP complements the characterisation of INP. For example, particles with similar physical and chemical properties can have different ice nucleating abilities.

1.5. Aerosols Properties and their Effect on Ice Nucleation

Heterogeneous ice nucleation is determined by two conditions: temperature and water vapour saturation ratio with respect to ice.[1] For immersion mode, where formation of ice happens in the bulk of water, nucleation seems to be unaffected by vapour/droplet interfaces.[70] Only temperature is important because the INP is already surrounded by supercooled water and the INP does not interact with water vapour. Water vapour does influence the ice nucleation by other modes and by the growth of water droplets (which can affect the ice nucleation by immersed particles indirectly) and ice crystals, but that will not be covered here. The physical and chemical properties of the INP determine the freezing temperature of a volume of supercooled water; however, predictions of nucleation based on these properties are not possible.[1] Chemical composition, crystalline structure (for crystals only), coatings, size and surface area, and time are some of the factors that determine the nucleating temperature of particles.[28] In general, INP are solid and insoluble in water, although some might be liquid. Common INP found in clouds that have been highly studied are mineral dust, soot, bioaerosols, ammonium sulphate, and organic acids among others.[71-72]

1.5.1. Ice Nucleation of Different Aerosols

Mineral dust particles are probably the most relevant INP globally. They nucleate ice efficiently and are relatively abundant in the atmosphere.[73] Soot particles are a bit more complicated than mineral dust particles because their composition depends on the original fuel and the combustion method.[74] It has been observed that soot particles' efficiency for ice nucleation depends on the organic carbon content. The ice nucleation activity decreases with higher organic carbon content.[75] In general, the more hydrophilic an INP is, the better ice nucleation efficiency it will have, but this is not always the case as some bioaerosols are some of the most efficient INP known.[6] Table 1.2 contains a comparison of the freezing temperatures of different organic and inorganic INP larger than 1 µm.

The ice nucleation of bioaerosols has a long range because only a small fraction of microorganisms can nucleate ice efficiently while others cannot. This is because specific microorganisms have evolved to induce frost damage on plants to extract nutrients from the host (usually plants).[76-77] Their ability to nucleate ice is very selective and is not just a coincidence. For example, it has been suspected that cold-resistant bacteria have the potential to nucleate ice, but so far, the results have been negative. Of all microorganisms, only selected fungi and bacteria have been found to nucleate ice through specific membrane proteins.[78-79] One of the best-known examples is the Gram-negative bacteria *Pseudomonas syringae* with onset temperatures of around -2 °C.[80]

There are other types of aerosols that can nucleate ice including salts, volcanic ashes and artificial particles.[33] The latter lack relevance due to their absence in the atmosphere. Some natural aerosols like volcanic ashes and sea salt spray can affect the climate, but due to their high solubility, salts cannot provide a surface for nucleation (unless they are completely dry), so in the end they are not important INP in the immersion mode by themselves. Still, they can become coatings of other important INP and modify their properties. Other species can also alter the surface properties of other INP by reacting with or coating the surface of these particles. This is important because in clouds, aerosols are subjected to different types of situations. For example, it has been reported that coating of ammonium sulphate can improve the nucleation of mineral dust particles.[36] It is also possible that some coatings suppress the ice nucleation ability of particles.[81] For example, it was reported that coatings of SOA on mineral dust particles supress the nucleation by mineral particles decreasing their efficiency as INP.[81] Organic particles like POA and SOA are highly hydrophobic; therefore, their potential as efficient CCN or IN is low.[82-83] SOA are the better CCN and IN of the two due to their higher level of oxidation. These oxygen-rich functional groups on the surface increase the interactions with water and decreasing its surface tension which in turn results in a higher nucleation efficiency.[84]

Table 1.2 Comparison of the freezing temperatures of common ice nucleating particles larger than 1 µm.

Particle type	Temperature (℃)			
Organic				
Acetylene soot	-34[85]			
Kerosene soot	-28[86]			
Pollen	-14[87]			
Birch pollen	-12[87]			
Leaf litter	-9.0[88]			
Bacteria	-7.0[89]			
P. Syringae	-3.5[90]	-9.0[91]		
E. Herbicola	-3.4[92]			
Inorganic				
Quartz	-12[93]			
Kaolinite	-23[94]	-22[95]	21[96]	-10[93]
Montmorillonite	-19[94]	-13[6]	-14[96]	-8.0[94]
Illite	-23[72]	-12[93]		
Hematite	-10[93]			
Albite	-11[93]			
Calcite	-14[93]			
AgI	-4.5[6]	-8.7[97]	-5.0[98]	
Volcanic ash	-18[99]			

1.5.2. Ice Nucleation by Nanoparticles and Nanosized Particles

One characteristic of INP that seems to have a directly proportional relation to ice nucleation efficiency is size. In general, larger particles are considered better INP than their smaller counterparts because they create smaller contact angles with the ice embryo due to a larger surface area. Observations of ice nucleation by mineral dust particles have led to the conclusion that smaller particles require a higher ice super saturation or lower temperatures to activate.[100] Because nanoparticles and particles < 200 nm are not as efficient at nucleating ice as their larger counterparts, most research focuses on the latter particles. Even climate models focus on the effect of the more efficient INP despite their lower abundance in the atmosphere. The concentration of particles < 1 µm is 10 to 10,000 cm^{-3} while the concentration of particles > 1 µm is < 10 cm^{-3}.[101]

On the other hand, there is an increasing concern for the effect of nanoparticulate pollution on human health.[102] Nanoparticles are even considered a major cause of premature infant mortality by the World Health Organization.[7-8] Recent research has been focusing increasingly on smaller INP such as nanoparticles and particles consisting of emerging contaminants.[79] Chapters 2, 3, and 4 of this work focus mainly on nanoparticles and particles < 200 nm and their ice nucleation properties.

1.6. Measurement of Aerosols

As mentioned before, the different properties of an INP determine how efficiently it will nucleate ice, but to know its properties, it is necessary to measure them. Measurements of environmental samples can be done *in situ* and in the laboratory, both requiring different methodologies. In this section, we will explore different techniques used in the laboratory to analyse environmental samples.

1.6.1. Electron Microscopy Techniques

Knowing the particle size distribution in a sample can be useful to study the population of possible INP. Particle sizing techniques used in the laboratory vary in their fundamental principles and therefore can provide complementary information about the particle size distribution of a sample (Table 1.3). Two main techniques to study the size of particles are electron microscopy and optical techniques. Electron microscopy techniques are frequently used to study the morphology and size of nanoparticles as well as micron-sized particles.[103] The Transmission Electron Microscope (TEM) is generally used to study the size of the smaller particles ($< 0.5\ \mu m^2$). It can also be used to calculate a number average diameter of particles by doing many observations, although overestimation is common.[104] These particles, however, need to have sufficient electron contrast to be seen by the microscope or to be treated with a high electron contrast stain (e.g. uranyl acetate).[105] The Scanning Electron Microscope (SEM) is another technique with lower magnification, but with the ability to provide topographic information of particles. This is very useful when studying agglomerates and aggregates of nanoparticles.[106] Atomic Force Microscopy (AFM) is similar to other microscopy techniques with the advantage of not requiring any treatment with stains prior to analysis.[107] For all these techniques, collection on a substrate is necessary prior to analysis. Common collection practices include filtration, and the use of impactors for collection on a vast variety of substrates.[103] Collection of aerosols can also be done directly onto an electron microscopy grid using electrostatic precipitation of the aerosols.

1.6.2. Optical Sizing Techniques

Optical sizing techniques differ from microscopy technique in that they provide the size distribution of a population of particles rather than the size of individual particles. Dynamic Light Scattering (DLS) correlates the intensity of the light scattered by particles in a liquid suspension to their sizes.[108] Due to the Brownian motion of particles, the intensity is not constant through time.[104] In DLS the intensity of scattered light can be correlated to the size of a particle because the Brownian motion of particles depends on their sizes.[2] Larger particles have slower Brownian motion and therefore the change in scattered light intensity is less than for smaller particles. An important aspect of DLS is that the sizes provided are hydrodynamic diameters, not the actual size of a particle. The equation used to calculate the hydrodynamic diameter is the Stokes-Einstein equation:

$$d = \frac{kT}{3\pi\eta D} \qquad (3)$$

Where k is the Boltzmann constant, T is the absolute temperature, η is the viscosity, and D is the translational diffusion coefficient of the particle. DLS, however, can be biased when the particle size difference in a sample is large, because the signal of larger particles tends to obscure the signal of smaller particles.[109] Other techniques similar to DLS also exist. Nanoparticle Tracking Analysis (NTA) is similar in principle to DLS.[104] This technique uses a camera to take a video of the particles and then, with an image analysis software, it can track the diffusion of particles to calculate their size.[110] This technique can provide better results than DLS when the sizes of particles in a sample vary greatly.

Sizing techniques are not limited to liquid suspensions. Other techniques exist that can provide the size distribution of particles in air. Most of these instruments are based on light diffraction for particle detection. Nevertheless, detection by light scattering can only be useful up to certain particle sizes.[2] Smaller particles cannot be discriminated that easily. Smaller particles first must be separated and then counted. An instrument that is routinely used to get the particle size distribution of particles under 0.1 μm is the Scanning Mobility Particle Sizer.[111] This instrument is based on the differential mobility of particles in an electric field.[108] The particles traverse through an electric field at different rates based on their sizes. Once separated, the number of particles is calculated using optical counters and the sizes are calculated based on mobility distribution.[63]

1.6.3. Chemical Characterisation of Aerosols

Chemical characterisation of aerosols can be performed *in situ* or by collecting the aerosols followed by analysis in the laboratory, usually by spectroscopic methods. Collection of aerosols is generally performed on filters, but other substrates can be used (like films and foils).[2] Most of the chemical instruments used to analyse particles collected on a filter cannot distinguish particle sizes. If the chemical analysis of a specific size range is wanted, classification must be done during collection.[112] One example is the use of a Micro-Orifice Uniform Deposit Impactor (MOUDI) which collects particles on different filters depending on their sizes.[113] Collecting samples for later analysis has been the most common way of getting the chemical composition of a sample due to its simplicity and low price.[103] *In situ* measurements, however, present some advantages over collection.[114] By analysing aerosols in the field, it is possible to obtain continuous measurements.[115] This means that collection methods can only give information about the atmosphere of certain time periods while *in situ* methods can provide information over a long period of time with no interruptions.[116] Other advantages include no need for storage, less contamination and near real-time data.[117]

The main chemical species of aerosols analysed are ions (cation and anions), carbonaceous materials (inorganic, organic, total, etc.), and elemental composition.[2, 118] For the analysis of ions, the most common technique used is Ion Chromatography for which samples need to be in solution prior to analysis, but other techniques are also used.[119-120]

Analysis of carbonaceous species can be divided by the type of carbon: total, dissolved, carbonate, elemental, and organic carbon.[2] Organic speciation can also be done to know the different organic molecules in a sample. Common techniques used are Gas Chromatography coupled with Mass Spectrometry (GC-MS) for volatile and semi-volatile compounds.[121-122] Aerosol Mass Spectrometry can be used for real-time analysis.[123] Soft ionisation techniques like Matrix-assisted laser desorption/ionisation MS are useful for large molecules (like biomolecules).[124] Elemental composition can be obtained using techniques such as X-ray fluorescence, X-ray photoelectron spectroscopy and the most commonly used Inductively Coupled Plasma Mass Spectrometry for metals.[2]

Table 1.3 Size and composition of particles that can be analysed by common techniques used in the study of aerosols. Taken from Georgakopoulos et al., 2009.[125]

Method	Size	Composition
Optical microscopy	~0.2 um	Biological identification
Scanning Electron Microscopy	~20 nm	Elemental analysis with EDS
Transmission Electron Microscopy	1Å	Elemental analysis with EDS
Atomic Force Microscopy	0.1 nm	-
Aerosol Mass Spectrometry	~50 nm	Ion fragments

1.7. Research Objectives

The hypothesis of this work was that particles <200 nm (herein called nanosized particles) are relevant in ice nucleation. The specific aims were the following:

- To develop a technique to determine the size of particles in snow with minimal perturbation of the original state of the particles.
- To find the most abundant sizes of particles in arctic and subarctic snow and determine if they are relevant INP (i.e., whether their ice nucleation efficiency is comparable to important atmospheric INP).
- To compare the ice nucleating properties between snow-borne particles from remote locations in the arctic with urban areas like Montreal.
- To compare the ice nucleating properties between snow-borne particles from highly contaminated areas like oil sands regions with urban areas like Montreal to determine whether pollution has a significant effect on natural INP.

To achieve our goal, we studied the chemical composition, ice nucleation properties and the size distribution of particles in snow from different northern locations. We focused on snow because snow is a natural phenomenon that can provide valuable information about the atmosphere. Particles get trapped within snowflakes through 3 different pathways: serving as the INP, scavenged by falling snow, and by fallout of aerosols onto ground snow.[126] Ground snow can contain more particles than falling snow if the time between falling and collection is long. In these cases, most particles come from the fallout of aerosols rather than scavenging or nucleation. Even in the case where snow is collected directly from falling snow, most particles in snow are from scavenging and not from nucleation. This is because one single particle is required for the nucleation of an entire ice crystal while many particles can be trapped by scavenging or fallout. Nevertheless, just because one particle nucleated an ice crystal does not mean that the other particles trapped in the same ice crystal are not efficient INP.

1.8. Structure of the Thesis

This thesis is in the form of 3 manuscripts each corresponding to a chapter except for the introduction. Chapter 2 was published as “Nazarenko, Y.; Rangel-Alvarado, R. B.; Kos, G.; Kurien, U.; Ariya, P. A., Novel aerosol analysis approach for characterization of nanoparticulate matter in snow. Environmental Science and Pollution Research 2017, 24 (5), 4480-4493”. This manuscript outlines our efforts to develop a technique which would allow us to study the size distribution of particles in snow samples by aerosolisation and subsequent drying of a liquid. We created this technique so that the particulate content suspended in a non-gaseous sample could be sized without modification of the original size of particles, i.e., minimisation of particle aggregation and separation without the need of pre-concentration procedures.

Chapter 3 was published as “Rangel-Alvarado, R. B.; Nazarenko, Y.; Ariya, P. A., Snow-borne nanosized particles: Abundance, distribution, composition, and significance in ice nucleation processes. Journal of Geophysical Research: Atmospheres 2015, 120 (22)”. This manuscript summarises our work on the study of particulate matter in arctic and subarctic snow. The main component of this study is the characterisation of the ice nucleation capabilities of particles < 200 nm. The technique developed in chapter 2 was utilised to obtain the particle size distributions of the different snow samples and was crucial to decipher the most abundant particle sizes in the samples. The findings of subcellular structures by electron microscopy enabled us to conclude a biological or partially biological origin of these particles. A related paper published as "Nazarenko, Y.; Kurien, U.; Nepotchatykh, O.; Rangel-Alvarado, R. B.; Ariya, P. A., Role of snow and cold environment in the fate and effects of nanoparticles and select organic pollutants from gasoline engine exhaust. Environmental Science: Processes & Impacts 2016, 18 (2), 190-199" where we also studied urban snow, but is not part of this thesis appeared on Royal Society of Chemistry editorial highlight.

Chapter 4 is a manuscript submitted to Environmental Science & Technology as "Rangel-Alvarado, R. B.; Willis, C. E.; Kirk, J. L.; St. Louis, V. L.; Lehnherr, I.; Amyot, M.; Bélanger, D.; Ariya, P. A., Athabasca Oil Sand Snow Contains Efficient Ice Nucleating Particles". This paper further expands on the study of nanoscale particles in snow as in chapter 3, but this time the focus of the study was on highly contaminated snow and how pollutants affect the ice nucleation of snow-borne particles. The second part of this manuscript details the effect of mercury(II) coatings on the ice nucleation of components of mineral dust.

References

1. Hoose, C.; Möhler, O., Heterogeneous ice nucleation on atmospheric aerosols: a review of results from laboratory experiments. *Atmospheric Chemistry and Physics* **2012,** *12* (20), 9817-9854.
2. Kulkarni, P.; Baron, P. A.; Willeke, K., *Aerosol measurement: principles, techniques, and applications*. John Wiley & Sons: 2011.
3. Solomon, S., et al. Cambridge University Press: Cambridge, UK and New York, NY, USA, 2007; p 996.
4. Stocker, T.; Qin, D.; Plattner, G.; Tignor, M.; Allen, S.; Boschung, J.; Nauels, A.; Xia, Y.; Bex, B.; Midgley, B., IPCC, 2013: climate change 2013: the physical science basis. Contribution

of working group I to the fifth assessment report of the intergovernmental panel on climate change. **2013**.

5. Murray, B.; O'sullivan, D.; Atkinson, J.; Webb, M., Ice nucleation by particles immersed in supercooled cloud droplets. *Chemical Society Reviews* **2012,** *41* (19), 6519-6554.

6. Ariya, P.; Sun, J.; Eltouny, N.; Hudson, E.; Hayes, C.; Kos, G., Physical and chemical characterization of bioaerosols–Implications for nucleation processes. *International Reviews in Physical Chemistry* **2009,** *28* (1), 1-32.

7. WHO, World Health Organization. International Agency for Research on Cancer. Outdoor Air Pollution a Leading Environmental Cause of Cancer Deaths. *International Agency for Research on Cancer: Diesel Engine Exhaust Carcinogenic* **2013**.

8. WHO, World Health Organization. 7 million premature deaths annually linked to air pollution. *World Health Organization* **2014**.

9. Kanakidou, M.; Seinfeld, J.; Pandis, S.; Barnes, I.; Dentener, F.; Facchini, M.; Dingenen, R. V.; Ervens, B.; Nenes, A.; Nielsen, C., Organic aerosol and global climate modelling: a review. *Atmospheric Chemistry and Physics* **2005,** *5* (4), 1053-1123.

10. Saxena, P.; Hildemann, L. M., Water-soluble organics in atmospheric particles: A critical review of the literature and application of thermodynamics to identify candidate compounds. *Journal of atmospheric chemistry* **1996,** *24* (1), 57-109.

11. Bond, T. C.; Streets, D. G.; Yarber, K. F.; Nelson, S. M.; Woo, J. H.; Klimont, Z., A technology-based global inventory of black and organic carbon emissions from combustion. *Journal of Geophysical Research: Atmospheres* **2004,** *109* (D14).

12. Sun, J.; Ariya, P. A., Atmospheric organic and bio-aerosols as cloud condensation nuclei (CCN): A review. *Atmospheric Environment* **2006,** *40* (5), 795-820.

13. Jones, A. M.; Harrison, R. M., The effects of meteorological factors on atmospheric bioaerosol concentrations—a review. *Science of the Total Environment* **2004,** *326* (1-3), 151-180.

14. Cavalli, F.; Facchini, M.; Decesari, S.; Mircea, M.; Emblico, L.; Fuzzi, S.; Ceburnis, D.; Yoon, Y.; O'Dowd, C.; Putaud, J. P., Advances in characterization of size-resolved organic matter in marine aerosol over the North Atlantic. *Journal of Geophysical Research: Atmospheres* **2004,** *109* (D24).

15. Aller, J. Y.; Kuznetsova, M. R.; Jahns, C. J.; Kemp, P. F., The sea surface microlayer as a source of viral and bacterial enrichment in marine aerosols. *Journal of aerosol science* **2005,** *36* (5-6), 801-812.

16. Jaenicke, R., Abundance of cellular material and proteins in the atmosphere. *Science* **2005,** *308* (5718), 73-73.

17. Skeie, R.; Berntsen, T.; Myhre, G.; Pedersen, C. A.; Ström, J.; Gerland, S.; Ogren, J., Black carbon in the atmosphere and snow, from pre-industrial times until present. *Atmospheric Chemistry and Physics* **2011,** *11* (14), 6809-6836.

18. Chughtai, A.; Brooks, M.; Smith, D., Hydration of black carbon. *Journal of Geophysical Research: Atmospheres* **1996,** *101* (D14), 19505-19514.

19. Volkamer, R.; Jimenez, J. L.; San Martini, F.; Dzepina, K.; Zhang, Q.; Salcedo, D.; Molina, L. T.; Worsnop, D. R.; Molina, M. J., Secondary organic aerosol formation from anthropogenic air pollution: Rapid and higher than expected. *Geophysical Research Letters* **2006,** *33* (17).

20. Tsigaridis, K.; Lathiere, J.; Kanakidou, M.; Hauglustaine, D., Naturally driven variability in the global secondary organic aerosol over a decade. *Atmospheric Chemistry and Physics* **2005,** *5* (7), 1891-1904.

21. Chung, S. H.; Seinfeld, J. H., Global distribution and climate forcing of carbonaceous aerosols. *Journal of Geophysical Research: Atmospheres* **2002,** *107* (D19).

22. Hoffmann, T., Final report of the 5th framework programme of the EU project OSOA (origin and formation of secondary organic aerosol). *contract EVK2-CT-1999-00016* **2001**.

23. Decesari, S.; Facchini, M.; Matta, E.; Mircea, M.; Fuzzi, S.; Chughtai, A.; Smith, D., Water soluble organic compounds formed by oxidation of soot. *Atmospheric Environment* **2002,** *36* (11), 1827-1832.

24. Chughtai, A.; Williams, G.; Atteya, M.; Miller, N.; Smith, D., Carbonaceous particle hydration. *Atmospheric Environment* **1999,** *33* (17), 2679-2687.

25. Penner, J. E.; Andreae, M.; Annegarn, H.; Barrie, L.; Feichter, J.; Hegg, D.; Jayaraman, A.; Leaitch, R.; Murphy, D.; Nganga, J., Aerosols, their direct and indirect effects. In *Climate Change 2001: The Scientific Basis. Contribution of Working Group I to the Third Assessment Report of the Intergovernmental Panel on Climate Change*, Cambridge University Press: 2001; pp 289-348.

26. Zender, C. S.; Miller, R.; Tegen, I., Quantifying mineral dust mass budgets: Terminology, constraints, and current estimates. *Eos, Transactions American Geophysical Union* **2004,** *85* (48), 509-512.

27. Andreae, M.; Rosenfeld, D., Aerosol–cloud–precipitation interactions. Part 1. The nature and sources of cloud-active aerosols. *Earth-Science Reviews* **2008,** *89* (1), 13-41.

28. DeMott, P. J.; Prenni, A. J.; Liu, X.; Kreidenweis, S. M.; Petters, M. D.; Twohy, C. H.; Richardson, M.; Eidhammer, T.; Rogers, D., Predicting global atmospheric ice nuclei distributions and their impacts on climate. *Proceedings of the National Academy of Sciences* **2010,** *107* (25), 11217-11222.

29. Krueger, B. J.; Grassian, V. H.; Cowin, J. P.; Laskin, A., Heterogeneous chemistry of individual mineral dust particles from different dust source regions: the importance of particle mineralogy. *Atmospheric Environment* **2004,** *38* (36), 6253-6261.

30. Formenti, P.; Elbert, W.; Maenhaut, W.; Haywood, J.; Osborne, S.; Andreae, M., Inorganic and carbonaceous aerosols during the Southern African Regional Science Initiative (SAFARI 2000) experiment: Chemical characteristics, physical properties, and emission data for smoke from African biomass burning. *Journal of Geophysical Research: Atmospheres* **2003,** *108* (D13).

31. Klaver, A.; Formenti, P.; Caquineau, S.; Chevaillier, S.; Ausset, P.; Calzolai, G.; Osborne, S.; Johnson, B.; Harrison, M.; Dubovik, O., Physico-chemical and optical properties of Sahelian and Saharan mineral dust: in situ measurements during the GERBILS campaign. *Quarterly Journal of the Royal Meteorological Society* **2011,** *137* (658), 1193-1210.

32. Dusek, U.; Frank, G.; Hildebrandt, L.; Curtius, J.; Schneider, J.; Walter, S.; Chand, D.; Drewnick, F.; Hings, S.; Jung, D., Size matters more than chemistry for cloud-nucleating ability of aerosol particles. *Science* **2006,** *312* (5778), 1375-1378.

33. Calvo, A.; Alves, C.; Castro, A.; Pont, V.; Vicente, A.; Fraile, R., Research on aerosol sources and chemical composition: past, current and emerging issues. *Atmospheric Research* **2013,** *120*, 1-28.

34. Ginoux, P.; Garbuzov, D.; Hsu, N. C., Identification of anthropogenic and natural dust sources using Moderate Resolution Imaging Spectroradiometer (MODIS) Deep Blue level 2 data. *Journal of Geophysical Research: Atmospheres* **2010,** *115* (D5).

35. Ryu, S.; Kwon, B.; Kim, Y.; Kim, H.; Chun, K., Characteristics of biomass burning aerosol and its impact on regional air quality in the summer of 2003 at Gwangju, Korea. *Atmospheric research* **2007,** *84* (4), 362-373.

36. Möhler, O.; Büttner, S.; Linke, C.; Schnaiter, M.; Saathoff, H.; Stetzer, O.; Wagner, R.; Krämer, M.; Mangold, A.; Ebert, V., Effect of sulfuric acid coating on heterogeneous ice nucleation by soot aerosol particles. *Journal of Geophysical Research: Atmospheres* **2005,** *110* (D11).

37. Seinfeld, J. H.; Pandis, S. N., *Atmospheric chemistry and physics: from air pollution to climate change*. John Wiley & Sons: 2012.

38. Wang, J.; Hoffmann, A. A.; Park, R. J.; Jacob, D. J.; Martin, S. T., Global distribution of solid and aqueous sulfate aerosols: Effect of the hysteresis of particle phase transitions. *Journal of Geophysical Research: Atmospheres* **2008,** *113* (D11).

39. Stoiber, R. E.; Jepsen, A., Sulfur dioxide contributions to the atmosphere by volcanoes. *Science* **1973,** *182* (4112), 577-578.

40. Derevianko, G. J.; Deutsch, C.; Hall, A., On the relationship between ocean DMS and solar radiation. *Geophysical Research Letters* **2009,** *36* (17).

41. Smith, S. J.; Aardenne, J. v.; Klimont, Z.; Andres, R. J.; Volke, A.; Delgado Arias, S., Anthropogenic sulfur dioxide emissions: 1850–2005. *Atmospheric Chemistry and Physics* **2011,** *11* (3), 1101-1116.

42. Pathak, R. K.; Wu, W. S.; Wang, T., Summertime PM 2.5 ionic species in four major cities of China: nitrate formation in an ammonia-deficient atmosphere. *Atmospheric Chemistry and Physics* **2009,** *9* (5), 1711-1722.

43. Schaap, M.; Spindler, G.; Schulz, M.; Acker, K.; Maenhaut, W.; Berner, A.; Wieprecht, W.; Streit, N.; Müller, K.; Brüggemann, E., Artefacts in the sampling of nitrate studied in the "INTERCOMP" campaigns of EUROTRAC-AEROSOL. *Atmospheric Environment* **2004,** *38* (38), 6487-6496.

44. Pinder, R. W.; Davidson, E. A.; Goodale, C. L.; Greaver, T. L.; Herrick, J. D.; Liu, L., Climate change impacts of US reactive nitrogen. *Proceedings of the National Academy of Sciences* **2012,** *109* (20), 7671-7675.

45. McCubbin, D. R.; Apelberg, B. J.; Roe, S.; Divita, F., Livestock ammonia management and particulate-related health benefits. ACS Publications: 2002.

46. Hinds, W. C., *Aerosol technology: properties, behavior, and measurement of airborne particles*. 2, illustrated ed.; John Wiley & Sons, Inc.: New York, NY, 1999; p 483.

47. Andronache, C., Estimated variability of below-cloud aerosol removal by rainfall for observed aerosol size distributions. *Atmospheric Chemistry and Physics* **2003,** *3* (1), 131-143.

48. Mishima, O.; Stanley, H. E., The relationship between liquid, supercooled and glassy water. *Nature* **1998,** *396* (6709), 329.

49. Kalikmanov, V. I., Classical nucleation theory. In *Nucleation theory*, Springer: 2013; pp 17-41.

50. Debenedetti, P. G., *Metastable liquids: concepts and principles*. Princeton University Press: 1996.

51. Cantrell, W.; Heymsfield, A., Production of ice in tropospheric clouds: A review. *Bulletin of the American Meteorological Society* **2005,** *86* (6), 795-807.

52. Sassen, K.; Dodd, G. C., Homogeneous nucleation rate for highly supercooled cirrus cloud droplets. *Journal of the atmospheric sciences* **1988,** *45* (8), 1357-1369.

53. Koop, T., et al., Water activity as the determinant for homogeneous ice nucleation in aqueous solutions. *Nature* **2000,** *406* (6796), 611-614.

54. Sanz, E.; Vega, C.; Espinosa, J.; Caballero-Bernal, R.; Abascal, J.; Valeriani, C., Homogeneous ice nucleation at moderate supercooling from molecular simulation. *Journal of the American Chemical Society* **2013,** *135* (40), 15008-15017.

55. Rosenfeld, D.; Woodley, W. L., Deep convective clouds with sustained supercooled liquid water down to-37.5 C. *Nature* **2000,** *405* (6785), 440.

56. Pruppacher, H. R.; Klett, J. D.; Wang, P. K., Microphysics of clouds and precipitation. Taylor & Francis: 1998.

57. Fletcher, N. H., *The physics of rainclouds*. Cambridge University Press: 2011.

58. Ragone, D. V., Thermodynamics of Materials, Volume 1. *Thermodynamics of Materials, Volume 1, by David V. Ragone, pp. 336. ISBN 0-471-30885-4. Wiley-VCH, October 1994.* **1994**, 336.

59. Vali, G., Nucleation terminology. *Bulletin of the American Meteorological Society* **1985,** *66* (11), 1426-1427.

60. Bigg, E., The formation of atmospheric ice crystals by the freezing of droplets. *Quarterly Journal of the Royal Meteorological Society* **1953,** *79* (342), 510-519.

61. Levine, J., Statistical explanation of spontaneous freezing of water droplets. **1950**.

62. Vali, G., Repeatability and randomness in heterogeneous freezing nucleation. *Atmospheric Chemistry and Physics* **2008,** *8* (16), 5017-5031.

63. Chen, J.-P., et al., Parameterizing ice nucleation rates using contact angle and activation energy derived from laboratory data. *Atmos. Chem. Phys.* **2008,** *8*, 7431–7449.

64. Niedermeier, D.; Shaw, R.; Hartmann, S.; Wex, H.; Clauss, T.; Voigtländer, J.; Stratmann, F., Heterogeneous ice nucleation: exploring the transition from stochastic to singular freezing behavior. *Atmospheric Chemistry and Physics* **2011,** *11* (16), 8767-8775.

65. Vali, G.; Stansbury, E., Time-dependent characteristics of the heterogeneous nucleation of ice. *Canadian Journal of Physics* **1966,** *44* (3), 477-502.

66. Vali, G., Quantitative evaluation of experimental results on the heterogeneous freezing nucleation of supercooled liquids. *Journal of the atmospheric sciences* **1971,** *28,* 402-409.

67. Murray, B.; Broadley, S.; Wilson, T.; Atkinson, J.; Wills, R., Heterogeneous freezing of water droplets containing kaolinite particles. *Atmospheric Chemistry and Physics* **2011,** *11* (9), 4191-4207.

68. Diehl, K.; Debertshäuser, M.; Eppers, O.; Schmithüsen, H.; Mitra, S.; Borrmann, S., Particle surface area dependence of mineral dust in immersion freezing mode: investigations with freely suspended drops in an acoustic levitator and a vertical wind tunnel. *Atmospheric Chemistry and Physics* **2014,** *14* (22), 12343-12355.

69. Hiranuma, N.; Augustin-Bauditz, S.; Bingemer, H.; Budke, C.; Curtius, J.; Danielczok, A.; Diehl, K.; Dreischmeier, K.; Ebert, M.; Frank, F., A comprehensive laboratory study on the immersion freezing behavior of illite NX particles: a comparison of 17 ice nucleation measurement techniques. *Atmospheric Chemistry and Physics* **2015,** *15* (5), 2489-2518.

70. Marcolli, C., Deposition nucleation viewed as homogeneous or immersion freezing in pores and cavities. *Atmos. Chem. Phys. Discuss.* **2013,** *13* (6), 16367-16456.

71. Simmel, M.; Heinrich, H.; Diehl, K., Ice Initiation for Various Ice Nuclei Types and its Influence on Precipitation Formation in Convective Clouds. In *Nucleation and Atmospheric Aerosols*, O'Dowd, C.; Wagner, P., Eds. Springer Netherlands: 2007; pp 427-431.

72. Diehl, K.; Wurzler, S., Heterogeneous drop freezing in the immersion mode: Model calculations considering soluble and insoluble particles in the drops. *Journal of the atmospheric sciences* **2004,** *61* (16), 2063-2072.

73. Atkinson, J. D.; Murray, B. J.; Woodhouse, M. T.; Whale, T. F.; Baustian, K. J.; Carslaw, K. S.; Dobbie, S.; O'Sullivan, D.; Malkin, T. L., The importance of feldspar for ice nucleation by mineral dust in mixed-phase clouds. *Nature* **2013,** *498* (7454), 355.

74. Möhler, O.; Linke, C.; Saathoff, H.; Schnaiter, M.; Wagner, R.; Mangold, A.; Krämer, M.; Schurath, U., Ice nucleation on flame soot aerosol of different organic carbon content. *Meteorologische Zeitschrift* **2005,** *14* (4), 477-484.

75. Crawford, I.; Möhler, O.; Schnaiter, M.; Saathoff, H.; Liu, D.; McMeeking, G.; Linke, C.; Flynn, M.; Bower, K.; Connolly, P., Studies of propane flame soot acting as heterogeneous ice nuclei in conjunction with single particle soot photometer measurements. *Atmospheric Chemistry and Physics* **2011,** *11* (18), 9549-9561.

76. Lindow, S. E.; Arny, D. C.; Upper, C. D., Bacterial ice nucleation: a factor in frost injury to plants. *Plant physiology* **1982,** *70* (4), 1084-1089.

77. Lindow, S., The role of bacterial ice nucleation in frost injury to plants. *Annual review of phytopathology* **1983,** *21* (1), 363-384.

78. Kawahara, H., The structures and functions of ice crystal-controlling proteins from bacteria. *Journal of bioscience and bioengineering* **2002,** *94* (6), 492-496.

79. O'Sullivan, D.; Murray, B. J.; Ross, J. F.; Webb, M. E., The adsorption of fungal ice-nucleating proteins on mineral dusts: a terrestrial reservoir of atmospheric ice-nucleating particles. *Atmospheric Chemistry and Physics* **2016,** *16* (12), 7879-7887.

80. Després, V.; Huffman, J. A.; Burrows, S. M.; Hoose, C.; Safatov, A.; Buryak, G.; Fröhlich-Nowoisky, J.; Elbert, W.; Andreae, M.; Pöschl, U., Primary biological aerosol particles in the atmosphere: a review. *Tellus B: Chemical and Physical Meteorology* **2012,** *64* (1), 15598.

81. Möhler, O.; Benz, S.; Saathoff, H.; Schnaiter, M.; Wagner, R.; Schneider, J.; Walter, S.; Ebert, V.; Wagner, S., The effect of organic coating on the heterogeneous ice nucleation efficiency of mineral dust aerosols. *Environmental Research Letters* **2008,** *3* (2), 025007.

82. Petters, M.; Kreidenweis, S., A single parameter representation of hygroscopic growth and cloud condensation nucleus activity. *Atmospheric Chemistry and Physics* **2007,** *7* (8), 1961-1971.

83. Novakov, T.; Corrigan, C., Cloud condensation nucleus activity of the organic component of biomass smoke particles. *Geophysical Research Letters* **1996,** *23* (16), 2141-2144.

84. Kotzick, R.; Niessner, R., The effects of aging processes on critical supersaturation ratios of ultrafine carbon aerosols. *Atmospheric Environment* **1999,** *33* (17), 2669-2677.

85. DeMott, P. J., An exploratory study of ice nucleation by soot aerosols. *Journal of applied meteorology* **1990,** *29* (10), 1072-1079.

86. Diehl, K.; Mitra, S., A laboratory study of the effects of a kerosene-burner exhaust on ice nucleation and the evaporation rate of ice crystals. *Atmospheric Environment* **1998,** *32* (18), 3145-3151.

87. Diehl, K.; Matthias-Maser, S.; Jaenicke, R.; Mitra, S., The ice nucleating ability of pollen:: Part II. Laboratory studies in immersion and contact freezing modes. *Atmospheric Research* **2002,** *61* (2), 125-133.

88. Diehl, K.; Quick, C.; Matthias-Maser, S.; Mitra, S.; Jaenicke, R., The ice nucleating ability of pollen: Part I: Laboratory studies in deposition and condensation freezing modes. *Atmospheric Research* **2001,** *58* (2), 75-87.

89. Levin, Z.; Yankofsky, S. A., Contact versus immersion freezing of freely suspended droplets by bacterial ice nuclei. *Journal of climate and applied meteorology* **1983,** *22* (11), 1964-1966.

90. Maki, L. R.; Galyan, E. L.; Chang-Chien, M.-M.; Caldwell, D. R., Ice nucleation induced by Pseudomonas syringae. *Applied microbiology* **1974,** *28* (3), 456-459.

91. Kozloff, L.; Schofield, M.; Lute, M., Ice nucleating activity of Pseudomonas syringae and Erwinia herbicola. *Journal of bacteriology* **1983,** *153* (1), 222-231.

92. Rogers, J.; Stall, R.; Burke, M., Low-temperature conditioning of the ice nucleation active bacterium, Erwinia herbicola. *Cryobiology* **1987,** *24* (3), 270-279.

93. Zimmermann, F.; Weinbruch, S.; Schütz, L.; Hofmann, H.; Ebert, M.; Kandler, K.; Worringen, A., Ice nucleation properties of the most abundant mineral dust phases. *Journal of Geophysical Research: Atmospheres* **2008,** *113* (D23).

94. Pitter, R.; Pruppacher, H., A wind tunnel investigation of freezing of small water drops falling at terminal velocity in air. *Quarterly Journal of the Royal Meteorological Society* **1973,** *99* (421), 540-550.

95. Salam, A.; Lohmann, U.; Crenna, B.; Lesins, G.; Klages, P.; Rogers, D.; Irani, R.; MacGillivray, A.; Coffin, M., Ice nucleation studies of mineral dust particles with a new continuous flow diffusion chamber. *Aerosol Science and Technology* **2006,** *40* (2), 134-143.

96. Ettner, M.; Mitra, S.; Borrmann, S., Heterogeneous freezing of single sulfuric acid solution droplets: laboratory experiments utilizing an acoustic levitator. *Atmospheric Chemistry and Physics* **2004,** *4* (7), 1925-1932.

97. Schaller, R.; Fukuta, N., Ice nucleation by aerosol particles: Experimental studies using a wedge-shaped ice thermal diffusion chamber. *Journal of the atmospheric sciences* **1979,** *36* (9), 1788-1802.

98. Zimmermann, F.; Ebert, M.; Worringen, A.; Schütz, L.; Weinbruch, S., Environmental scanning electron microscopy (ESEM) as a new technique to determine the ice nucleation capability of individual atmospheric aerosol particles. *Atmospheric Environment* **2007,** *41* (37), 8219-8227.

99. Shaw, R. A.; Durant, A. J.; Mi, Y., Heterogeneous surface crystallization observed in undercooled water. *The Journal of Physical Chemistry B* **2005,** *109* (20), 9865-9868.

100. Welti, A.; Lüönd, F.; Stetzer, O.; Lohmann, U., Influence of particle size on the ice nucleating ability of mineral dusts. *Atmospheric Chemistry and Physics* **2009,** *9* (18), 6705-6715.

101. Raes, F.; Van Dingenen, R.; Vignati, E.; Wilson, J.; Putaud, J.-P.; Seinfeld, J. H.; Adams, P., Formation and cycling of aerosols in the global troposphere. *Atmospheric environment* **2000,** *34* (25), 4215-4240.

102. Slezakova, K.; Morais, S.; do Carmo Pereira, M., Atmospheric Nanoparticles and Their Impacts on Public Health. **2013**.

103. McMurry, P. H., A review of atmospheric aerosol measurements. *Atmospheric Environment* **2000,** *34* (12-14), 1959-1999.

104. Domingos, R. F.; Baalousha, M. A.; Ju-Nam, Y.; Reid, M. M.; Tufenkji, N.; Lead, J. R.; Leppard, G. G.; Wilkinson, K. J., Characterizing manufactured nanoparticles in the environment: multimethod determination of particle sizes. *Environmental science & technology* **2009,** *43* (19), 7277-7284.

105. Leppard, G. G., Nanoparticles in the environment as revealed by transmission electron microscopy: detection, characterisation and activities. *Current Nanoscience* **2008,** *4* (3), 278-301.

106. Kasparian, J.; Frejafon, E.; Rambaldi, P.; Yu, J.; Vezin, B.; Wolf, J.; Ritter, P.; Viscardi, P., Characterization of urban aerosols using SEM-microscopy, X-ray analysis and Lidar measurements. *Atmospheric environment* **1998,** *32* (17), 2957-2967.

107. Friedbacher, G.; Grasserbauer, M.; Meslmani, Y.; Klaus, N.; Higatsberger, M. J., Investigation of environmental aerosol by atomic force microscopy. *Analytical Chemistry* **1995,** *67* (10), 1749-1754.
108. Hinds, W.; Reist, P., Aerosol measurement by laser doppler spectroscopy—I. Theory and experimental results for aerosols homogeneous. *Journal of Aerosol Science* **1972,** *3* (6), 501-514.
109. Starchev, K.; Wilkinson, K.; Buffle, J., Application of fluorescence correlation spectroscopy to the study of environmental systems. *Fluorescence Correlation Spectroscopy: Theory and Applications* **2000**, 251-275.
110. Filipe, V.; Hawe, A.; Jiskoot, W., Critical evaluation of Nanoparticle Tracking Analysis (NTA) by NanoSight for the measurement of nanoparticles and protein aggregates. *Pharmaceutical research* **2010,** *27* (5), 796-810.
111. Wang, S. C.; Flagan, R. C., Scanning electrical mobility spectrometer. *Aerosol Science and Technology* **1990,** *13* (2), 230-240.
112. Marple, V. A.; Willeke, K., Impactor design. *Atmospheric Environment (1967)* **1976,** *10* (10), 891-896.
113. Marple, V. A.; Rubow, K. L.; Behm, S. M., A microorifice uniform deposit impactor (MOUDI): Description, calibration, and use. *Aerosol Science and Technology* **1991,** *14* (4), 434-446.
114. Wexler, A. S.; Johnston, M. V., What have we learned from highly time-resolved measurements during EPA's Supersites Program and related studies? *Journal of the Air & Waste Management Association* **2008,** *58* (2), 303-319.
115. Sullivan, R. C.; Prather, K. A., Recent advances in our understanding of atmospheric chemistry and climate made possible by on-line aerosol analysis instrumentation. *Analytical Chemistry* **2005,** *77* (12), 3861-3886.
116. Solomon, P. A.; Sioutas, C., Continuous and semicontinuous monitoring techniques for particulate matter mass and chemical components: a synthesis of findings from EPA's particulate matter supersites program and related studies. *Journal of the Air & Waste Management Association* **2008,** *58* (2), 164-195.
117. Chow, J. C., Measurement methods to determine compliance with ambient air quality standards for suspended particles. *Journal of the Air & Waste Management Association* **1995,** *45* (5), 320-382.
118. Chow, J. C.; Doraiswamy, P.; Watson, J. G.; Chen, L.-W. A.; Ho, S. S. H.; Sodeman, D. A., Advances in integrated and continuous measurements for particle mass and chemical composition. *Journal of the Air & Waste Management Association* **2008,** *58* (2), 141-163.
119. Simon, P. K.; Dasgupta, P. K., Continuous automated measurement of gaseous nitrous and nitric acids and particulate nitrite and nitrate. *Environmental science & technology* **1995,** *29* (6), 1534-1541.
120. Weber, R.; Orsini, D.; Daun, Y.; Lee, Y.-N.; Klotz, P.; Brechtel, F., A particle-into-liquid collector for rapid measurement of aerosol bulk chemical composition. *Aerosol Science & Technology* **2001,** *35* (3), 718-727.
121. Ho, S. S. H.; Yu, J. Z., Determination of airborne carbonyls: Comparison of a thermal desorption/GC method with the standard DNPH/HPLC method. *Environmental science & technology* **2004,** *38* (3), 862-870.
122. Ho, S. S. H.; Yu, J. Z., In-injection port thermal desorption and subsequent gas chromatography–mass spectrometric analysis of polycyclic aromatic hydrocarbons and n-alkanes in atmospheric aerosol samples. *Journal of Chromatography A* **2004,** *1059* (1-2), 121-129.

123. Jayne, J. T.; Leard, D. C.; Zhang, X.; Davidovits, P.; Smith, K. A.; Kolb, C. E.; Worsnop, D. R., Development of an aerosol mass spectrometer for size and composition analysis of submicron particles. *Aerosol Science & Technology* **2000,** *33* (1-2), 49-70.
124. Harris, W. A.; Reilly, P. T.; Whitten, W. B., Aerosol MALDI of peptides and proteins in an ion trap mass spectrometer: Trapping, resolution and signal-to-noise. *International Journal of Mass Spectrometry* **2006,** *258* (1-3), 113-119.
125. Georgakopoulos, D.; Després, V.; Fröhlich-Nowoisky, J.; Psenner, R.; Ariya, P.; Pósfai, M.; Ahern, H.; Moffett, B.; Hill, T., Microbiology and atmospheric processes: biological, physical and chemical characterization of aerosol particles. *Biogeosciences* **2009,** *6* (4), 721-737.
126. Warren, S. G.; Wiscombe, W. J., A model for the spectral albedo of snow. II: Snow containing atmospheric aerosols. *Journal of the Atmospheric Sciences* **1980,** *37* (12), 2734-2745.

Chapter 2

2. Novel Aerosol Analysis Approach for Characterization of Nanoparticulate Matter in Snow

My contributions to this paper were the following:

Yevgen Nazarenko and I developed the technique in this paper. We decided to develop this technique because we needed something to study particles in melted snow with minimal perturbation of their original state. We believed aerosolization would be a good way to minimize aggregation of particles. I used this technique to obtain the particle size distribution of arctic and subarctic snow samples. Arctic samples come from remote locations where particle concentrations are low, but concentrations of dissolved material like salts are high. Due to the nature of the technique (where drying is used to remove aerosolized water), dissolved materials become an interference that can enlarge the size of particles. I used dialysis to minimize interference from salts and other dissolved materials. I evaluated the efficiency of dialysis and the technique itself with standard solutions of common components found in snow at concentration relevant to snow studies. The developed technique was later used in the other research projects of this study for the acquisition of particle size distribution of snow samples.

The paper is reproduced in this thesis with the permission of Springer.

Manuscript published in Environmental Science and Pollution Research 24:4480–4493, February 2017

Novel Aerosol Analysis Approach for Characterization of Nanoparticulate Matter in Snow

Yevgen Nazarenko[1] & Rodrigo B. Rangel-Alvarado[2], Gregor Kos[1], Uday Kurien[1], and Parisa A. Ariya*[1,2]

[1]Department of Atmospheric and Oceanic Sciences, and [2]Department of Chemistry, McGill University, 801 Sherbrooke St. W., Montreal, QC H3A 2K6, Canada

*Corresponding author

R.B. Rangel-Alvarado and Y. Nazarenko contributed equally to this work

Abstract. Tropospheric aerosols are involved in several key atmospheric processes: from ice nucleation, cloud formation, and precipitation to weather and climate. The impact of aerosols on these atmospheric processes depends on the chemical and physical characteristics of aerosol particles, and these characteristics are still largely uncertain. In this study, we developed a system for processing and aerosolization of melted snow in particle-free air, coupled with a real-time measurement of aerosol size distributions. The newly developed technique involves bringing snow-borne particles into an airborne state, which enables application of high-resolution aerosol analysis and sampling techniques. This novel analytical approach was compared to a variety of complementary existing analytical methods as applied for characterization of snow samples from remote sites in Alert (Canada) and Barrow (USA), as well as urban Montreal (Canada). The dry aerosol measurements indicated a higher abundance of particles of all sizes, and the 30 nm size dominated in aerosol size distributions for the Montreal samples, closely followed by Barrow, with about 30% fewer 30 nm particles, and about four times lower 30 nm particle abundance in Alert samples, where 15 nm particles were most abundant instead. The aerosolization technique, used together with nanoparticle tracking analysis and electron microscopy, allowed measurement of a wide size range of snow-borne particles in various environmental snow samples. Here, we discuss the application of the new technique to achieve better physicochemical understanding of atmospheric and snow processes. The results showed high sensitivity and reduction of particle aggregation, as well as the ability to measure a high-resolution snow-borne particle size distribution, including nanoparticulate matter in the range of 10 to 100 nm.

Keywords. Particles in snow, Nanoparticulate, Atmospheric aerosols, Aerosol, Ice nucleation, Ice nuclei, Nanoparticles, Ultrafine particles, Aerosolization, Cloud condensation nuclei.

2.1. Introduction

Cloud formation processes play a key role in climate change because water vapor and cloud droplets absorb and emit infrared light, thereby influencing the global radiation budget and water cycle.[1] Consequently, nucleation of water droplets and ice crystals in the atmosphere is a focus of a large body of research.[2-4] Pure water droplets that contain no particulate matter do not form ice crystals at temperatures above −38 °C. Without ice nucleating particles in water droplets, temperature has to be lower than −38 °C for water to freeze by homogeneous ice nucleation,[5] which occurs when water starts crystallizing on its own by self-assembly of water molecules.[6] For ice to form in the atmosphere at temperatures warmer than −38 °C, airborne particles must be present to initiate heterogeneous ice nucleation, during which ice crystallization starts on a surface. The airborne particles providing their surfaces for initiation of ice crystallization are called ice nuclei (IN) and can be of various sizes and composed of diverse materials.[7-8] Similarly, water droplets rarely form at the conditions found in the atmosphere. This process requires water vapor supersaturation of several hundred percent. Instead, atmospheric water droplets usually form heterogeneously in the presence of particles called cloud condensation nuclei (CCN).[9] One of the most common IN and CCN in the atmosphere is mineral dust,[10] which originates in locations such as the Sahara Desert. Mineral dust is considered one of the most efficient ice forming nuclei, partly due to its abundance in global atmospheric aerosols. Certain marine-, vegetation-, and soil-derived aerosols, bacteria, fungi, and their fragments also efficiently nucleate ice.[11-19] Recently, research pointed to ice nucleating activity of nanosized organic compounds, possibly peptides, as well as nanosized inorganic compounds such as metal oxides.[20] In addition to the above categories of ice nuclei incorporated in the snow crystals, snowpack contains pollution particles.[21-26] These include aerosols from engine exhaust,[27-28] power plants,[29] mining activities,[30] and other pollution sources. Characterization of particles in snow is a crucial element of research to understand the sources and properties of particles in the atmosphere and, consequently, their effects on weather, climate, and pollution.[21, 31] The physicochemical characterization and quantification of snow-borne particles, especially nanometric material, are technically challenging due to instrumental limitations of traditionally used analytical techniques for counting, sizing, and physicochemical analysis. Specifically, electron microscopy techniques are expensive and time-consuming and require staining with carcinogenic uranium-based compounds to detect most organic particles, which are otherwise nearly electron-transparent. Organic particles are also unstable under the electron beam.[32] Nanoparticle tracking analysis (NTA) is expected to have a progressively reducing efficiency of detection of particles, particularly smaller than 50–100 nm, as light scattering efficiency of smaller particles declines.[33] Particle detection efficiency also fluctuates depending on their physicochemical nature, which influences how efficiently they scatter light. Dynamic light scattering is biased towards larger sizes and cannot analyze melted snow samples in original state, requiring pre-concentration. This leads to a challenge in determining the role of different types and sizes of particles found in snow matrices using the traditional particle analysis techniques. Another problem that accompanies sample preparation for traditional analytical techniques that require dry or pre-concentrated samples is agglomeration of particulate matter. Pre-concentration, if needed to improve detection,[34] can itself alter the original particles that are being analyzed.

This study presents a first-of-its-kind systematic characterization of nanoparticles in snow, which involved the development of a new aerosol-mediated characterization technique. The purpose of this technique is to analyze particles in snow independent of their ice-nucleating abilities. We also tested the applicability of existing complementary analytical techniques to environmental snow samples obtained from High Arctic and urban locations. New types of characterization data were obtained for snow samples from Alert, Nunavut in Canada; Barrow, Alaska in the USA; and from the urban site of Montreal, Quebec, Canada.

2.2. Materials and Methods

2.2.1. Sampling and Storage

We collected samples at several sites in Alaska, USA (2009) and Nunavut (2006) and Montreal, Quebec (in 2006 and 2014), Canada. Samples from Alaska were collected in Barrow (71.31° N, 156.6° W), approximately 400 m to the southeast of the Barrow Arctic Research Center (BARC). Snow originated from a relatively pristine snow region in a designated clean air sector, as part of the 2009 international Ocean-Atmosphere-Sea Ice-Snowpack (OASIS) campaign.

Samples obtained from Alert, Nunavut (74.70° N, 95.05° W) were collected at the northern tip of Ellesmere Island at a pristine site in the vicinity of the Environment Canada Global Atmosphere Watch (GAW) station in the High Arctic in May and June 2006. Local contamination from a military base was a generator, an incinerator, and vehicle traffic. Sampling was performed upwind approximately 6.5 km away from the base on a flat plateau with restricted vehicle traffic.

Arctic snow collection and storage have previously been described in detail elsewhere.[21, 23, 35-38] Arctic snow from the top 3 cm of the snowpack was collected into 950-mL amber glass jars (Daniels Scientific, Charleston, SC, USA), with PTFE-lined lids, pre-cleaned as previously described.[20] A sterile HDPE spoon was used to transfer snow (Bel-Art Products, Inc., Wayne, NJ, USA). The Barrow (Alaska) and Alert (Nunavut) samples were kept in a −20 °C walk-in freezer until shipped to Montreal by plane in commercial coolers filled with ice packs (Coleman Company, Inc., Wichita, KS, USA) and snow. The snow samples did not warm up above −5 °C before reaching the laboratory at McGill University in Montreal, QC, Canada where they were immediately transferred to a −20 °C freezer.

Fresh snow samples from Montreal were collected at two sites. The first location was near McGill University downtown campus in Mont-Royal Park, away from any trails and vehicular or pedestrian traffic at −11 °C in February of 2006. Snow collection occurred in a wooded area of the abovementioned park (45° 35′ N, 70° 52′ W) after a heavy snowfall. Montreal receives regular fresh snow precipitation approximately 5 months a year. The second set of snow samples was obtained during a light snowfall, also in Mont-Royal Park (45° 30′ 45″ N, 73° 35′ 15″ W) immediately following a heavy nightly snowfall. Collection time was between 1 and 3 p.m. on March 23, 2014. Meteorological conditions were as follows: air temperature between 0 and −1 °C, light snow, with wind NNE ~43 km/h, UV index of 2 (low), RH 87%, atmospheric air pressure

1014.4 mb, and visibility of 4 km (The Weather Channel, LLC 2014). The collection site was not subject to human or pet traffic. We also avoided collection in the vicinity of freshly fallen vegetation and animal tracks or droppings. Following collection of snow, we brought the snow samples in the pre-cleaned jars, certified according to EPA standards (U.S.EPA 1992), to the laboratory in a wheeled cooler. The distance between the sampling location and the laboratory was around 2 km. Upon delivery to the laboratory, the jars were immediately placed in a freezer. The 2006 samples were kept in a −20 °C freezer and the recent 2014 samples in a −39 °C freezer. Our above-referenced studies confirmed that these storage conditions maintain snow in near-pristine condition. The elapsed time between collection and precipitation was less than 2 hours in all locations.

2.2.2. Processing of Melted Snow

After transfer from the original storage containers, snow samples were stored in sterile Falcon™ 50-mL Conical Centrifuge Tubes (Corning Life Sciences, Inc.) at −39 °C until processed. Processing of melted snow by filtration and/or dialysis was intended to determine contribution of different particle size fractions to chemical composition of particulate matter in snow (total organic carbon) and explore influence of dissolved matter on measurement results. The samples were allowed to melt at room temperature (23 °C) and then a fraction of each sample filtered through a Millex syringe filter with a hydrophilic polyvinylidene fluoride (PVDF) membrane, 0.22 µm pore size, part no. SLVV033RS (EMD Millipore Corp., Billerica, MA, USA). Another fraction of each sample was dialyzed using a Standard Grade Regenerated Cellulose membrane (Spectrum Laboratories, Inc., Rancho Dominguez, CA, USA) with a molecular weight cutoff of 5–8 kDa. The filled membrane tubes were dialyzed at room temperature (23 °C) in a bath of ultrapure water (EMD Millipore Corp.) with stirring for 5 days. The water bath was replaced once daily.

2.2.3. Chemical Analysis of Melted Snow

Unprocessed and filtered melted snow samples were analyzed for total organic carbon (TOC) and by ion chromatography (IC) using standard automatic procedures on an Aurora 1030W TOC Analyzer (O.I. Corp., College Station, TX) and a Dionex ICS-500 ion chromatograph. The methodologies of these analyses are described in detail in Supplementary Information.

2.2.4. Nanoparticle Tracking Analysis of Melted Snow

Unprocessed, filtered, and/or dialyzed snow samples were analyzed on a NanoSight NS500 instrument (Malvern Instruments, Ltd., Malvern, Worcestershire, UK). The principle of operation of the instrument lies in using a microscope equipped with a CCD camera to digitally film scattered light from individual particles in liquid samples illuminated by a 532 nm laser beam. A ×20 magnification was used for the microscope. The camera was set to take 1 min videos operating at 30 frames per second. The NanoSight NTA 3.0 Software was then used to process the videos using the Stokes-Einstein equation for calculating the hydrodynamic size of each particle individually. The instrument's specifications mention the theoretical range of detectable particle size from 10 to 2000 nm. However, the particle and liquid properties likely limited this range in our experiments on both ends of the operating particle size range. Two samples from each location were analyzed. Each sample was analyzed 10 times using a new subsample and these measurements were averaged. The NTA technique has gained popularity in the last few years[34, 39] but has not been used or optimized for snow samples.

2.2.5. Generation of Melted Snow Aerosol

The central novelty of this work is the aerosol-mediated snow analysis technique. The system for aerosolization of melted snow we built is diagramed in Figure 2.1.

Unprocessed, filtered, and/or dialyzed snow samples were aerosolized in the system. The setup consisted of three modules for (1) primary liquid droplet aerosol generation, (2) aerosol drying, and (3) dry aerosol stream analysis and collection. All the elements where aerosol transport occurred were positioned in a straight horizontal line to minimize aerosol particle losses due to impaction. Note, however, that the diagram shows these elements compactly. The elements of the setup were connected with electrically conductive silicone tubing (TSI, Inc., Shoreview, MN) to minimize electrostatic aerosol particle losses.

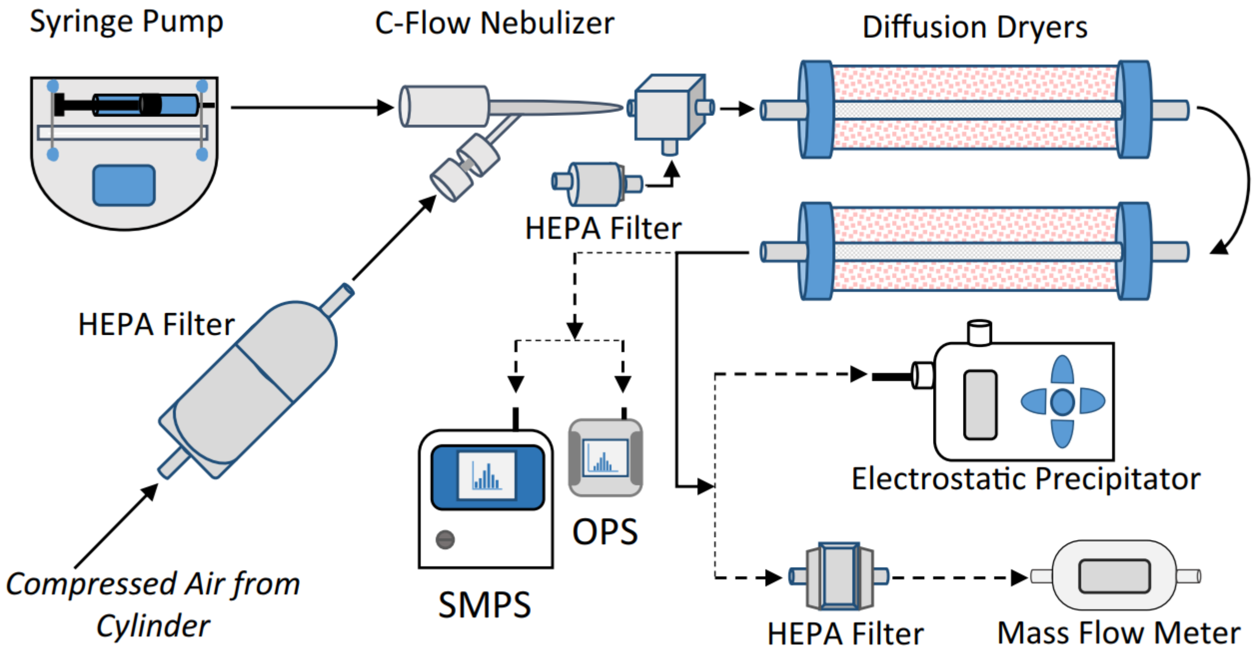

Figure 2.1 Setup for collection of samples for electron microscopy through the aerosol phase. HEPA Filter high-efficiency particulate air filter, SMPS scanning mobility particle sizer, OPS optical particle sizer.

The melted snow samples were drawn into an autoclaved all-glass syringe that was installed into a syringe pump (GenieTouch™, Kent Scientific Corp., Torrington, CT, USA). The syringe pump quantitatively fed the melted snow into an autoclaved C-Flow 700d PFA Nebulizer (Savillex Corporation, Minnetonka, MN, USA). The nebulizer was connected to the syringe with autoclaved low-volatile grade, platinum-cured silicone tubing. The liquid feed rate to the nebulizer was set at

500 μL/min. Dry air from a cylinder was passed to the nebulizer at a pressure of 60 psi through a large high-efficiency particulate air (HEPA) filter, Whatman™ HEPA -Cap 150 (Little Chal font, Buckinghamshire, UK). This resulted in the output air flow rate from the nebulizer of 0.9 SL/min (SL: liters at standard temperature and pressure, 273.15 K, 100 kPa). We checked the output airflow rate with a mass flow meter, model 4040 (TSI Inc.). The mass flow meter was equipped with another HEPA filter to prevent instrument contamination. Operation of the large HEPA filter in the nebulizer air supply line, at a flow rate substantially below nominal level, allowed obtaining clean air stream that was free of detectable particles. This step eliminated contamination with aerosol particles found in the air from the compressed air cylinder.

The aerosol stream containing aqueous droplets of melted snow particles was introduced into an in-housebuilt mixing element. The mixing element was a steel box with internal dimensions of 5 × 4 × 4 cm and three ports in its three facets. The mixing element too had a HEPA filter connected to it. This HEPA filter was open to the atmosphere, which allowed makeup air to be drawn into the mixing element for dilution of the sample stream to reach the total flow rate, drawn by the measurement instruments (1.75 L/min). The diluted aerosol then passed to an in-house-made double diffusion dryer. In a typical diffusion dryer, the aerosol stream travels through a tubular diffusion screen (wire mesh tube) surrounded by a desiccant (silica gel). Relative humidity (RH) inside the diffusion screen tubes is reduced due to diffusion of water molecules into the desiccant-filled space, leading to water evaporation from the aerosol droplets. The process of aerosol drying in the diffusion dryer removes water from the droplets generated by the atomizer, leaving any nonvolatile particles dry and solutes precipitated. Each of the two diffusion dryers consisted of two transparent polycarbonate cylindrical silica gel-filled capsules, 16 in. long and 3 in. in diameter. The tubular diffusion screens inside the diffusion dryers were 0.5 in. in diameter.

Temperature and RH was checked in the output aerosol stream at the exit from the double diffusion dryer. For these measurements, we used an RH/temperature (RH/T) probe, model PROBE-SHT2X (Aginova, Inc., Freehold, NJ, USA) with a data transmitter/logger, and model iCelsius Wireless IPROBE-3000-0001 (Aginova, Inc.). During snow aerosolization, the RH and temperature of the aerosol stream just before electrostatic sampling were routinely measured at 2.2–2.7% and 22–23 °C, respectively.

2.2.6. Collection of Samples for Electron Microscopy

Another novel aspect of this work is aerosol-mediated preparation of snow samples for electron microscopy. Several alternative methods of sample preparation, technically applicable to analysis of snow, such as drying a drop of liquid sample directly on an electron microscopy grid, have been described by Domingos et al.[34] In our approach, the dry aerosol stream generated from processed or unprocessed melted snow was sampled directly into an electrostatic precipitator, ESPnano Model 100 (ESPnano, Spokane, WA, USA), at the exit from the double diffusion dryer at an aspiration inlet flow rate of 0.1 L/min. The excessive aerosol was released into the atmosphere without restriction. The electrostatic precipitator uses a corona discharge to simultaneously charge and collect aerosol particles onto media such as EM grids. We operated the instrument at 5 kV and 100 s sampling duration with a 15 s purge before sampling. The aerosolization module was operated for at least 30 s before the start of each cycle of sampling with the electrostatic precipitator to ensure a stable particle size distribution throughout sampling.

For electrostatic sample collection, we used FCF200-CuEB grids (Formvar carbon film on 200-mesh copper extra thick option B grids, 25–50 nm Formvar and 3–4 nm carbon). This choice of grids was made to ensure a mechanically robust conductive surface for collection of fast-moving charged particles. The grids were loaded and unloaded from the electrostatic precipitatorcompatible sample holder keys inside a Class II Biosafety Cabinet (NuAire, Inc., Plymouth, MN, USA) to prevent potential contamination with airborne particles found in ambient air.

2.2.7. Transmission Electron Microscopy

Analysis of the EM-grids with samples collected using electrostatic precipitation was conducted using a Tecnai G2F20 S/ TEM with a field emission gun (FEI Comp., Hillsboro, OR, USA). The microscope was operated at 200 kV. The images were acquired with an UltraScan™ 1000 2 k × 2 k CCD Camera System, Model 895 (Gatan, Inc., Pleasanton, CA, USA). Energy-dispersive X-ray spectroscopy (EDS) was performed with a Genesis EDS Analysis System (EDAX, Inc., Mahwah, NJ, USA).

We also investigated the samples after staining them with 0.75% uranyl formate. The staining solution was prepared by dissolving 37.5 mg of uranyl formate powder (Electron Microscopy Sciences, Inc., Hatfield, PA, USA) in boiling hot ultrapure water. The test tube was wrapped in aluminum foil to reduce exposure to light. After complete dissolution, we added 150 µL of 5 M solution of sodium hydroxide. The mixture was then shaken in a test tube shaker for 5 min. The resulting solution was cooled to near-room temperature and filtered using the same type of Millex syringe filter with a 0.22 µm pore size that we used for melted snow filtration. The resulting staining solution was kept in a refrigerator at 4 °C wrapped in aluminum foil and used within 5 days. For safety, all the above procedures to prepare the staining solution were performed in a chemical fume hood to prevent any inhalation exposure to aerosols potentially generated during the handling and processing of uranyl formate, and all the liquid and solid waste was disposed of according to the local regulations. Alternatively, a 2% aqueous solution of uranyl acetate (SPI Supplies, Inc., West Chester, PA, USA) was used for staining the samples followed by airdrying.

Imaging of these samples was done using a FEI Tecnai 12 Biotwin TEM microscope (FEI Comp.), equipped with a tungsten filament, at 120 kV.

2.2.8. Aerosol Size Distribution Analysis

Aerosol particle size distributions in the output aerosol stream exiting from the double diffusion dryer were measured with a NanoScan™ scanning mobility particle sizer (SMPS), Model 3910 (TSI, Inc.), and an optical particle sizer (OPS), model 3330 (TSI, Inc.). The NanoScan™ SMPS is a particle electrical mobility-based instrument with a measurement size range of 10 nm to 420 nm and measurement time of 60 s for size distribution measurements. Its inlet sampling flow rate is 0.75 L/min. The OPS is a single-particle optical counting instrument with a measurement size range of 0.3–10 μm in 16 aerosol particle size channels. The OPS's inlet sampling flow rate is 1 L/min.

Blank samples were obtained before each sampling session by operating the nebulizer without any liquid feed and then with ultrapure water that was either unfiltered or filtered through PVDF membrane filters with 0.22 μm pore size, the same type as those used for filtration of snow samples. Two samples from each location were analyzed. Each sample was nebulized and analyzed five times, and these measurements were averaged.

2.3. Results and Discussion

The work encompassed the development of the aerosol-mediated snow analysis technique in parallel with application of alternative techniques: electron microscopy and NTA, as well as a complementary characterization of total organic carbon. The samples for electron microscopy were prepared by particle collection from aerosol phase, and this way of collecting particles, as we show below, has the advantage of preventing agglomeration of particles. Figure 2.2 depicts a flowchart showing various snow processing procedures and analytical techniques outlined in the "Materials and methods" section in the sequence they were performed.

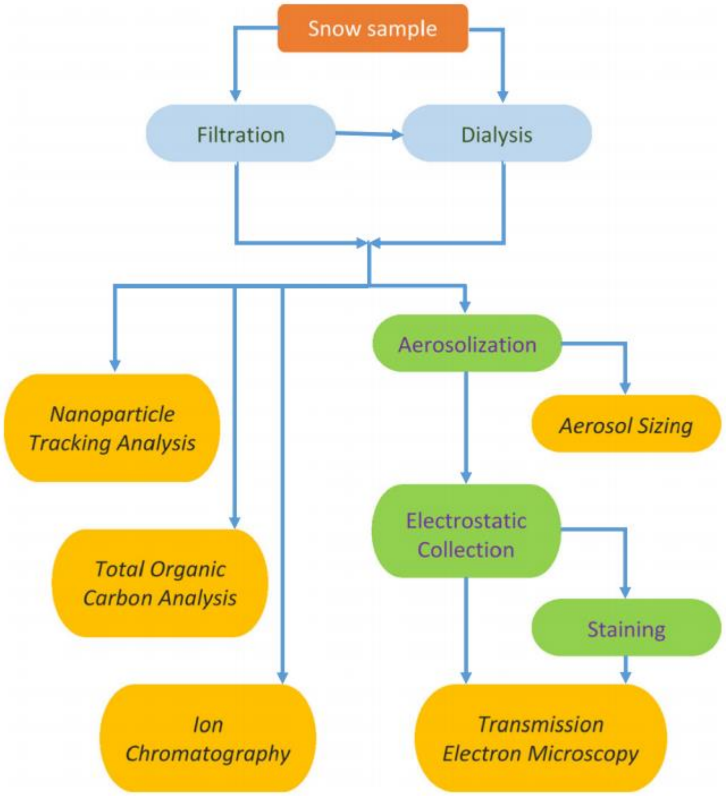

Figure 2.2 Snow processing procedures and analyses.

2.3.1. Direct Characterization of Liquid Melted Snow Samples

The first step of the work was to characterize snow samples by NTA—an established technique, yet only recently applied to analysis of snow samples. We collected snow samples from different locations and sampling campaigns in original state and processed by filtration and/or dialysis, as outlined in Figure 2.2. Filtration was required to determine the potential or absence thereof of the larger particles to obscure detection of smaller particles and to determine the fraction of total organic carbon in the large particles. Dialysis was aimed at reducing concentration of dissolved substances (salts and organics) to determine their potential to affect size distribution measurements. Application of dialysis was a novel approach for snow samples. NTA found a higher abundance and larger sizes of particles in snow samples from Montreal, compared to samples from Alert and Barrow, as seen in Figure 2.3. Expectedly, the unfiltered samples had a higher abundance of larger particles compared to the filtered samples. Most unprocessed samples' hydrodynamic diameter distributions (NTA distributions) showed several modes (peaks); however, all distributions had the maximum peak between 100 and 200 nm. Filtration (0.22 μm pore size) dramatically reduced concentrations of particles with hydrodynamic diameter larger than a little over 200 nm. We note that hydrodynamic diameter, measured by NTA, includes the double electric layer. All filtered samples from all three locations (Alert, Barrow and Montreal) seemed to produce a generally similar shape of the hydrodynamic particle size distribution with the highest mode ranging from 100 to 200 nm. At this mode, the highest absolute particle concentration per 1 mL of melted snow of about $(1.2 \pm 0.2) \times 10^6$ cm^{-3} was observed in melted 2006 Montreal snow sample, followed by Alert, with about $(8.2 \pm 1) \times 10^5$ cm^{-3}. The lowest concentration of 100– 200 nm particles was measured in the Barrow sample: about $(5 \pm 0.5) \times 10^5$ cm^{-3}. Barrow, however, had another peak at 300 nm, where particle concentration was $(2 \pm 1) \times 10^5$ cm^{-3}.

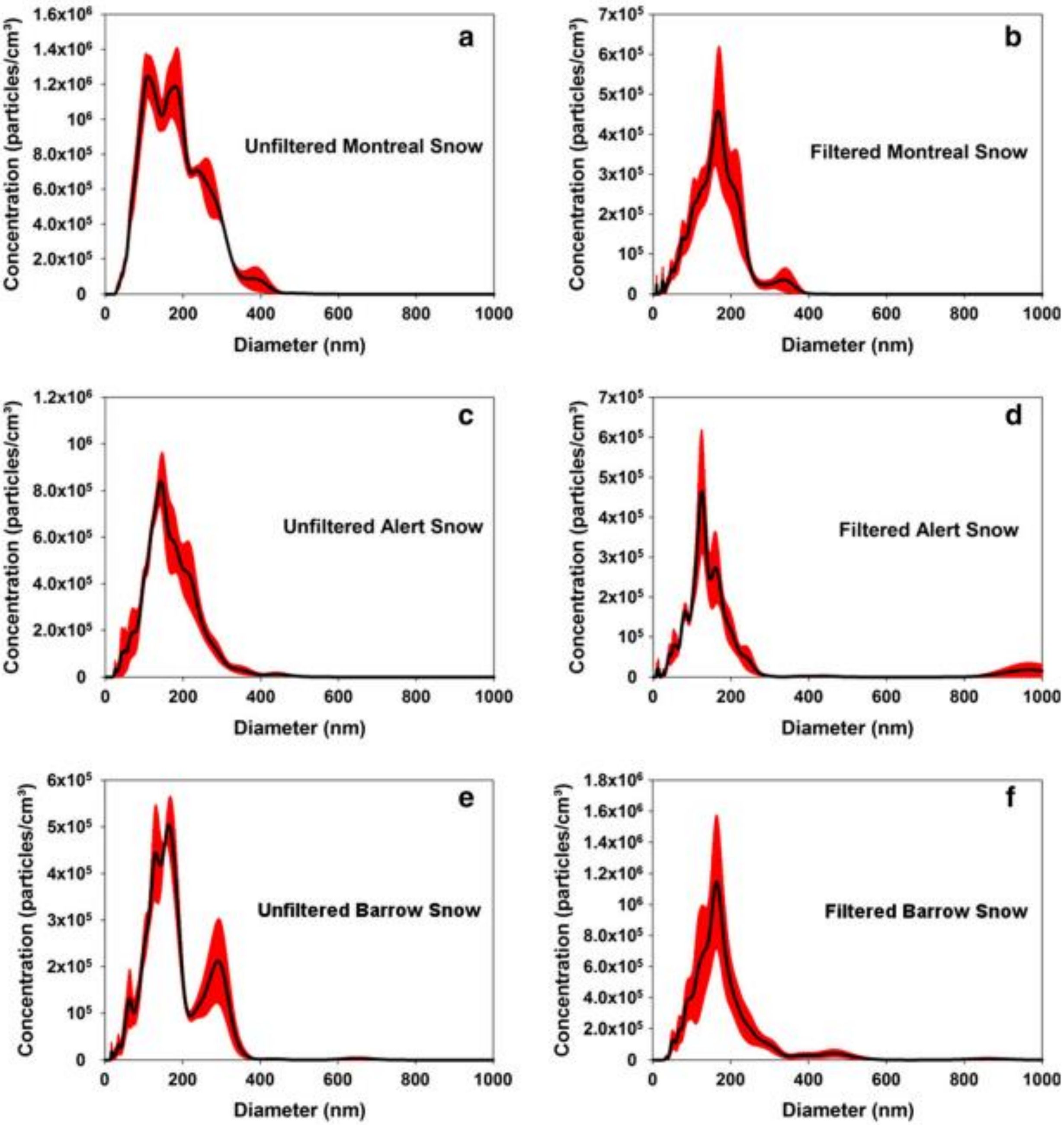

Figure 2.3 Hydrodynamic particle size distributions of snow samples from (a, b) Montreal 2006, (c, d) Alert, and (e, f) Barrow. All samples were analyzed both unprocessed and filtered using a syringe filter with pores of 0.22 μm in diameter. a, c, e. Adapted with permission from Supporting Information for (Rangel-Alvarado et al. 2015). Error bars indicate ±1 standard error of the mean.

Unprocessed samples from downtown Montreal (2006) showed a distribution with few larger particles, up to 900 nm, whereas particle size distributions of melted snow from Alert and Barrow showed particles up to around 400 nm. As the urban location of Montreal has multiple potential sources of large aerosol particles compared to the remote locations of Barrow and Alert lacking vegetation and with substantially lower anthropogenic activity, the observed higher abundance of larger particles was expected.

After filtration aimed at removing particles larger than about 200 nm, the distributions expectedly tended to become mono-modal, with a maximum peak still around 100 and 200 nm, but about 50% lower absolute concentration of these most abundant particles, with the exception of Barrow, where it increased. The trend was even more pronounced for the dialyzed Alert sample (Figure A.1) where dialysis also seemed to remove or lower the concentration of particles in the size range of 600 to 800 nm.

Soluble particles originally present in the snowpack, including soluble ice nuclei, dissolve when snow is melted. By nature, dialysis reduces soluble material, which may contribute to particle coatings, so reduction of soluble substances in melted snow was expected to lead to a reduction of both hydrodynamic and aerosol diameters of particles. Therefore, dialysis was indeed important to measure primary particle size in melted snow more accurately.

Soluble materials are of high importance due to their effects on ice nucleating properties of atmospheric particles. It has been reported that insoluble particles coated by soluble components, such as ammonium sulfate, may have altered ice nucleating properties and possibly other characteristics compared with the core insoluble particles themselves.[40-41]

To investigate the ionic content in the melted snow (soluble salts) and the effects of dialysis on it, we performed ion chromatography, which showed a substantial reduction of ionic content in all samples after performing dialysis (Table 2.1).

Table 2.1 Comparison of ion content in the original and dialyzed snow.

	Ions and their concentration, mg/L								
Sample	Sulfate	Phosphate	Chloride	Nitrite	Sodium	Potassium	Magnesium	Calcium	Ammonium
Alert 1	0.39	< 0.1	12.76	< 0.1	7.12	0.23	0.87	1.01	< 0.1
σ	0.06	< 0.1	0.26	< 0.1	0.22	0.02	0.04	0.07	< 0.1
Alert 1*	0.65	< 0.1	0.82	< 0.1	0.38	0.15	0.07	1.36	< 0.1
σ	0.05	< 0.1	0.06	< 0.1	0.15	0.03	0.02	0.16	< 0.1
Alert 2	0.43	< 0.1	16.78	< 0.1	7.13	0.26	0.98	0.74	< 0.1
σ	0.06	< 0.1	0.14	< 0.1	0.31	0.02	0.06	0.08	< 0.1
Alert 2*	0.36	< 0.1	0.41	< 0.1	0.26	0.05	0.04	0.81	< 0.1
σ	0.04	< 0.1	0.08	< 0.1	0.15	0.02	0.01	0.11	< 0.1
Barrow 1	0.68	< 0.1	13.59	< 0.1	5.24	0.21	0.66	1.06	< 0.1
σ	0.02	< 0.1	11.05	< 0.1	4.13	0.03	0.50	0.35	< 0.1
Barrow 1*	0.55	< 0.1	0.68	< 0.1	0.30	0.05	0.08	1.08	< 0.1
σ	0.02	< 0.1	0.03	< 0.1	0.13	0.00	0.00	0.01	< 0.1
Barrow 2	0.53	< 0.1	7.91	< 0.1	3.70	0.19	0.51	0.58	< 0.1
σ	0.04	< 0.1	0.07	< 0.1	0.14	0.02	0.02	0.05	< 0.1
Barrow 2*	0.52	n. d.	3.45	n. d.	0.43	2.38	n. d.	1.19	n. d.
σ	0.01	n. d.	0.03	n. d.	0.13	0.03	n. d.	0.09	n. d.
Mtl 2006	0.82	n. d.	0.29	n. d.	0.48	0.09	n. d.	0.86	n. d.
σ	0.02	n. d.	0.01	n. d.	0.10	0.02	n. d.	0.04	n. d.
Mtl 2006*	0.46	n. d.	0.53	n. d.	0.27	n. d.	n. d.	0.71	n. d.
σ	0.02	n. d.	0.57	n. d.	0.14	n. d.	n. d.	0.10	n. d.
Mtl 2014	1.47	n. d.	11.40	n. d.	4.74	n. d.	0.59	5.16	n. d.
σ	0.01	n. d.	0.06	n. d.	0.16	n. d.	0.02	0.06	n. d.
Mtl 2014*	0.20	n. d.	0.07	n. d.	0.28	n. d.	n. d.	0.67	n. d.
σ	0.00	n. d.	0.01	n. d.	0.14	n. d.	n. d.	0.13	n. d.

*dialyzed samples

This decrease was expected since most of the ions found in the unprocessed samples are soluble in water and can diffuse through the dialysis membrane effectively. However, we also observed that the concentrations of sulfate and calcium ions did not reduce as drastically as the concentrations of the other measured ions. For some samples, the concentration of calcium increased instead by a bit, and it was a consistent trend among those samples.The manufacturer (Spectrum Laboratories, Inc.) of the dialysis membrane we used indicated that the membrane could be a source of up to 0.5 mg/L of sulfur, which is comparable to the concentrations we observed in the original and dialyzed samples. However, the manufacturer did not find the membrane to leach any detectable concentration of calcium ions. Consistently, previous research showed that calcium ions bind to cellulose dialysis membranes.[42] A possible explanation for increasing calcium ion concentration may be that calcium ions are bound to colloidal matter in melted snow that does not pass through the dialysis membrane and may be released when ionic strength decreases in the process of dialysis. Further research, which is beyond the scope of this publication, is recommended to clarify the situation.

We did not observe a clear correlation between the total concentrations of different ions measured by IC and concentrations of aerosol particles, which mean that the influence of particles formed from dissolved substances had no significant influence on the aerosol size distributions, similar to observations by other researchers.[43] The concentrations of various ions, as measured by IC, even in undialyzed samples, were also below the concentrations used for generation of salt crystal aerosols from saline solutions with particle size in the region of interest for melted snow (TSI, Inc. 2005). We note that generation of salt crystal aerosols from saline solutions is a well-established technique in aerosol science.[44] Moreover, even undialyzed samples had salt concentrations (almost exclusively Na+ and Cl− as other ions were generally <1 mg/L) lower or on the borderline with those required to produce any interfering salt aerosol. For example, it can be seen that higher concentrations than what we had in dialyzed and even undialyzed (Table 1) samples of salts are needed to produce dry aerosol particles in the size range of interest: 120 mg/L of NaCl for 50 nm mode diameter, 12 mg/L for 35 nm mode diameter, and 1 mg/L for ∼30 nm mode diameter. In the latter case, no distinct mode is observed when salt concentration is only 1 mg/L. In our distributions, we observed a more distinct mode at 15 nm for Alert and secondary modes at this size for Montreal and Barrow. Moreover, we had the same mode at 15 nm for both undialyzed and dialyzed samples. The effects of filtration on total organic carbon concentration differed substantially between snow samples. The concentration of organic carbon in the most recent Montreal snow sample (2014) changed little after filtering out particles larger than 200 nm (Table 2.2).

Table 2.2 Total organic carbon in snow samples.

Sample	Average, mg/L	σ	%CV
Arctic snow sample (Alert, Nunavut)	0.723	0.047	6.530
Filtered Arctic snow sample (Alert, Nunavut)	0.496	0.040	8.184
Montreal snow sample (2014)	1.484	0.018	1.239
Filtered Montreal snow sample (2014)	1.410	0.090	6.367
Montreal snow sample (2006)	2.803	0.045	1.589
Filtered snow sample (2006)	0.980	0.049	5.051

Therefore, most particulate organic matter in it was in the size fraction <200 nm and in the molecularly dissolved form that passed through the filter. On the contrary, for the 2006 Montreal snow sample, removal of particles with diameters greater than 200 nm by filtration led to an almost threefold drop of total organic carbon (TOC), meaning that most particulate organic matter by mass in the 2006 Montreal snow sample was in the size fraction larger than 200 nm. The substantially higher TOC in unfiltered 2006 Montreal sample compared to the 2014 Montreal sample points to the presence of an initially higher abundance of large (>200 nm) organic matter-containing particles in the 2006 Montreal snow sample, relative to the combined contribution of small particles (<200 nm) and dissolved organic carbon. The sources of these particles are both anthropogenic and biogenic. Approximately 20 to 50% of the total organic fine aerosol mass at the continental mid-latitudes originate from fossil fuel burning, domestic and biomass burning, and naturally from viruses, bacteria, fungal spores, and plant debris.[45] We note that microorganisms are mostly larger than the filter pore size we used,[46-47] so their removal is expected to also contribute to the observed lowering of TOC after filtration. In the Montreal snow samples, anthropogenic particles likely represent a larger percentage of the total aerosol, compared to snow at Alert due to absence of considerable immediate sources of organic matter emission in Alert and presence of considerable emission sources in the Montreal area. Indeed, we observed the lowest TOC among all analyzed samples in the samples from Alert, where it was approximately half the level in the lowest TOC Montreal sample from 2014. With respect to the content of dissolved organic matter, small (<200 nm) organic particles: about a third of TOC in the sample from Alert constituted large particles corresponding to TOC removed by filtration, and the remaining two thirds of the TOC were small particles and dissolved organic matter.

When we examined particulate matter, collected by electrostatic precipitation from the aerosolized melted snow, by TEM, we observed a high on-grid concentration of particles of various electron contrast and crystalline, as well as amorphous structures (Figure 2.4a–f). However, dialyzed versions of the same samples were dominated by smaller particles (20–100 nm) with low electron contrast. We note a very low occurrence of agglomerates, not excluding a possible presence of electron-transparent agglomerates that transmission electron microscopy (TEM) cannot detect. We then "washed" a portion of the samples directly on EM-grids to remove soluble matter and stained them, along with original unwashed samples, with uranyl acetate and uranyl formate to view organic particles as well. Uranyl formate and uranyl acetate are negative stains—they leave organic particles unstained and near transparent to the electron beam while staining the background. Stained samples presented a high concentration of particles showing as light dots at the dark background of other high-electron-contrast particles and the stained substrate, as well as particles with low electron contrast (Figure 2.4g–i).

Most of the high-electron-contrast particles exhibited what looked like a coating surrounding the particles, similar to recent observations of such features in sea spray aerosol particles.[48] This coating had lower electron contrast than the core particles.

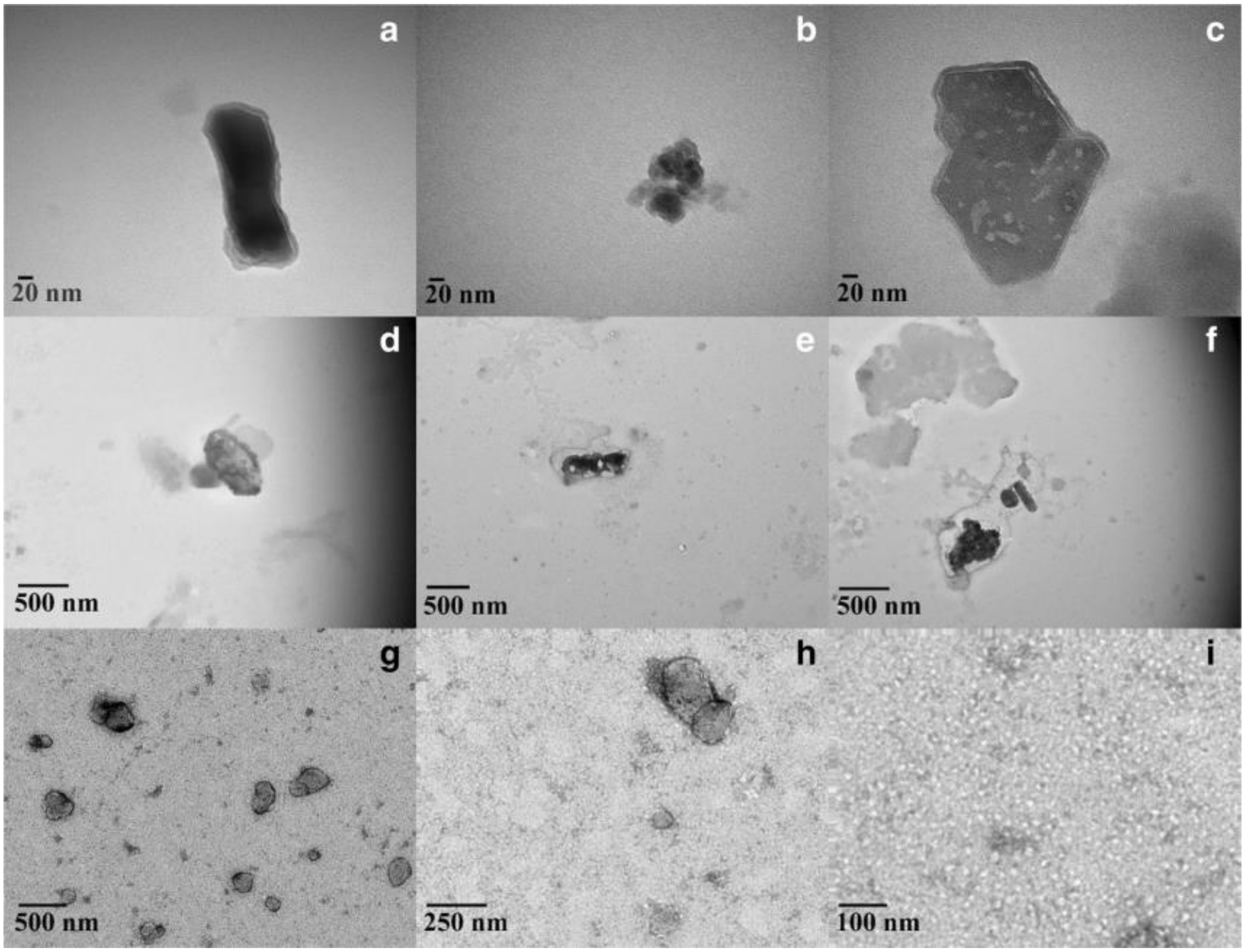

Figure 2.4 Representative high- and mid-resolution TEM images of aerosolized particles. a–c With prior dialysis and d–i without any prior processing. a–f. Stained with uranyl formate and g–i stained with uranyl acetate.

The electron microscopy images of dialyzed samples did not show residue from precipitation of dissolved matter and formation of salt crystals, supporting the abovementioned evidence for effectiveness of dialysis in reducing effects of dissolved substances. TEM of any blank samples (not shown) did not reveal electron-contrast particles beyond very low contamination with metallic copper particles in the very first background sample, where these particles likely originated from the electrostatic precipitator itself, brand new and used for the first time since acquisition. This contamination was not observed in subsequent samples under our operating conditions.

The particles visible by TEM in samples from all three locations were found by EDS to contain carbon and silicon in detectable quantities (Figures A.2–A.4), silicon likely originating from mineral dust and carbon from either organic or carbonaceous matter. Only the sample from Montreal contained sodium, potassium, calcium, magnesium, and chlorine within electron contrast particles, and these elements were probably detected due to their elevated concentration in the urban snow where salt is applied to deice roadways and sidewalks and could be carried by wind as aerosol to areas of snow sampling. The sample from Alert contained the lowest number of detected elements: besides carbon, oxygen, and silicon, EDS found tellurium in it. The sample from Barrow, besides carbon and silicon, contained chromium, nickel, and iron—likely from mineral dust. It must be noted that the copper detected by EDS is in the region of spectra that indicates it came from the TEM-grids, made out of copper, and it was feasible to only investigate select particles by EDS due to the high cost of the technique, so the presented data may not be exhaustive with respect to all particles present in the samples. Ions of iron, chromium, and nickel that were present in the EDS spectra (Figures A.2–A.4) were likely mostly in an insoluble form within colloidal particles. The EDS data are complementary to the IC results, which analyzed ions in the entire volume of melted snow samples.

2.3.2. Aerosol-Mediated Characterization of Melted Snow Samples

The aerosol measurements indicated a higher abundance of particles of all sizes in aerosol size distributions for the Montreal samples, closely followed by Barrow, as seen in Figure 2.5 and Table 2.3. We saw much fewer large particles (0.3– 10 μm) in the dialyzed filtered samples, which indicates that filtration effectively removes >0.3 μm particles, but the effect may be clearly seen only when the sample is also dialyzed, again pointing to the necessity of dialysis in terms of increased definition of the aerosol size distributions. Dialysis also reduced the concentration of larger particles (Figure 2.5) and somewhat reduced small particles as well (Figure 2.6).

Table 2.3 Comparison of the mode diameters and concentrations for different locations of snow sampling. The concentrations are at corresponding primary and secondary mode particle diameter and expressed as dN/dlogDp, where dN is the number-based concentration of particles in the particle size range delimited by the upper and lower particle size boundaries of the corresponding measurement bin. Dp is the difference between these upper and lower instrument measurement bin boundaries.

Sample	Primary mode diameter (nm)	Concentration × 10^5, cm^{-3}	Secondary mode diameter (nm)	Concentration × 10^5, cm^{-3}
Alert snow sample	10	20	30	15
Dialyzed alert snow sample	10	7	30	2
Barrow snow sample	30	40	10	20
Dialyzed Barrow snow sample	10	2	30	1
Montreal snow sample	30	40	10	10
Dialyzed Montreal snow sample	10	2	30	1

However, after dialysis, despite substantial differences in concentrations of large particles between filtered and unfiltered samples, no change of mode diameters occurred. We note that some particles may have been lost to the walls of the dialysis tubing. We did not observe as dramatic a reduction of aerosol particles after filtration of the undialyzed samples. It was expected that filtration would remove large particles. We, therefore, conclude that soluble substances, originally present in undialyzed melted snow, must have formed a substantial fraction of large aerosol particles, and dialysis remediated the masking problem of particles derived from soluble substances revealing a size distribution of larger aerosol particles, including larger ice nuclei, more representative of that in the melted snow samples. Therefore, desalination by dialysis of melted snow samples was found to be an important additional experimental step, which allowed improving definition of aerosol size distributions of snow-borne particles by reducing interference from salt particles and other soluble matter that may otherwise condense after aerosol drying.

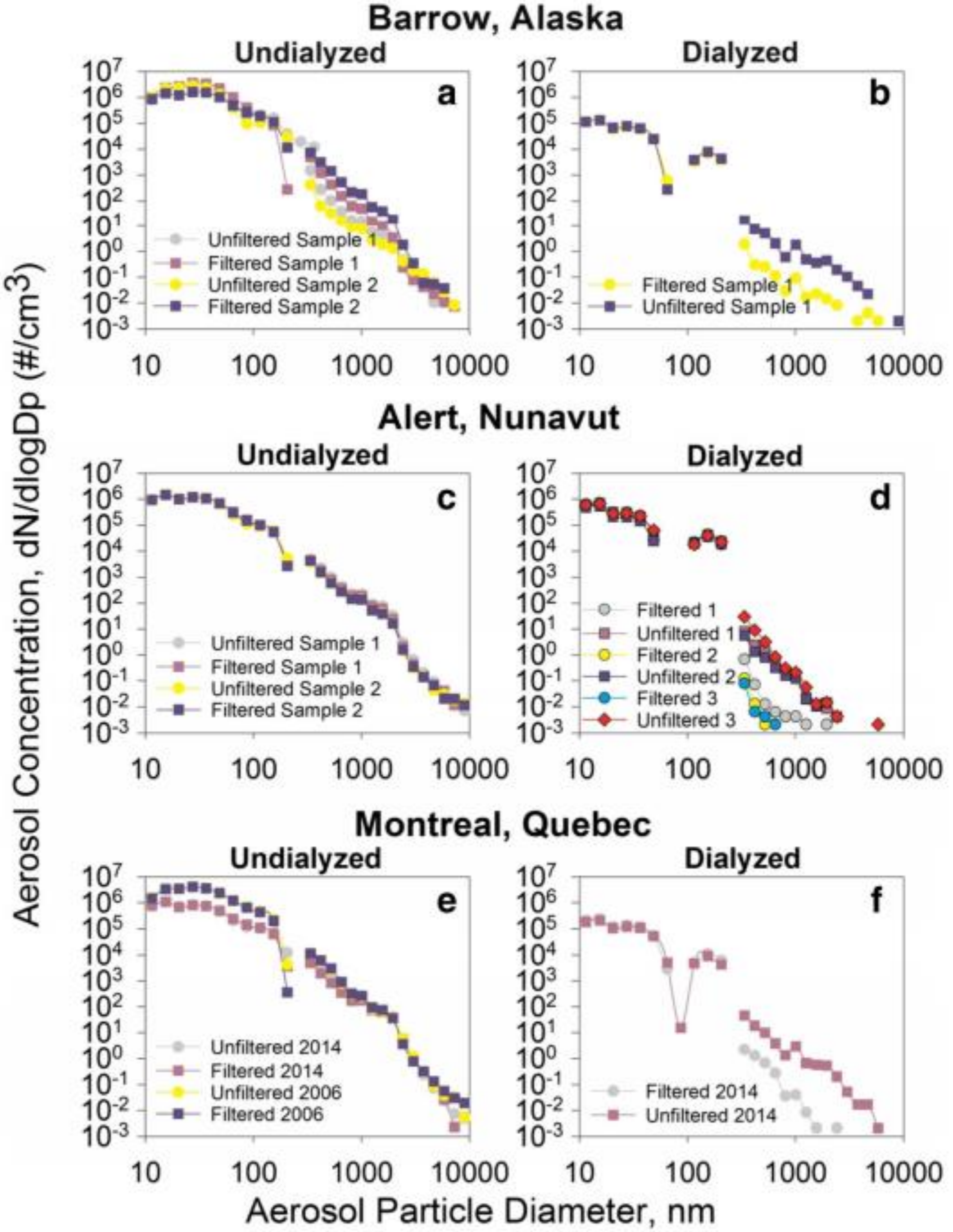

Figure 2.5 Aerosol particle size distributions of the aerosolized snow samples measured using the NanoScan scanning mobility particle sizer (SMPS) and the optical particle sizer (OPS).

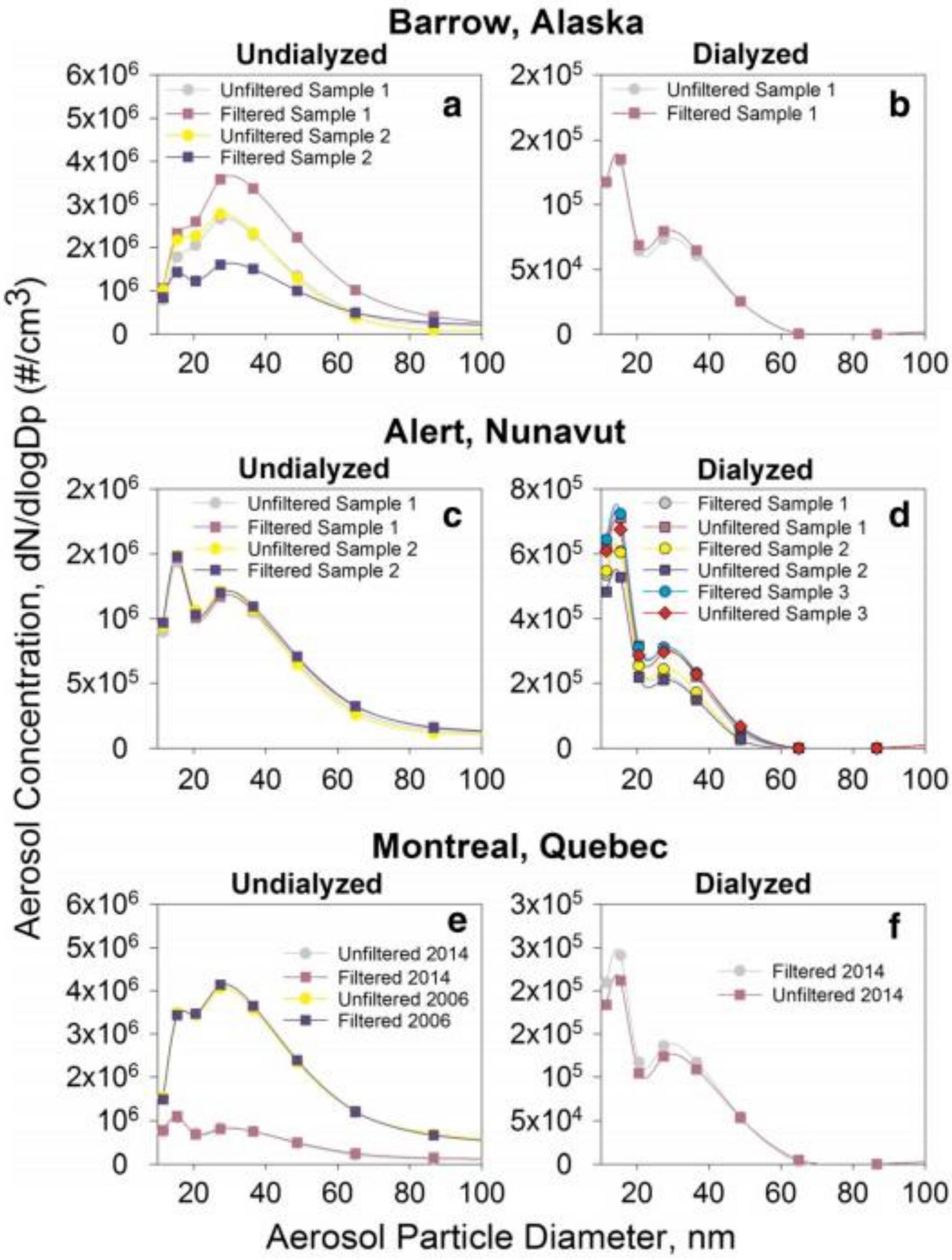

Figure 2.6 High-resolution aerosol nanoparticle size distributions of the aerosolized snow samples measured with the NanoScan scanning mobility particle sizer (SMPS).

When the nebulizer was operated without any liquid feed (blank sample group 1), the NanoScan™ and the OPS registered only occasional single particles, indicating a very clean background. The ultrapure water aerosol size distributions (blank sample group 2) were substantially below the size distributions of aerosolized melted snow samples and are, therefore, not shown in Figures 2.5 and 2.6.

2.3.3. Verification of the Aerosol-Mediated Characterization Technique

To rule out any significant effect of particles formed from soluble substances that may still remain after dialysis in the melted snow samples, including any residual salts, which may precipitate or crystallize during drying of aerosol, we prepared and analyzed a number of 2-, 3-, and 4-fold dilutions of select filtered and unfiltered dialyzed samples by mixing the melted snow samples with ultrapure water. This standard approach was successfully used before to rule out effects of soluble substances on aerosol size distribution.[43] The aerosol size distributions of these original and diluted samples did not reveal any changes of the aerosol size distributions for any samples (Figure A.5). At the same time, aerosol concentrations in different aerosol size channels changed proportionally to the degree of dilution of the original melted snow samples, which was expected and confirms that these particles originated from insoluble particles, originally present in the melted snow. We, therefore, conclude that the concentration of particles formed due to precipitation and crystallization of any soluble matter in dialyzed snow samples was insignificant and did not distort the aerosol size distributions.

As an additional test of the robustness of the aerosolization technique coupled with dialysis, we tested diluted standard TiO_2 suspension (rutile, 20%wt in water, 30–50 nm, US Research Nanomaterials, Inc., Houston, TX, USA) with a soluble salt (NaCl) and a soluble organic material (oxalic acid), both reagents from Sigma Aldrich, Inc. (St. Louis, MI, USA). We used two different concentrations of NaCl. The first was 28 mg/L of NaCl—equivalent to 17 mg/L of chloride, corresponding to the highest concentration of chloride measured in undialyzed snow samples. The second was 1 mg/L of NaCl (typical concentration after dialysis of snow samples). We chose the concentration of oxalic acid based on the measurements of this organic substance in cloud water at Mount Lu and Mount Heng as reported by Sun et al.[49] Note that the concentration in Sun et al.[21] is reported in microequivalents per liter. Therefore, the concentration of 630 µg/L we used here corresponds to 10 µeq/L of oxalic acid ($H_2C_2O_4 \cdot 2H_2O$) as reported in Sun et al.[21] We note that dialysis is expected to greatly reduce concentrations of soluble organic substances too (<5–8 kDa), including oxalic acid, so the original 630 µg/L is a high estimate. As seen in Figure 2.7, soluble materials at low concentration, typical of post-dialysis samples (1 mg/L NaCl and 630 µg/L oxalic acid) do not have an effect on aerosol particle concentrations or the particle size distribution of TiO_2, whereas soluble material at high concentration (as found in melted snow prior to dialysis) do modify the aerosol concentration and particle size distribution. It is clear that dialysis is an effective and crucial step when using the aerosol-mediated technique we developed for analysis of samples with high concentrations of soluble materials.

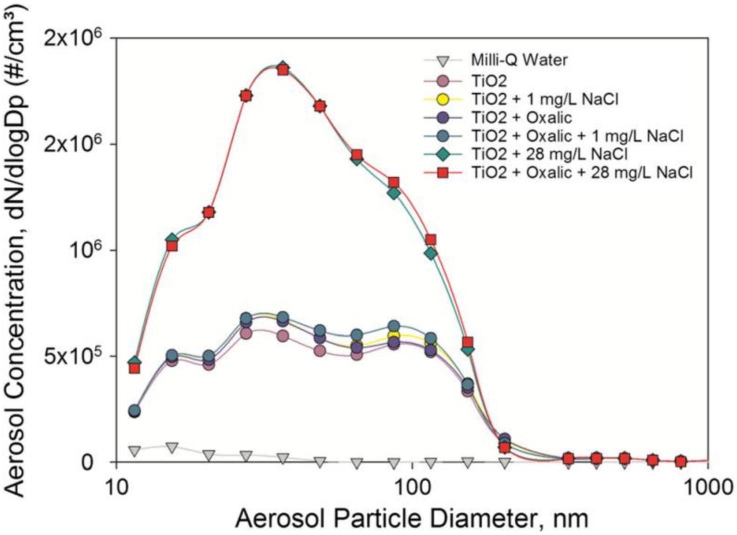

Figure 2.7 Aerosol particle size distributions measured using the NanoScan scanning mobility particle sizer (SMPS) and the optical particle sizer (OPS) of the aerosolized TiO_2 colloid solutions with or without added solutes: oxalic acid and different concentrations of NaCl. Oxalic acid concentration is 630 µg/L.

The NTA's ability to detect particles by the light they scatter sharply reduces below a certain size, which, depending on optical properties of particles, can be between 10 and 50 nm or sometimes even larger, according to the manufacturer of the instrument. Therefore, the aerosolization technique, involving real-time aerosol measurements by the SMPS and OPS systems, has a superior particle size measurement range—down to 10 nm with the instrument we used. The NTA size distributions predictably contrast in their not showing a high number of small nanoparticles. The aerosolization-based SMPS measurement showed a high abundance ($\sim 10^6$ cm^{-3}) of aerosol particles down to the smallest measurable size of 10 nm for all snow samples (Figure 2.6).

In summary, we developed a new technique, at the core of which is aerosolization of melted snow with subsequent drying of aqueous droplets in airborne state. The melted snow is processed before aerosolization by dialysis and optionally by filtration, which allows removing larger particles (>200 or >100 μm, depending on the filter used) and soluble substances, including salts, such as chlorides, sulfates, etc. Thus, when processed melted snow is aerosolized, and the minute droplets are dried, an aerosol of core snow-borne (nano)particles is produced. These particles are then analyzed by real-time aerosol analyzers to determine particle size distributions. The particles are also collected on TEM-grids using electrostatic precipitation for electron microscopy and EDS to determine their elemental composition. In this study, the use of this new technique was complemented with analysis by NTA, providing a more comprehensive set of information about snow-borne (nano)particles. Compared to the traditionally used direct liquid-to-grid sample transfer, the aerosol-mediated approach allows amplification of deposited particle density on EM-grids while minimizing particle agglomeration. Another advantage of the new approach is the higher particle size resolution and a comparatively more extensive measurement size range of provided by the aerosol analyzers compared to traditional techniques for particle measurement in liquid phase, such as nanoparticle tracking analysis.

2.4. Concluding Remarks and Future Work

This study presents a novel technique based on aerosolization of processed melted snow. The processing by dialysis of melted snow samples before aerosolization is an important step to reduce interference effects of soluble substances on the measured size distributions. Dialyzing melted snow that we suggest here could also become an important method in research of effects of soluble substances, such as biogenic chemicals and anthropogenic pollutants, on ice nucleating properties of atmospheric aerosols.

The developed technique combines sizing and counting of individual dried aerosol particles with their collection by electrostatic precipitation. Consequently, acquisition of particle size distributions of snow-borne particles is complemented with their simultaneous characterization by electron microscopy and energy-dispersive X-ray spectroscopy. The samples prepared through aerosolization and subsequent collection of dispersed particles are suitable for analysis by other techniques in future research.

In this study, a variety of snow samples were characterized, providing new information about the similarities and differences in composition and physicochemical features of particulate matter in snow while demonstrating broad applicability and usefulness of the new aerosolization technique.

The developed technique has a high sensitivity and minimizes particle aggregation. The results demonstrate the added value of the new technique in its ability to measure a high-resolution snow-borne particle size distribution, including between 10 and 100 nm, where other techniques are limited. Future research should focus on segregating size distributions of different categories of ice nucleating particles found in snow from non-ice nuclei.

Acknowledgements. We thank Mr. Jean-Philippe Guay for building the diffusion dryers and the mixing elements, Ms. Katherine Velghe for conducting TOC, and Ms. Monique Riendeau for conducting IC analyses of the melted snow. We would like to express special thanks to TSI, Inc. and personally to Ms. Sherrie Elzie and Ms. Sarah Sakamoto for providing the NanoScan™ and the OPS instruments. We also kindly thank the anonymous reviewers for their valuable feedback that helped improve the final manuscript. The study is jointly funded by Natural Science and Engineering Research Council of Canada, Environment Canada, Canadian Foundation for Innovation, and FRQNT. Dr. Yevgen Nazarenko is supported by Fonds de recherche du Québec—Nature et technologies. The views expressed in the manuscript are solely of the authors and do not necessarily reflect those of the funding agencies.

References

1. Archer, D., *Global warming: understanding the forecast*. John Wiley & Sons: 2012.
2. Kärcher, B., Atmospheric ice formation processes. In *Atmospheric Physics*, Springer: 2012; pp 151-167.
3. Murray, B.; O'sullivan, D.; Atkinson, J.; Webb, M., Ice nucleation by particles immersed in supercooled cloud droplets. *Chemical Society Reviews* **2012,** *41* (19), 6519-6554.
4. Yakobi-Hancock, J. D.; Ladino, L. A.; Abbatt, J. P., Review of recent developments and shortcomings in the characterization of potential atmospheric ice nuclei: focus on the tropics. *Revista de Ciencias* **2013,** *17* (3), 15-34.
5. Koop, T., et al., Water activity as the determinant for homogeneous ice nucleation in aqueous solutions. *Nature* **2000,** *406* (6796), 611-614.
6. Khvorostyanov, V. I.; Curry, J. A., *Thermodynamics, kinetics, and microphysics of clouds*. Cambridge University Press: 2014.
7. Barkan, J.; Alpert, P.; Kutiel, H.; Kishcha, P., Synoptics of dust transportation days from Africa toward Italy and central Europe. *Journal of Geophysical Research: Atmospheres* **2005,** *110* (D7).
8. Xuan, J.; Sokolik, I. N.; Hao, J.; Guo, F.; Mao, H.; Yang, G., Identification and characterization of sources of atmospheric mineral dust in East Asia. *Atmospheric Environment* **2004,** *38* (36), 6239-6252.

9. Ariya, P.; Sun, J.; Eltouny, N.; Hudson, E.; Hayes, C.; Kos, G., Physical and chemical characterization of bioaerosols–Implications for nucleation processes. *International Reviews in Physical Chemistry* **2009,** *28* (1), 1-32.

10. Archuleta, C. M.; DeMott, P.; Kreidenweis, S., Ice nucleation by surrogates for atmospheric mineral dust and mineral dust/sulfate particles at cirrus temperatures. *Atmospheric Chemistry and Physics* **2005,** *5* (10), 2617-2634.

11. Bigg, E. K.; Leck, C., Cloud-active particles over the central Arctic Ocean. *Journal of Geophysical Research: Atmospheres* **2001,** *106* (D23), 32155-32166.

12. Fröhlich-Nowoisky, J.; Nespoli, C. R.; Pickersgrill, D.; Galand, P.; Müller-Germann, I.; Nunes, T.; Cardoso, J. G.; Almeida, S. M.; Pio, C.; Andreae, M., Diversity and seasonal dynamics of airborne archaea. *Biogeosciences* **2014,** *11* (21), 6067-6079.

13. Georgakopoulos, D.; Després, V.; Fröhlich-Nowoisky, J.; Psenner, R.; Ariya, P.; Pósfai, M.; Ahern, H.; Moffett, B.; Hill, T., Microbiology and atmospheric processes: biological, physical and chemical characterization of aerosol particles. *Biogeosciences* **2009,** *6* (4), 721-737.

14. Mortazavi, R.; Attiya, S.; Ariya, P. In *Microbial analysis of arctic snow and frost flowers: what next generation sequencing method can reveal*, AGU Fall Meeting Abstracts, 2014.

15. Mortazavi, R.; Attiya, S.; Ariya, P., A next generation sequencing of Arctic bacteria in snow and frost flowers: identification, abundance and freezing nucleation. *Atmospheric Chemistry & Physics Discussions* **2014,** *14* (23).

16. Mortazavi, R.; Attiya, S.; Ariya, P., Arctic microbial and next-generation sequencing approach for bacteria in snow and frost flowers: selected identification, abundance and freezing nucleation. *Atmospheric Chemistry and Physics* **2015,** *15* (11), 6183-6204.

17. Mortazavi, R.; Hayes, C. T.; Ariya, P. A., Ice nucleation activity of bacteria isolated from snow compared with organic and inorganic substrates. *Environmental Chemistry* **2008,** *5* (6), 373-381.

18. Schnell, R.; Vali, G., Biogenic ice nuclei: Part I. Terrestrial and marine sources. *Journal of the Atmospheric Sciences* **1976,** *33* (8), 1554-1564.

19. Vali, G.; Christensen, M.; Fresh, R.; Galyan, E.; Maki, L.; Schnell, R., Biogenic ice nuclei. Part II: Bacterial sources. *Journal of the Atmospheric Sciences* **1976,** *33* (8), 1565-1570.

20. Rangel-Alvarado, R. B.; Nazarenko, Y.; Ariya, P. A., Snow-borne nanosized particles: Abundance, distribution, composition, and significance in ice nucleation processes. *Journal of Geophysical Research: Atmospheres* **2015,** *120* (22).

21. Ariya, P.; Kos, G.; Mortazavi, R.; Hudson, E.; Kanthasamy, V.; Eltouny, N.; Sun, J.; Wilde, C., Bio-Organic Materials in the Atmosphere and Snow: Measurement and Characterization. In *Atmospheric and Aerosol Chemistry*, Springer: 2013; pp 145-199.

22. Ariya, P.; Domine, F.; Kos, G.; Amyot, M.; Côté, V.; Vali, H.; Lauzier, T.; Kuhs, W.; Techmer, K.; Heinrichs, T., Snow–a photobiochemical exchange platform for volatile and semi-volatile organic compounds with the atmosphere. *Environmental Chemistry* **2011,** *8* (1), 62-73.

23. Kos, G., Ariya, P. A., Volatile organic compounds in snow in the Quebec-Windsor Corridor. *J. Geophys. Res.* **2010,** *115* (D1).

24. Nemirovskaya, I.; Kravchishina, M., Biogeochemical features of the distribution of organic compounds and particulate matter in the snow-ice cover in East Antarctica. *Geochemistry International* **2015,** *53* (5), 430-440.

25. Radke, L. F.; Hobbs, P. V.; Eltgroth, M. W., Scavenging of aerosol particles by precipitation. *Journal of Applied Meteorology* **1980,** *19* (6), 715-722.

26. Skeie, R.; Berntsen, T.; Myhre, G.; Pedersen, C. A.; Ström, J.; Gerland, S.; Ogren, J., Black carbon in the atmosphere and snow, from pre-industrial times until present. *Atmospheric Chemistry and Physics* **2011,** *11* (14), 6809-6836.

27. Kuoppamäki, K.; Setälä, H.; Rantalainen, A.-L.; Kotze, D. J., Urban snow indicates pollution originating from road traffic. *Environmental pollution* **2014,** *195*, 56-63.

28. Nazarenko, Y.; Kurien, U.; Nepotchatykh, O.; Rangel-Alvarado, R. B.; Ariya, P. A., Role of snow and cold environment in the fate and effects of nanoparticles and select organic pollutants from gasoline engine exhaust. *Environmental Science: Processes & Impacts* **2016,** *18* (2), 190-199.

29. Barrie, L. A., The fate of particulate emissions from an isolated power plant in the oil sands area of western Canada. *Annals of the New York Academy of Sciences* **1980,** *338* (1), 434-452.

30. Williamson, B.; Udachin, V.; Purvis, O.; Spiro, B.; Cressey, G.; Jones, G., Characterisation of airborne particulate pollution in the Cu smelter and former mining town of Karabash, South Ural Mountains of Russia. *Environmental Monitoring and assessment* **2004,** *98* (1-3), 235-259.

31. Rosenfeld, D., Suppression of rain and snow by urban and industrial air pollution. *Science* **2000,** *287* (5459), 1793-1796.

32. Egerton, R.; Li, P.; Malac, M., Radiation damage in the TEM and SEM. *Micron* **2004,** *35* (6), 399-409.

33. Jacobson, M. Z., *Fundamentals of atmospheric modeling*. Cambridge university press: 2005.

34. Domingos, R. F.; Baalousha, M. A.; Ju-Nam, Y.; Reid, M. M.; Tufenkji, N.; Lead, J. R.; Leppard, G. G.; Wilkinson, K. J., Characterizing manufactured nanoparticles in the environment: multimethod determination of particle sizes. *Environmental science & technology* **2009,** *43* (19), 7277-7284.

35. Kos, G., Ariya, P. A., Determination of a wide range of volatile and semivolatile organic compounds in snow by use of solid-phase micro-extraction (SPME). *Anal. Bioanal. Chem.* **2006,** *385* (1), 57-66.

36. Kos, G.; Ariya, P. In *Determination of Volatile Organic Compounds in Snow and Air in Alert, Nunavut*, AGU Fall Meeting Abstracts, 2006.

37. Mortazavi, R.; Kos, G.; Ariya, P. In *A comparison study of volatile organic compound species and concentrations in snow samples from rural sites in south-western Quebec and at Alert, Nunavut*, AGU Fall Meeting Abstracts, 2006.

38. Poulain, A. J.; Garcia, E.; Amyot, M.; Campbell, P. G.; Ariya, P. A., Mercury distribution, partitioning and speciation in coastal vs. inland High Arctic snow. *Geochimica et Cosmochimica Acta* **2007,** *71* (14), 3419-3431.

39. Filipe, V.; Hawe, A.; Jiskoot, W., Critical evaluation of Nanoparticle Tracking Analysis (NTA) by NanoSight for the measurement of nanoparticles and protein aggregates. *Pharmaceutical research* **2010,** *27* (5), 796-810.

40. Baustian, K.; Wise, M.; Tolbert, M., Depositional ice nucleation on solid ammonium sulfate and glutaric acid particles. *Atmospheric Chemistry and Physics* **2010,** *10* (5), 2307-2317.

41. Wise, M. E.; Baustian, K. J.; Tolbert, M. A., Internally mixed sulfate and organic particles as potential ice nuclei in the tropical tropopause region. *Proceedings of the National Academy of Sciences* **2010,** *107* (15), 6693-6698.

42. Reed, K., Binding of calcium by cellulose membranes and Sephadex. *Biochemical and biophysical research communications* **1973,** *50* (4), 1136-1142.

43. Lee, I.-S.; Kim, H. J.; Lee, D. H.; Hwang, G. B.; Jung, J. H.; Lee, M.; Lim, J.; Lee, B. U., Aerosol Particle Size Distribution and Genetic Characteristics of Aerosolized Influenza A H 1 N 1 Virus Vaccine Particles. *Aerosol and Air Quality Resarch* **2011,** *11* (3), 230-237.
44. Borrego, C.; Brebbia, C. A., *Air Pollution XV*. WIT Press: 2007; Vol. 101.
45. Kanakidou, M.; Seinfeld, J.; Pandis, S.; Barnes, I.; Dentener, F.; Facchini, M.; Dingenen, R. V.; Ervens, B.; Nenes, A.; Nielsen, C., Organic aerosol and global climate modelling: a review. *Atmospheric Chemistry and Physics* **2005,** *5* (4), 1053-1123.
46. Kokhanovsky, A. A., *Light scattering reviews 3: light scattering and reflection*. Springer Science & Business Media: 2008.
47. Talaro, K.; Chess, B., Foundations in Microbiology. McGraw Hill, Boston: 2008.
48. Prather, K., Influence of sea spray aerosols on cloud and climate. *250th American Chemical Society National Meeting & Exposition,*

Boston, p 155 **2015**.
49. Sun, X.; Wang, Y.; Li, H.; Yang, X.; Sun, L.; Wang, X.; Wang, T.; Wang, W., Organic acids in cloud water and rainwater at a mountain site in acid rain areas of South China. *Environmental Science and Pollution Research* **2016,** *23* (10), 9529-9539.

Chapter 3

3. Snow-Borne Nanosized Particles: Abundance, Distribution, Composition, and Significance in Ice Nucleation Processes

My contributions to this paper were the following:

I was responsible for the measurement of the ice nucleation abilities of particles < 200 nm and larger particles as well as for the calculation of the cumulative concentration of active ice nuclei at each temperature. I performed further physical and chemical characterization of these particles (microscopy, mass spectrometry, ion chromatography, and carbon content) and analysis of the data to understand the reason why the particles are efficient ice nuclei. Most of the writing was done by myself with inputs from Yevgen Nazarenko and Parisa Ariya. Yevgen Nazarenko and I contributed equally to collection of samples and the measurement of the particle distributions. The identification of microorganisms was described in Mortazavi 2008.[1]

A implication of this paper was to increase the awareness of nanosized particles (< 200 nm) as important atmospheric ice nucleating particles. Currently these particles have a higher recognition, specially particles of biological origin such as subcellular components.[2] We used the technique mentioned in the previous chapter for the acquisition of the particle size distribution of our samples.

The paper is reproduced in this thesis with the permission of John Wiley & Sons, Inc.

Manuscript published in Journal of Geophysical Research: Atmospheres 120: 11,760-11,774,

November 2015

Snow-Borne Nanosized Particles: Abundance, Distribution, Composition, and Significance in Ice Nucleation Processes

Rodrigo B. Rangel-Alvarado[1] & Yevgen Nazarenko[2], and Parisa A. Ariya*[1,2]

[1]Department of Chemistry, and [2]Department of Atmospheric and Oceanic Sciences, McGill University, 801 Sherbrooke St. W., Montreal, QC H3A 2K6, Canada

*Corresponding author

R.B. Rangel-Alvarado and Y. Nazarenko contributed equally to this work

Abstract. Physicochemical processes of nucleation constitute a major uncertainty in understanding aerosol-cloud interactions. To improve the knowledge of the ice nucleation process, we characterized physical, chemical and biological properties of fresh snow using a suite of state-of-the-art techniques based on mass spectrometry, electron microscopy, chromatography, and optical particle sizing. Samples were collected at two North American Arctic sites, as part of international campaigns (2006 & 2009), and in the city of Montréal, Canada, over the last decade.

Particle size distribution analyses, in the range of 3 nm to 10 μm, showed that nanosized particles are the most numerous (38-71 %) in fresh snow, with a significant portion (11 to 19 %) less than 100 nm in size. Particles with diameters less than 200 nm consistently exhibited relatively high ice nucleating properties (on average ranged from -19.6 ± 2.4 to -8.1 ± 2.6 °C). Chemical analysis of the nanosized fraction suggests that they contain bioorganic materials, such as amino acids, as well as inorganic compounds with similar characteristics to mineral dust. The implication of nanoparticle ubiquity and abundance in diverse snow ecosystems are discussed in the context of their importance in understanding atmospheric nucleation processes.

Keywords. Nanosized Particles, Ice Nucleation, Particles in Snow

3.1. Introduction

Aerosols are airborne, condensed matter particles present as liquids, solids, or multi-phased, and are produced through anthropogenic and natural activities (Figure 3.1).[3-5] Little is known about the interaction of aerosol particles with and within clouds, and is highlighted as a major research uncertainty by the International Panel on Climate Change (IPCC).[6-7] The health implications of aerosols are also important due to growing evidence of the adverse health effects that nanoparticle air pollution causes.[8] As a notable example, the World Health Organization (WHO) named airborne particulate matter and, specifically, nanoparticles, a major cause of premature infant mortality.[9-10] Nanoparticles (1 to 100 nm[11]) are emitted into the atmosphere either directly or through gas-to-particle formation.[12] Yet, there is very limited research data on nanosized compounds that are in diverse environmental matrices and on the types of physical, chemical and biological processes, in which atmospheric nanoparticles are involved.

Snow is an important form of precipitation present near the ground surface, and can provide a snapshot of atmospheric physicochemical processes.[13] It is an omnipresent feature in polar and subpolar regions, as well as mountainous regions around the globe. The formation of snow in the atmosphere has been shown to drive local, regional and global climatic effects.[14] It also plays a central role in hydrological cycles, radiation and climate processes, such as precipitation,[15-16] which in turn causes removal of trace substances from the atmosphere, including select gaseous and particulate air pollutants.[17-18]

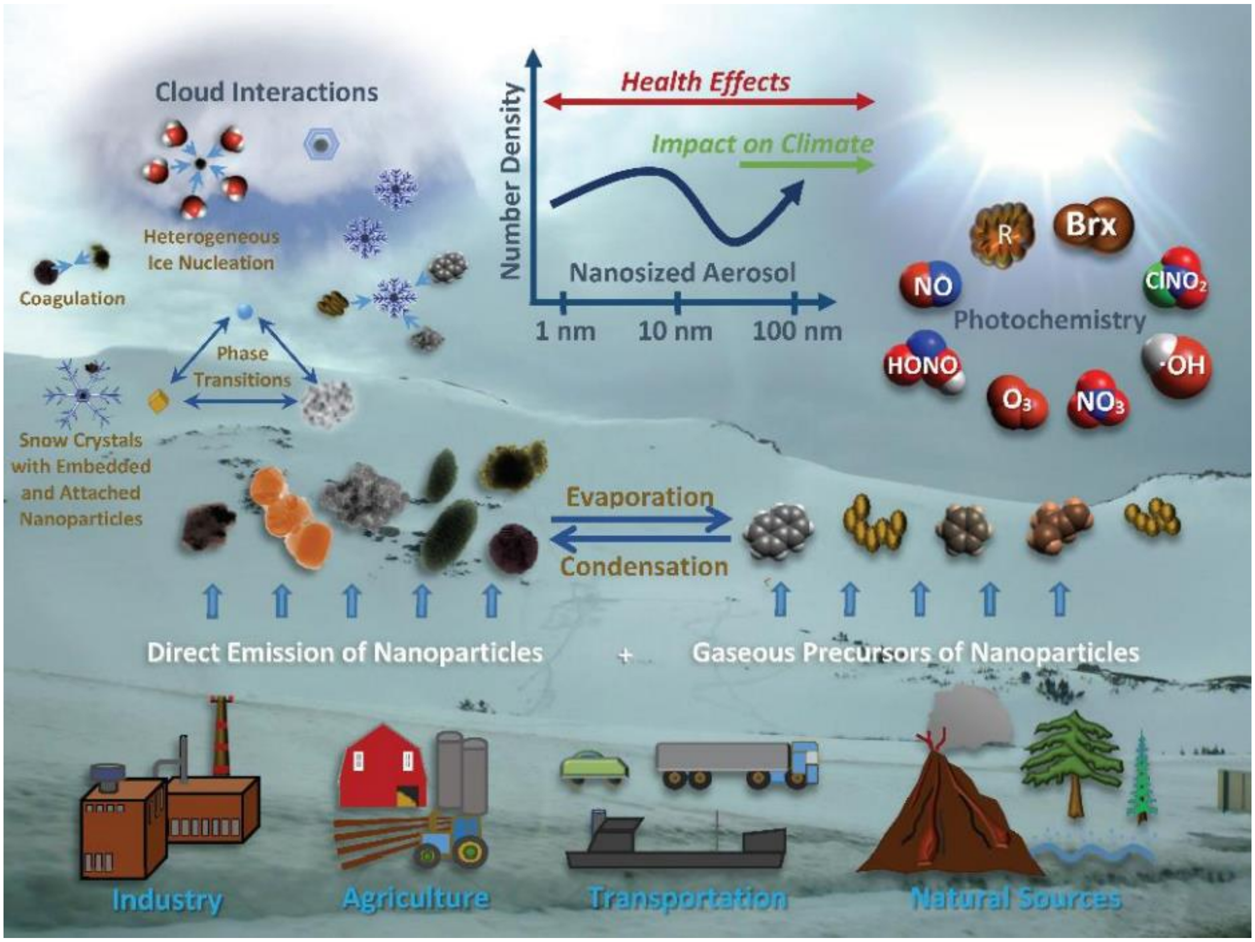

Figure 3.1 A simplified schematic of nanoparticle cycling in the atmosphere and snow-air interfaces. For simplicity, the splitting effects for clusters and the splintering effect of cloud microphysics are not shown.

The formation of snow starts with ice nucleation. When cooled, liquid water easily enters a metastable state, called supercooled water, remaining liquid well below its melting point, to temperatures as low as approximately −38 °C, or existing as a vapor at very high supersaturations.[19] In the atmosphere, such conditions are infrequent, with the exception of cirrus and other high tropospheric clouds.[20] More often, heterogeneous ice nuclei (IN) catalytically assist in the formation of ice or snow in the atmosphere at warmer temperatures. This heterogeneous ice nucleation process can occur by several mechanisms. When water vapor condenses directly onto a particle surface to form ice (deposition mode). When water vapor condenses directly onto the particle surface to form a water droplet which eventually freezes (freezing mode). When a water droplet comes into contact with an insoluble particle and freezes (contact mode). When an insoluble particle is already immersed in a water droplet and freezes (immersion mode).[14] It has been reported that the same aerosol particles will present different nucleation temperatures when acting in different nucleation modes. Moreover, factors, including solubility, surface tension, chemical impurities, volatility, morphology, contact angle, deliquescence, wettability, and chemical processes of aerosols are pivotal in understanding ice nucleation.[21-23]

The predominant global source of IN is currently considered to be mineral dust.[5, 24] Mineral dust exhibits size-dependent ice nucleation activity by deposition mode, which is less efficient at smaller particle sizes.[25] Although this is specific to the deposition mode, we can expect a similar trend for other modes.[21] Median freezing temperature induced by dust particles (200 - 800 nm in diameter) has been estimated at -33 to -35 °C.[26] In addition to mineral dust, carbonaceous particles have also been recognized as condensation IN,[27] as have plant and soil-borne organic particles.[28] Bioorganic particles, including bacteria, pollen, fungi and spores, that are known to possess ice-nucleating abilities, range in size from 500 nm to 80 µm. Although, recently, some fungal fragments smaller than 10 nm were found to be active in ice nucleation.[29] Among bioorganic ice nucleators, bacteria induce ice nucleation at the highest freezing temperatures, which can be as high as -2 °C (genus P*seudomonas*).[1, 30] Yet, due to the presumed scarcity of bioorganic particles in the atmosphere, there has not been sufficient evidence of their importance, for instance, in cirrus cloud formation.[31] Nevertheless, it has even been suggested that bacteria in the form of aerosols could act as condensation IN within the Arctic region.[32] It is worth mentioning that bacteria are typically micro-scale, and, correspondingly, most ice nucleation studies involving bacterial nucleators have been limited to larger particles of that size. Although smaller bacterial particles have been found in Arctic zones, their activity, as ice nucleators, has not yet been demonstrated.[33] Recent laboratory experiments point to size-dependent phase transitions of aerosol nanoparticles in mixed systems. Phase transitions, such as solubility and hygroscopic growth, can play an important role in the ice nucleation process, especially when considering the immersion mode.[34-35] As size plays a role in controlling these properties in nanoparticles, it is reasonable to think that size will affect nucleation by nanoparticles, along other properties such as contact angle. Currently, there is neither an atmospheric global model to explicitly include nanoparticles as relevant ice nucleating particles, nor does the IPCC consider them in major comparative modeling studies. However, of note is that nanoparticles are considered in human health impacts by both, the IPCC, and the WHO.[8] On another front, experimental challenges have so far precluded researchers from evaluating various hypotheses regarding the role of nanosized materials in snow formation.[25] Our group has recently developed novel methodologies overcoming some key challenges of the physico-chemical and morphological characterization and quantification of snow/ice materials.[1, 23, 36]

In this study, we set out to determine whether nanosized particles (operationally defined here as ≤ 200 nm in diameter) in air will affect the physical and chemical processes involved in the formation of snow and its transformations. We extensively characterized the physical, chemical and biological properties of snow from polar sites in Canada and the US, collected during the international experiments in Alert, Canada and Barrow, Alaska, and yearly over the last decade (2004-2014) at subpolar continental urban sites in Montréal and its surrounding suburbs. We provide evidence for the significant abundance of nanosized particles in snow, the importance of nanosized ice nucleators, and the potential role of biomaterials in nucleation processes.

3.2. Experimental and Methods

3.2.1. Sampling

Snow sampling sites, collection procedures, sampling and preservation protocols are described in detail elsewhere.[36-37] Snow samples were taken in 2006 and 2009, in Alert, Nunavut, Canada (82.5 °N; 62.3 °W; May – June, 2006) and in Barrow, Alaska, USA (71.3 °N; 156.8 °W; March 2009), respectively, and from 2004-2014 in the City of Montréal and in its suburbs, in Quebec, Canada. Briefly, samples were collected under sterilized conditions, using sterile equipment and clean suits, during snow precipitation events or within one hour of snowfall from the upper 3 cm of the snowpack. All samples were kept frozen immediately after collection at -10 ± 2 °C; many samples were analyzed within 24 hours following sampling, and others were frozen at -35 ± 2 °C, and were only thawed, within their gas-tight recipient container, immediately prior to analysis under clean conditions. To ensure high quality analysis, comparison of the blanks and dedicated frozen control samples from Alert and Barrow were performed, on a monthly basis. In addition to fresh surface snow, chemical and physical analysis of aged samples was performed.

As the thawing-refreezing cycle required for this analysis would disrupt particle size distribution in the samples,[38] only fresh samples from the series were used for all particle analyses in this study.

3.2.1.1. Barrow, AK, USA

Snow sampling was performed during the Ocean - Atmosphere - Sea Ice – Snowpack (OASIS) 2009 campaign in Barrow, AK, USA. Samples for microorganism analysis and volatile organic compounds (VOC) analysis were taken between March 4th and 20th. A field dedicated to snow studies in the clean air sector at 71.31° N, 156.6° W, 400 m southeast of the Barrow Arctic Research Center (BARC) was used for all sampling events. To limit local pollution, vehicle access to the site was restricted and all equipment was transported on foot with a hand-pulled sled. Sampling equipment included: sterile single-use containers, tools and glassware, pre-cleaned prior to departure by soaking in nutrient-free detergent, rinsing with 3 % hydrochloric acid, followed by three ultra-pure water rinses. For each event, sterile amber glass sample containers with a volume of 950 mL (Daniels Scientific) were filled with snow using a fresh, sterile, HDPE spoon (Fisher Scientific). As the snow samples originated from the top 3 cm of the snow surface, they are, therefore, heavily influenced by wind conditions and photochemistry. During snow sampling, snow temperature was measured using a long-stemmed thermometer (Fisher Scientific), and meteorological conditions were recorded (air temperature, wind direction, and cloud cover). Samples were stored in a walk-in freezer set to -20 °C until shipment in commercial coolers (Coleman). Once shipped out by airfreight (transit time 41 hours), the maximum temperature measured upon arrival to the laboratory at McGill University in Montréal was -10 °C, where storage continued in a freezer at -35 °C until analysis was initiated, by melting.

3.2.1.2. Alert, NU, Canada

Samples presented here were collected in Alert, NU on Ellesmere Island from May to June 2006. The study location was near the Alert meteorological station, chosen to avoid local contamination from a nearby military base. Sampling was performed on a flat plateau, upwind approximately 6.5 km away from the base. The site was accessed by truck parked downwind, with the final leg of approximately 500 m reached on foot in accordance with on-site regulations. All equipment was transported with a hand-pulled sled. For select sites in Alert, depth profile samples were collected from a snow pit dug with a pre-cleaned and sterilized shovel. Depth profiling was completed over the course of no more than 3 hours.

3.2.1.3. Montreal, QC, Canada and its Suburbs

Sterile snow sampling equipment was employed, using procedures as described above, and samples were kept frozen upon collection. Sampling was undertaken on a bi-weekly basis, during the winter months of December to April over a decade (2004-2014). Fresh snow samples were regularly analyzed within the same day. In addition to fresh surface snow, the depth profiles, as well as analysis of aged samples were performed for physical, biological and chemical characterization.

3.2.2. Aerosol Size Distributions

We used a NanoScan™ Scanning Mobility Particle Sizer (SMPS) model 3910 (TSI Inc.) to measure particle size distributions from aerosolized melted snow samples in terms of electrical mobility diameter, and an Optical Particle Sizer (OPS) model 3330 (TSI Inc.) to obtain particle size distributions as aerodynamic diameter. Melted snow was aerosolized using a C-Flow 700d PFA Nebulizer (Savillex Corporation) for a total aerosol flow rate of 0.9 SL/min (SL stands for liters at standard temperature and pressure, 273.15 K, 100 kPa). The aerosol stream was dried using an in-house-built double diffusion dryer and diluted to 1 L/min with particle-free air to match the combined sampling flow rates of the NanoScan™ SMPS and the OPS. These instruments are factory-calibrated on a yearly basis with Polystyrene Latex (PSL) spheres, and for all the internal and external flow rates.

It is important to note that electrical mobility and aerodynamic diameters, measured by the two above-mentioned aerosol instruments, are different metrics based on different physicochemical particle properties. Two different particle size regions are measured using the two techniques. The NanoScan™ SMPS system effectively measures in the range 10 nm to ~350 nm, whereas the OPS system measures larger particle sizes – confidently within the size range of ~350 nm to 10 µm. The aerodynamic diameter measured by the OPS is similar to the electrical mobility diameter, under the assumption that particles are spherical with densities of 1.0 g/cm.[3] [39] We only make this assumption when discussing the SMPS and OPS aerosol particle size measurements, and not for any other results. When operated simultaneously, the two aerosol instruments perform particle size measurements from 10 nm to 10 µm.

The approach of melted snow aerosolization and subsequent sizing of the resulting airborne particles has a number of advantages over other techniques used to characterize particulate matter in snow. Nebulization with compressed air generates aqueous droplets containing particulate matter originally present in snow. When these droplets are dried by a diffusion dryer, only the core particles remain.[40] Desalination of the snow samples by dialysis prior to aerosolization minimizes salt particle formation and crystallization on aerosol particles in the drying process. Note that potential modifications of the original size distribution of soluble salts may have occurred as snow was melted. Aerosol size distributions were the average of 5 runs for each sample.

3.2.3. Hydrodynamic Diameter Distribution

The hydrodynamic size distributions of unprocessed snow were measured by Nanoparticle Tracking Analysis (NTA) using a Malvern NanoSight NS500 with a laser wavelength of 532 nm and an Electron Multiplying Charge Coupled Device (EMCCD) camera. The capture settings were set to a 29.0099 ms shutter speed, 309 camera gain, a 17.8 fps frame rate and a temperature of 26.6 °C. The hydrodynamic diameter, also called Stokes diameter, is by definition the diameter of a hypothetical rigid sphere that diffuses in a liquid at the same speed as the sample particle.[39] The diameter includes the electric double layer around the particle. This technique is based on the visualization of particles in a liquid medium and tracking their Brownian motion to determine the size of individual particles allowing analysis directly of the original unprocessed, as well as processed (filtration, dialysis) melted snow samples. Hydrodynamic diameter distributions were obtained by averaging 10 runs per sample. Weighed standard deviations were plotted.

3.2.4. Matrix-Assisted Laser Desorption/Ionization Time-Of-Flight Mass Spectrometry (MALDI-TOF-MS/MS)

Samples were filtered with a Millex syringe filter with a 0.22 µm pore size hydrophilic PVDF membrane, concentrated using a Thermo ModulyoD-115 freeze dryer for 1 day and desalted with a ZipTip C18 reversed phase column in order to lower matrix-cluster formation that can generate background interference in the analysis of peptides.[41] A 50:50 acetonitrile to water solution and 0.1 % trifluoroacetic acid (TFA) aqueous solution were used to wet and equilibrate the ZipTip column. Passing a sample through the column binds the peptides in the sample onto the ZipTip column. The ZipTip was washed with a 0.1 % aqueous TFA solution to remove excess salts. Elution of peptides into the matrix was performed with the same 50:50 acetonitrile to water solution and 0.1 % TFA solution. Concentrated and desalted samples were deposited on a pre-spotted AnchorChip PAC II 384/96 α-cyano-4-hydroxycinnamic acid (HCCA) by spotting two to three 0.5 μL drops of the solution. MALDI spectra were collected using a Bruker AUTOFLEX III time-of-flight mass spectrometer (TOF-MS/MS) operating in linear positive ion mode. The MALDI/LDI ionization source was a 355 nm frequency tripled Nd:YAG SmartBeam™ laser (Bruker). The resolution of the instrument in linear mode is ≥ 5, 000 with a mass accuracy of ≤ 20 ppm for protein samples.

3.2.5. Electrospray Ionization Mass Spectrometry (ESI/MS)

Snow samples were analyzed without further processing other than melting at room temperature. Mass spectra were collected using an Agilent Technologies 6130 Series Quadrupole LC/MS System with an electrospray ionization (ESI) source. The ESI-MS instrument has an isotopic resolution at 10,000 u/sec and a mass accuracy within the calibrated mass range of ± 0.13 u in scan mode. The mass range used was from 1000 to 2000 Da, positive scan, N_2 as drying gas at 350 °C flowing at 11 L/min. The fragmentation voltage was set to 70 V, capillary voltage to 3000 V, with the flow rate of melted snow at 150 μL/min, and a total run time of 5 min.

3.2.6. Total Organic Carbon (TOC)

Unprocessed samples of freshly melted snow were analyzed with an Aurora 1030W TOC analyzer using a persulfate oxidation method. A 5 ml aliquot of water was used from each sample. To detect total inorganic carbon, 0.5 ml of 5 % phosphoric acid was added to the subsample and combusted at 700 °C. Afterwards, to detect organic carbon, 2 ml of 10 % sodium persulfate was added and combusted at 980 °C. The resulting CO_2 gas from these two reactions was detected separately by a nondispersive infrared sensor (NDIR). Each sample was processed in duplicate or triplicate. External standards (0 and 5 ppm) were included in each batch of samples to ensure consistency of results between analyses.

3.2.7. High-Resolution Transmission Electron Microscopy with Energy Dispersive X-Ray Spectroscopy (HR-TEM-EDS)

Snow samples were stored in 50 mL sterile plastic conical tubes at -20 °C until processed. The samples were melted and filtered, as mentioned above, and pre-concentrated and freeze dried using a Thermo ModulyoD-115 freeze dryer for 1 day prior to HR-TEM. Aliquots of 5 μL concentrated samples were deposited on glow discharged carbon film coated copper electron microscopy grids. The droplets were kept on the grids for one minute, followed by blotting off the excess liquid with an edge of a piece of filter paper. The samples were stained with 2 % uranyl acetate (SPI-Chem) and air-dried before being imaged using a FEI Tecnai 12 Biotwin TEM microscope (FEI Electron Optics) equipped with a tungsten filament, at 120 kV. Alternatively, uranyl formate (Electron Microscopy Sciences (EMS)) was used to stain replicate samples. Images were acquired using an Advanced Microscopy Techniques, Corp. (AMT) XR80C CCD Camera System.

3.2.8. Drop-Freezing Assays

Microphysics experiments were performed on snow from each of the three sampled sites. All snow samples were left to melt at room temperature (23 ± 0.5 °C) in their gas-tight containers. Drop-freezing assays were performed, as described by Vali,[42] with several samples from each site, using both filtered and unfiltered samples, as well as centrifuged. Samples were centrifuged using a Hermle Z200M/H bench-top centrifuge at 4000 rpm for 15 min (about 1000 g). For each sample, 240 droplets were placed on a cooling plate (in-house made copper plate) and the temperature of the plate (starting at ~0°C) cooled at a rate of 1 °C/min. The temperature, at which each droplet froze, was recorded.[1] All experiments were run with filtered versions of the same samples. Filtration was performed as described above. The copper plate was evenly coated with Vaseline petroleum jelly. The samples were loaded as 10 μL droplets. Ultra-pure water droplets from a

Simplicity 185 Ultrapure Water System (Millipore Corporation) and tap water were used as blank controls.

3.2.8.1. Ice Nucleation Data Analysis

For comparison of drop-freezing assay populations, we performed the analysis using the MATLAB function ttest2, which tests the null hypothesis that data in 2 different populations are independent random samples from normal distributions with equal means and equal but unknown variances at a 95 % confidence level.

3.2.9. Ion Chromatography

For ion analysis of snow samples, a Dionex ICS-500 Ion Chromatography system was used along with a separation column Dionex AS14 with 3.5 mM Na_2CO_3/ 1.0 mM $NaHCO_3$, as mobile phase for anions, and a separation column Dionex CS12 with 20 nM methanesulfonic acid, as mobile phase for cations. Ions analyzed included: sulfate, phosphate, nitrate, chloride, sodium, potassium, magnesium, calcium and ammonium. The mobile phase flow rate for analysis of anions was 0.30 mL/min and for analysis of cations 0.25 mL/min. Detection was performed by suppressed conductivity using an Anion Self-Regenerating ASRS 300 2mm and a Cation Self-Regenerating CSRS Ultra II 2mm suppressor. The detection limit for all ions was 0.1 ppm. Analysis was performed in triplicate using 10 μL samples of melted snow.

3.2.10. Materials and Supplies

Chemical reagents were purchased from Sigma-Aldrich and gaseous compounds were obtained from Praxair. TraceClean wide mouth packers, amber glass for sampling and storage of snow samples were obtained from VWR International. DNA extraction and purification kits were obtained from Qiagen and Epicentre Technologies. Millex syringe filters with a 0.22 μm pore size hydrophilic PVDF membrane, as well as ZipTip C18 reversed phase columns, were obtained from

EMD Millipore Corporation. The pre-spotted AnchorChip used for MALDI-TOF was obtained from Bruker Biosciences Corporation. Along with the 0.22 μm pore size filter, we utilized 0.1 μm pore size filters, but as there was a lack of statistically significantly difference under our experimental conditions, we only discuss the results obtained with the 0.22 μm pore size filter in this publication.

3.3. Results and Discussion

3.3.1. Nanosized Particle Size Distributions

Size distributions of particles in aerosolized fresh snow samples as a function of the electrical mobility diameter as well as aerodynamic diameter are depicted in Figure 3.2a (red bars). We observed that in all studied snow samples from all three sites, there is a substantial fraction of particles that have electrical mobility diameters smaller than 200 nm (about two orders of magnitude higher in abundance than at larger sizes). It is worth mentioning that in Montréal, there are several sources of local pollution from the hospitals, motor vehicles, waste processing and other industry, water and wastewater treatment, and so forth.[43] This local pollution may have an effect on the snow particle size distribution.

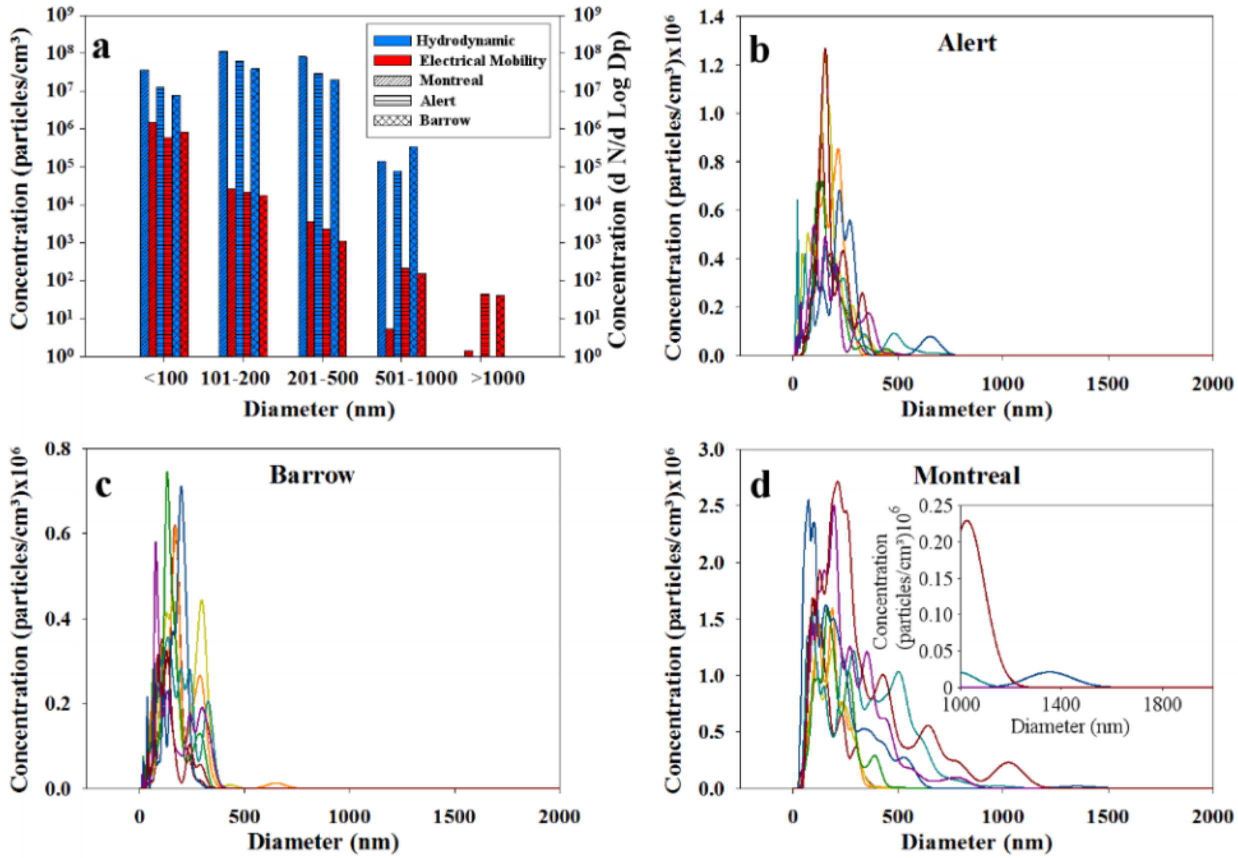

Figure 3.2 Size distributions of snow-borne particles. (a) Measured concentrations of particles as a function of particle size (logarithmic scale) using both nanoparticle tracking analysis (NTA) and aerosolization techniques in Montréal, Alert and Barrow. (b-d) Particle abundance as a function of hydrodynamic diameter for several snow samples from Montréal, Alert and Barrow sites; different colors represent different samples.

At electrical mobility diameters greater than 200 nm, we observe a decline in the concentration of particles. Furthermore, a decrease in particle concentration becomes more noticeable at aerodynamic diameters greater than 300 nm. Although we cannot correlate electrical mobility diameter with aerodynamic diameter directly, both provide a good approximation of the impact of size on the concentration of particles in snow. Conversion of electrical mobility into aerodynamic diameter is theoretically possible, though parameters, such as the shape of particles and their density, need to be known. These properties differ substantially depending on particle structure and composition. For simple aerosols or standard suspensions and colloid solutions, these parameters are available, however for environmental samples, the number of types of particles is so large that it becomes virtually impossible to perform an accurate conversion, and thus, as done by other researchers,[44-46] in order to prevent introduction of error of unknown scale, we report the original metrics without conversion. We also note that, although the dialysis of samples reduced potential formation of particles from soluble non-volatile constituents of melted snow during aerosol drying, the effect cannot be fully eliminated. As a result, a certain portion of smallest particles measured by the aerosol instruments are likely from substances dissolved in melted snow that persisted after dialysis.

To complement the aerosolization process, and to directly investigate particles in the liquid melted snow, we measured hydrodynamic diameter by NTA, as shown in Figure 3.2. The number density of particles measured by NTA (Figure 3.2a, blue bars) was consistently higher than when measured in aerosol phase as electrical mobility and aerodynamic diameter in the ranges of 101-200 and 201-500 nm, correspondingly, with a number density peak at approximately 200 nm (Figure 3.2b-d). Moreover, particles less than 500 nm in hydrodynamic diameter represented an absolute majority of the total observed particles in snow matrices, under the experimental conditions used. We note that the particle hydrodynamic diameter distributions (Figure 3.2b-d) are fitted to the total concentration measurement, so that the areas underneath the curves match the total particle concentrations in the samples. We cannot directly correlate the diameter measured by NTA to the electrical mobility diameter, nor with the aerodynamic diameter. We also could not assess whether the total concentration of aerosols correlates with the concentration of particles in snow meltwater, hence normalization of aerosol concentrations by volume of melted snow was not possible. Therefore, the value of aerosol measurements lies in determining most abundant particle sizes. However, we can confidently confirm that nanosized particles (≤ 200 nm) dominate the total aerosol distribution (Figure 3.2a).

3.3.2. Chemical Composition of the Observed Nanosized Materials and Particles

We identified a significant amount of total (dissolved and suspended) organic (TOC) compounds in snow samples, as listed in Table 3.1. In an earlier study, we had already confirmed presence of certain volatile and semi-volatile organic compounds in snow samples from the sampling sites during the same period.[37] With 2 samples analyzed per site for three locations, the total number of samples analyzed is quite limited, and indeed should not represent typical TOC values in the Arctic. These measurements merely represent the total carbon content of samples taken under experimental conditions, described herein. We expect much more variability with more samples over a wider range of Arctic regions were performed.[47-49] We therefore encourage additional research to provide a broader range of TOC content across a wider range of Arctic regions and different seasons.

To characterize the chemical composition of the nanosized fraction specifically, we performed MALDI-TOF analysis on pre-concentrated samples. We discarded the possibility of matrix interferences, as the observed peaks did not systematically correspond to known matrix cluster signatures (Figure B.2).

Table 3.1 Total Organic Carbon (TOC) and ion concentrations (ppm) in 2 snow samples from the 3 sampling sites (σ: standard deviation of at least 3 repeats; detection limit: 0.1 ppm). Data for different snow samples from Barrow, Alaska, USA; Alert, Nunavut and Montréal, Québec, Canada.

Sample (ppm)	TOC	SO_4^{2-}	PO_4^{3-}	Cl^-	NO_3^-	Na^+	K^+	Mg^{2+}	Ca^{2+}	NH_4^+
Alert 1	1.3	0.4	< 0.1	12.76	< 0.1	7.12	0.23	0.87	1.01	< 0.1
σ	0.0	0.1	< 0.1	0.26	< 0.1	0.22	0.02	0.04	0.07	< 0.1
Alert 2	1.5	0.4	< 0.1	16.78	< 0.1	7.13	0.26	0.98	0.74	< 0.1
σ	0.1	0.1	< 0.1	0.14	< 0.1	0.31	0.02	0.06	0.08	< 0.1

Barrow 1	2.5	0.7	< 0.1	13.59	< 0.1	5.24	0.21	0.66	1.06	< 0.1
σ	0.1	0.0	< 0.1	11.05	< 0.1	4.13	0.03	0.50	0.35	< 0.1
Barrow 2	2.2	0.5	< 0.1	7.91	< 0.1	3.70	0.19	0.51	0.58	< 0.1
σ	0.1	0.0	< 0.1	0.07	< 0.1	0.14	0.02	0.02	0.05	< 0.1
Montreal 1	4.0	0.8	< 0.1	0.29	< 0.1	0.48	0.09	< 0.1	0.86	< 0.1
σ	0.0	0.0	< 0.1	0.01	< 0.1	0.10	0.02	< 0.1	0.04	< 0.1
Montreal 2	1.5	1.5	< 0.1	11.40	< 0.1	4.74	< 0.1	0.59	5.16	< 0.1
σ	0.0	0.0	< 0.1	0.05	< 0.1	0.16	< 0.1	0.02	0.06	< 0.1

The measured MALDI-TOF spectra are inconsistent with inorganic materials, but are similar to those for bioorganic materials, such as macromolecules with mass-to-charge ratios from 1100 to 1350 Da,[41] consisting of compounds such as amino-acids or monomers. We certainly cannot suggest that HUmic LIke Substances (HULIS) were absent in the sample, or that they were not isolated by the column along with peptides. However, it must be noted that the molecular weights of most simple HULIS are relatively smaller in comparison with the molecular weights found in this study by MALDI. Furthermore, the repetition of specific mass units, as illustrated in the MALDI-TOF spectrum in Figure 3.3, suggests a possible polymeric structure. The patterns of monomer loss upon ionization are also indicative of macromolecules of polymeric nature.[50-51] We suggest specific amino acids, molecular weights of which match the above-mentioned mass decreases, so the potential polymers are likely peptides, and are shown in Figure 3.3a. Moreover, proteins and macromolecules have previously been observed in atmospheric aerosols,[52-53] as well as ice and snow.[54]

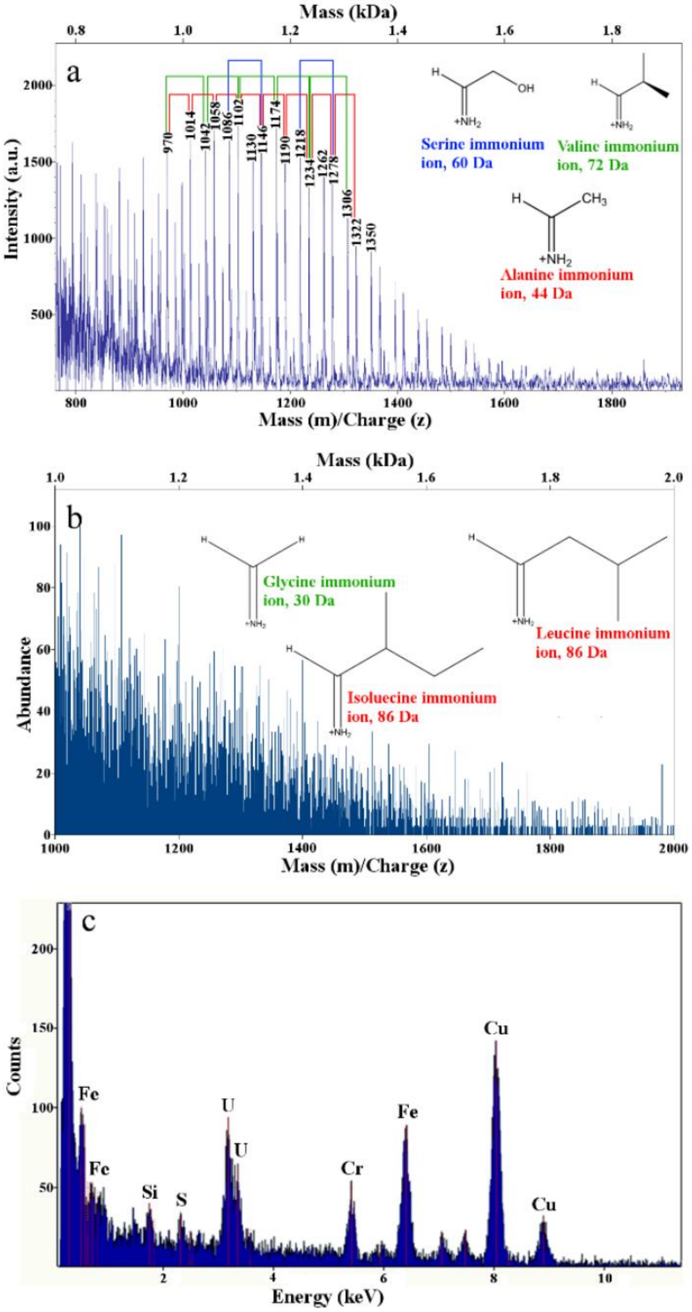

Figure 3.3 Examples of a) MALDI-TOF MS mass spectra depicting patterns related to bioorganic materials with suggested structures; b) ESI/MS spectra showing relatively high molecular mass with suggested structures in case the analyzed molecules are in fact peptides; c) EDS showing elements such as silicon and iron, which are usually found in ice nucleating mineral dust particles.

Even extracellular polymeric substances have been found in diamond dust from the Arctic.[55]

Using the soft ionization technique of electrospray mass spectrometry, shown in Figure 3.3b, we obtained an almost identical spectrum to MALDI-TOF mass/charge ratio range, supporting the existence of bioorganic materials such as various amino acids.

TEM images provided evidence for the existence of numerous sub-micron particles in snow samples with sizes of ~500 nm and smaller, as illustrated in Figure 3.4.

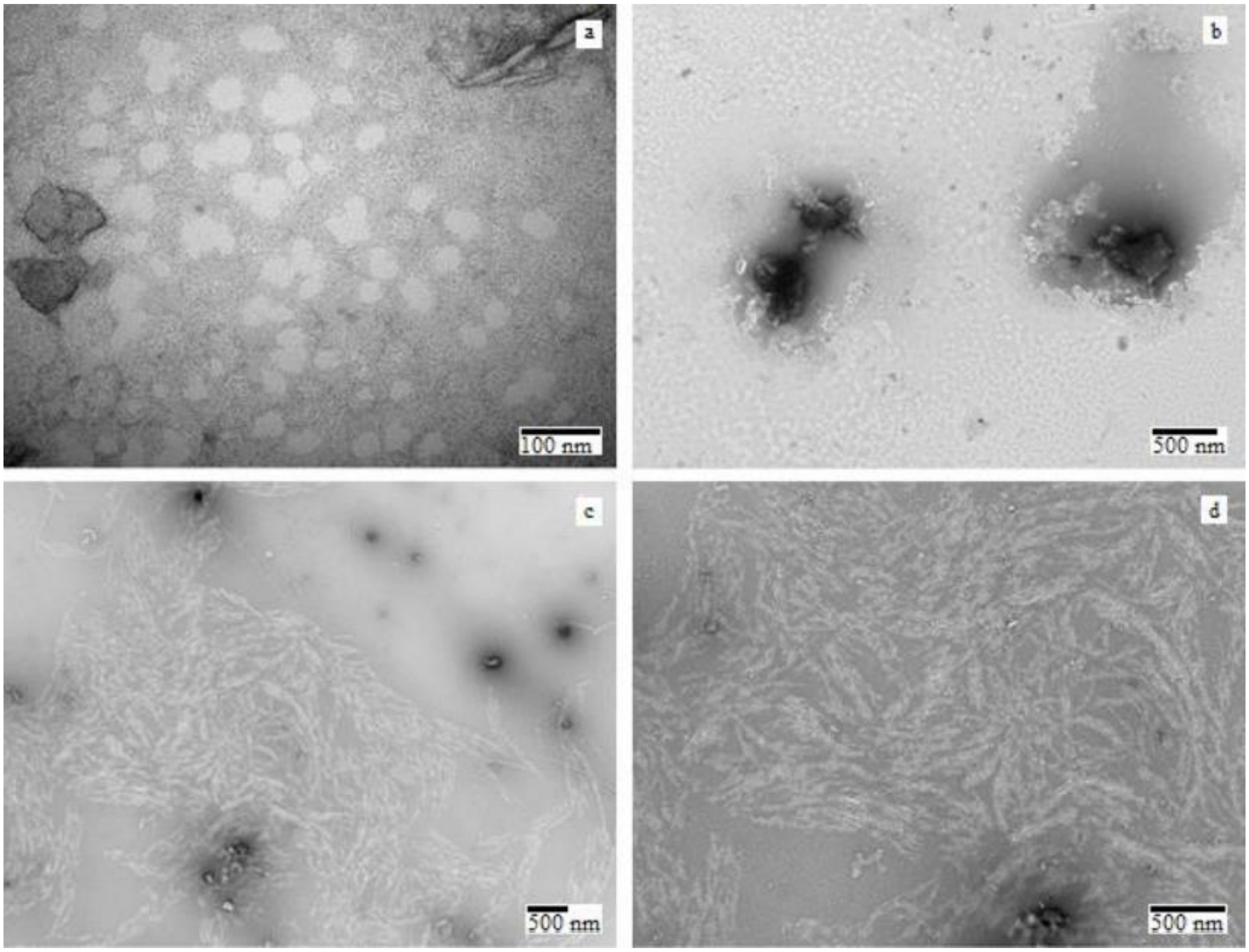

Figure 3.4 Electron microscopy images of filtered snow samples depicting filaments and vesicles likely of organic origin, and the probable presence of some inorganic compounds.

It is important to mention that sizes of these particles, identified by electron microscopy, do not match hydrodynamic diameter as only the electron-contrast cores of particles, excluding any electron-transparent coatings, are visible in TEM, and also because the hydrodynamic diameter includes the double electric layer. Nevertheless, we can observe that these particles are still nanosized, and dominate the electron microscopy images. Furthermore, the shape of these particles resembles globular structures (Figure 3.4 a-b), as well as fibrous structures (Figure 3.4 c-d) typically adopted by polymers and peptides/proteins.[56] High-electron-contrast particles are likely inorganic in nature, whereas low-electron-contrast particles are probably bioorganic in nature,[57] which is consistent with our mass spectrometry analysis shown in Figure 3.3. Note that the uranium-based negative stains we used do not bind to most organic matter leaving it low-contrast.[58]

EDS analysis also revealed presence of inorganic components in the snow samples containing elements common to inorganic particles, such as iron and silicon (Figure 3.3c), reported in literature.[24, 59-60] The electron micrographs, shown in Figure 3.4, suggest an abundance of particles that are likely organic in nature, as the negative stain did not bind to them revealing sharp boundaries between the particles and the background.[55, 61]

3.3.3. Nanosized Ice Nuclei

Figure 3.5 illustrates the cumulative nucleus distribution of over 20,000 data points in all three sampling locations, obtained by drop-freezing experiments. We had two distinct sampling sites at each location. The number of active nuclei at or above a certain temperature is $[\ln N_0 - \ln N(\theta)]V^{-1}$, where N_0 is the total number of drops in the experiment, $N(\theta)$ is the number of unfrozen drops at a certain temperature θ, and V is the volume of the drop. Note that the cumulative nuclei concentration is not a direct measure of the number concentration of particles in a solution or suspension. The shape of a logarithmically scaled spectrum offers insight into non-uniformities among nuclei since the various nuclei differ in their nucleating activities independently from one another.[42]

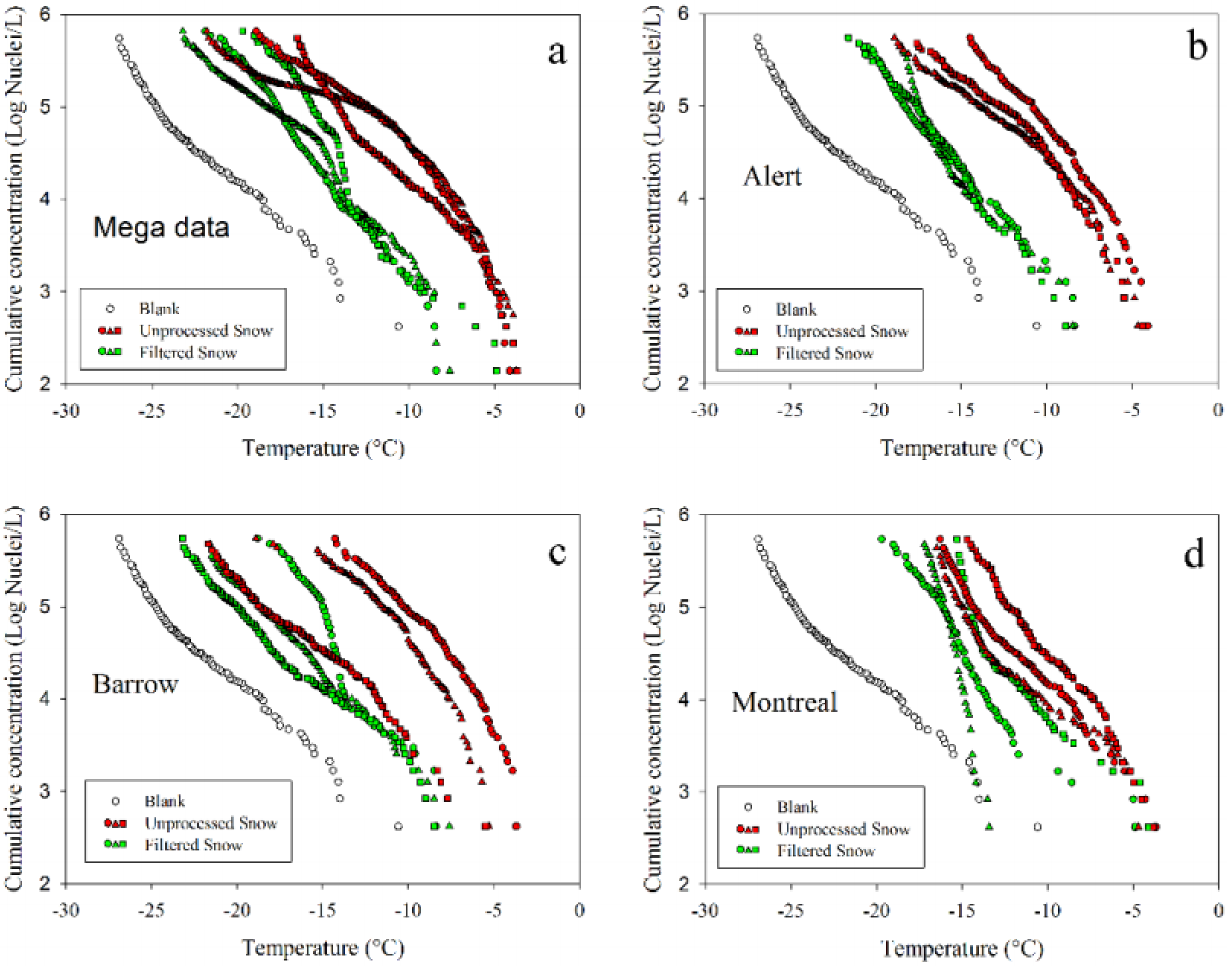

Figure 3.5 Comparison of the cumulative nucleus spectra (Log10, Ice Nuclei/Liter) of the top layers (3 cm) of surface snow samples. (a) All sampled sites; b) Alert, Nunavut; c) Barrow, Alaska; and d) Montréal, Québec. Same symbol shapes represent the same sample types in all regions. The mean freezing temperatures of unprocessed snow are for Barrow -12.52 °C (Standard Deviation (σ): 8.58); Alert -11.48 °C (σ: 2.94); and Montréal -12.82 °C (σ: 2.60). The mean freezing temperatures of filtered snow are for Barrow -17.3 °C (σ: 7.8); Alert -17.1 °C (σ: 6.3); and Montréal -15.0 °C (σ: 1.7).

We observed that the drop-freezing assay data points of freshly melted snow, with particles already immersed in water, vary within and across the sites (Figures 3.5, 3.6, 3.7) ranging from (-17.0 ± 2.5) to (-4.4 ± 0.7) °C (red curves). Interestingly, we also observed that the filtered snow samples (green curves) showed distinctly different ice nucleation patterns to their respective unfiltered counterparts (-19.6 ± 2.4 to -8.1 ± 2.6 °C). The mean freezing temperature of all data points (all locations) corresponding to unprocessed snow samples was -12.0 ± 6.4 °C, whereas the mean freezing temperature of all data points corresponding to filtered snow samples was -17.2 ± 7.1 °C. With these two mean temperature values, we performed a t-test with a significance level of 5 %. The p-values obtained suggest these two types of samples are two different populations.

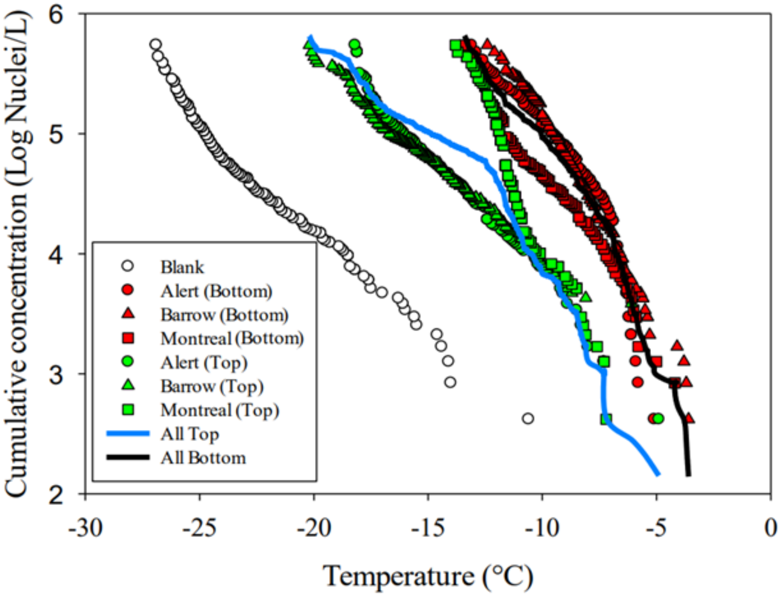

Figure 3.6 Cumulative nucleus spectrum of centrifuged snow samples. From Alert, Nunavut (●); Barrow, Alaska (▲); and Montréal, Québec (■). Green curves represent samples from the top 1 cm layer of centrifuged samples, and red curves represent samples from the bottom 1 cm layer of a 1.5 mL conical vial. The blue line is the average of samples from the top layer, whereas the black line is the average of samples from the bottom layer.

Ice nucleation study results suggest two different populations for unprocessed and filtered snow. However, there is a possibility that the filtering process leads to an alteration of select physical characteristics and/or the chemical composition of the particles,[62] which could in turn affect their nucleating ability. We therefore also centrifuged our snow samples to separate different particles without potential alterations from particle-filter interactions (Figure 3.6). The centrifugation process separates particles as a function of density. Since bacteria have been identified as the most efficient IN, we centrifuged our samples with an acceleration of about 1000 g (g force or relative centrifugal force) forcing large microorganisms like bacteria and any other high density particles like large mineral dust particles to settle to the bottom layer.[63] We performed drop-freezing experiments on droplets isolated from the top and bottom layers of the centrifuged samples (Figure 3.7). The statistical analysis indicated that the freezing temperatures of the top layer were lower than the ones at the bottom layer by ~ 4.4 °C, similar to the difference between filtered and unprocessed snow, shown in Figure 3.5. Statistical analyses on datasets from all sites indicated that both filtered and centrifuged populations of samples, representing snow without particles larger than 200 nm, exhibit significant differences from unperturbed snow samples (-13.2 ± 0.6 to -4.3 ± 0.8 °C), yet seem to be excellent IN (-17.6 ± 3.4 to -6.1 ± 1.2 °C). Conversely, it has been reported that the presence of soluble material coating inorganic particles can enhance their nucleating properties, one of the best known examples of this phenomenon being mineral dust particles coated by $(NH_4)_2SO_4$.[64-65] To eliminate the possible influence of dissolved ions on ice nucleation temperatures, we explored the ionic diversity in the studied snow matrices with the mean ion concentrations and standard deviations given in Table 3.1. We considered this especially important to check because salts such as $(NH_4)_2SO_4$ have been found in Arctic samples.[32] We determined it to be unlikely that compounds such as $(NH_4)_2SO_4$ would have a considerable effect on ice nucleation temperatures because, in most cases, the concentration of ammonium found in snow samples taken at different sites was below the detection limit.

Since there is no reference technique for measuring the number of nanosized ice nucleating particles in snow, to make an estimation, we use the assumption[24, 66-67] that approximately 0.1 % of these nanosized particles can exhibit ice nucleation abilities in the immersion mode. If this assumption is correct, our results suggest that snow nanosized particles' contributions to nucleation are significant, in comparison to micro-scale ice nucleating particles (Figure 3.2). Particles with diameters less than 200 nm amount to 38 – 71 % of all snow-borne particles, whereas nanoparticles account for ~ 11 % to 19 % of the total nuclei across a wide range of studied distinct snow types.

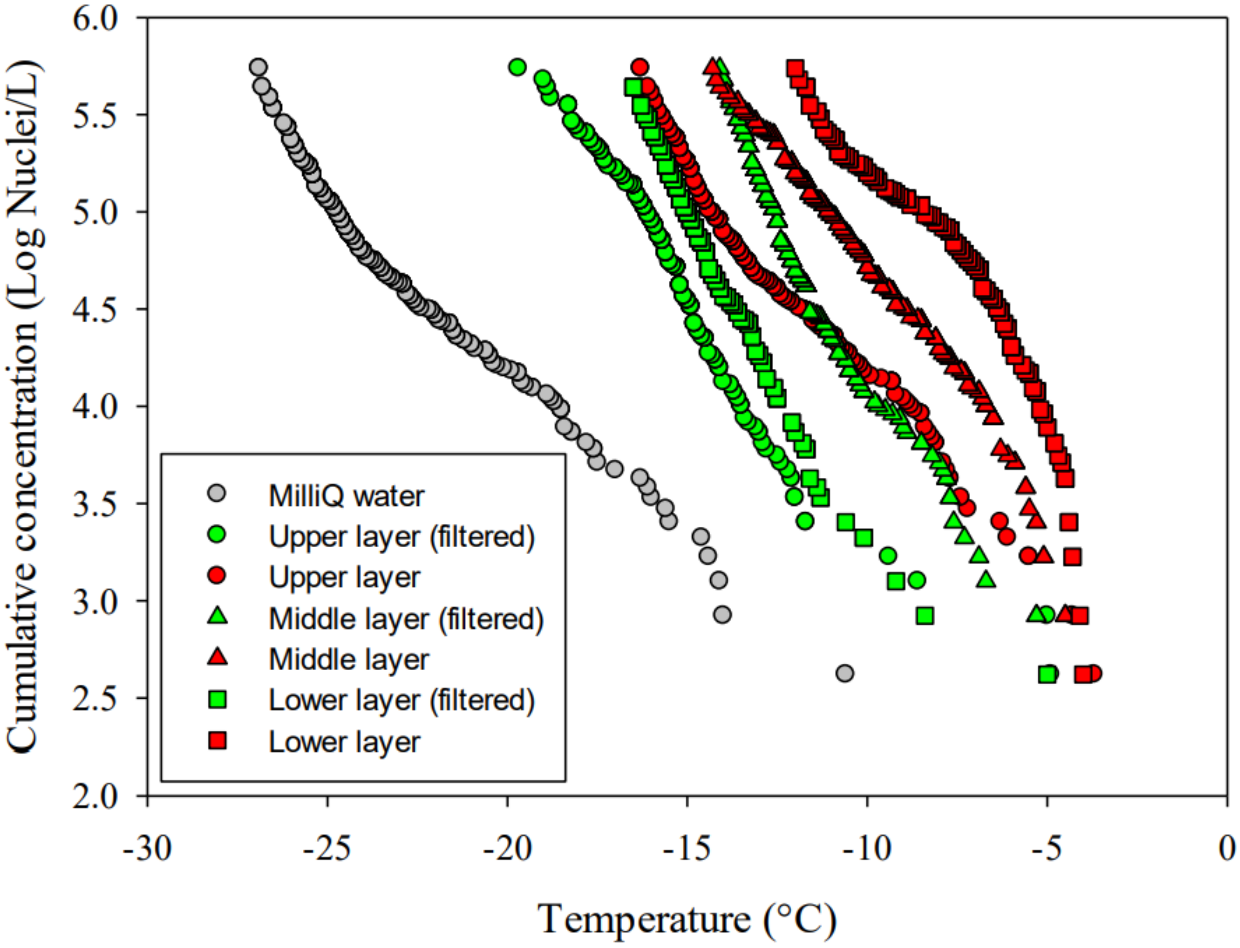

Figure 3.7 Cumulative nucleus spectrum of snow samples from Montréal, Québec, collected at different depths. Lower layer (■), 5 cm close to the ground, intermediate layer (▲), and top 3 cm of snow (●). Green curves represent samples containing particles with sizes smaller than 0.22 µm, and red curves represent unfiltered samples. Grey circles represent Milli-Q water for comparison.

In order to relate the particles in snow samples to their likely points of origin, we verified back trajectory data published in previous studies for the same dates in Barrow and Alert.[55, 61] Data from Barrow showed that most of the trajectories come from northern locations, that is, directly from the Arctic Ocean. This may explain the sea salt content within the samples. Similarly, data from

Alert showed that the air masses affecting the sampling area came primarily from northwest and southwest locations, again the Arctic Ocean, as well as some terrestrial locations, where organic particles could have originated from local vegetation.

3.3.4. Microbiological Diversity in Snow

Since bacterial species are considered to be among the most efficient identified IN, in a parallel study, we focused our research on the identity, population and ice nucleation ability of the bacterial and fungal communities in the different types of snow examined.[68] Complementary morphology of the identified taxa was obtained using TEM (Figure 3.8). Freezing point temperatures of bacterial isolates ranged from approximately -20 °C to -5 °C. These identified bacteria were generally larger than 1 µm. Therefore, the systematically elevated ice nucleation temperatures for nanosized particles observed in sampled snow at all snow collection sites cannot be explained. Microbial cellular materials, which are smaller in size, could, however, be a source of the observed nanoparticles, which are in agreement with the TEM observation of the vesicular and filament structures (Figure 3.4) in filtered snow samples, similar to some organic matter.[69-70]

It has been speculated that viruses could serve as potential nanosized IN.[71] We used several microscopy techniques and stains, routine for virus analysis,[72-73] for several samples taken during this study, but found no conclusive evidence of the presence of viruses within the samples. Nevertheless, this negative result does not entirely preclude the role of viruses in ice nucleation processes or lack thereof.

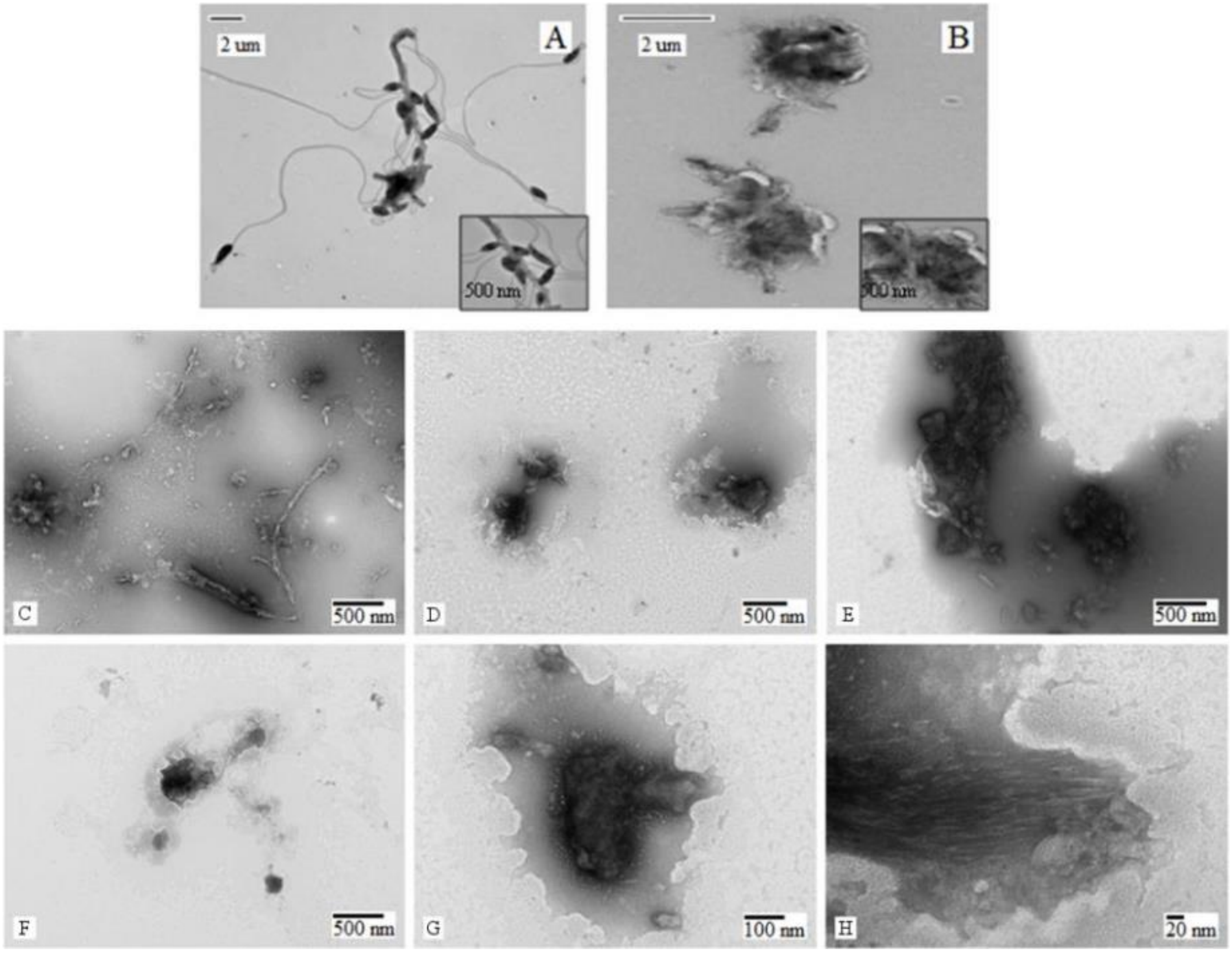

Figure 3.8 Electron microscopy images of snow samples. (A-B) Scanning Electron Microscopy (SEM) images of some microorganisms in different types of snow. (C-H) Transmission Electron Microscopy (TEM) images of filtered snow samples using a filter with a pore diameter of 0.22 μm.

3.3.5. Why do Nanosized Compounds Act as Efficient Ice Nuclei?

Both bioorganic compounds and inorganic nanoparticles were observed within our snow samples (Figure 3.4). Although inorganic compounds, containing elements such as iron are similar to nano dust particles, we cannot overrule iron containing biological remnants, which should be further studied. Our results support that some nanosized particles may exhibit similar ice nucleating temperatures as microscale mineral dust particles, under our experimental conditions. Since contact angle is a key parameter in determining the nucleation capability of particles,[74] further studies not only of size, but contact angle calculations under different environmental conditions, are recommended. Select theoretical studies have proposed that possible ice nucleation mechanisms are likely due to nanosized effects.[75-76] Considering the high abundance of the larger nanosized particles observed, ice nucleation may be altered due to possible additional active corner and edge sites for water uptake, larger total surface area, and complex surface curvatures. It is also conceivable that pores and cracks in these nanoparticles are inducing the formation of different crystal phases of ice that is more stable at warmer temperatures.[77] Adsorbed water molecules can be subjected to ideal conditions, which, at a nanosized level, form the first ice embryo from which ice can start growing.[77] We do not overrule the existence of other nanosized effects that have yet to be considered. Further research should be focused on understanding the nature of nanosized ice nucleators, namely their composition, phase, configuration, surface properties and evaluate whether these nanosized ice nucleators are mostly bioorganic in origin or not.

3.4. Concluding Remarks and Future Work

This work provides the snow-borne size-aggregated particle number density, distribution and chemical composition of snow, as well as microphysical data on ice nucleation of snow at various conditions at two Arctic sites during field campaigns and data, collected in Montréal over a decade (2004 – 2014). We showed for the first time that nanosized particles are the most abundant particle size in snow and that nanoparticles are abundant over a wide range of ecosystems studied. This study expands our previous understanding of the ubiquity of nanosized nuclei in precipitation.[78-79] As the phenomenon of ice-nucleating nanoparticles seems to be widespread in North American snow, these particles may have potential implications in cloud formation and consequently influence precipitation, biogeochemistry, ecosystem health and climate change. Further research should focus on understanding the nature of nanosized particles as ice nucleators. Specifically, their composition, configuration, surface properties, including active sites, size distribution, and mechanism(s) of initiation of ice nucleation should be investigated. In a changing climate with increases in the incidence of extreme weather, the transport of non-native chemicals to the polar regions is intensifying, and this in turn will potentially affect the diversity and distribution of chemicals in the polar regions, resulting in melting and refreezing of snow and ice. Lastly, since some snow-borne nanoparticles can have health effects,[9-10] further research on environmental and human toxicology is also recommended.

Acknowledgements. We cordially thank Drs. Mortazavi, Kos, Zuend, Yau, Vali, Li, Bottenheim, Shepson, and Mr. Saade for their help with field campaigns' logistics, with certain sampling and analysis procedures, and for providing valuable suggestions. We are grateful to Montréal Children's Hospital, TIS, Inc. and personally Ms. Sarah Sakamoto and Ms. Sherrie Elzie for access to a suite of nanoparticle analyzers. We also thank Jim (Avik) Ghoshdastidar for his help in proofreading the manuscript. We are grateful to the anonymous reviewers of this manuscript for their valuable suggestions that helped improve the manuscript. We acknowledge financial support from the Natural Sciences and Engineering Research Council of Canada, the Canada Foundation for Innovation, Fonds de recherche du Québec - Nature et technologies and from Environment Canada. All data used for this paper will be made available upon request to the corresponding author Parisa A. Ariya (parisa.ariya@mcgill.ca).

References

1. Mortazavi, R.; Hayes, C. T.; Ariya, P. A., Ice nucleation activity of bacteria isolated from snow compared with organic and inorganic substrates. *Environmental Chemistry* **2008,** *5* (6), 373-381.
2. O'Sullivan, D.; Murray, B. J.; Ross, J. F.; Webb, M. E., The adsorption of fungal ice-nucleating proteins on mineral dusts: a terrestrial reservoir of atmospheric ice-nucleating particles. *Atmospheric Chemistry and Physics* **2016,** *16* (12), 7879-7887.

3. Levin, Z.; Cotton, W. R., *Aerosol pollution impact on precipitation: a scientific review*. Springer Science & Business Media: 2008.

4. Andreae, M.; Rosenfeld, D., Aerosol–cloud–precipitation interactions. Part 1. The nature and sources of cloud-active aerosols. *Earth-Science Reviews* **2008,** *89* (1), 13-41.

5. Szyrmer, W.; Zawadzki, I., Biogenic and anthropogenic sources of ice-forming nuclei: A review. *Bulletin of the American Meteorological Society* **1997,** *78* (2), 209-228.

6. Stocker, T.; Qin, D.; Plattner, G.; Tignor, M.; Allen, S.; Boschung, J.; Nauels, A.; Xia, Y.; Bex, B.; Midgley, B., IPCC, 2013: climate change 2013: the physical science basis. Contribution of working group I to the fifth assessment report of the intergovernmental panel on climate change. **2013**.

7. Solomon, S., et al. Cambridge University Press: Cambridge, UK and New York, NY, USA, 2007; p 996.

8. Slezakova, K.; Morais, S.; do Carmo Pereira, M., Atmospheric Nanoparticles and Their Impacts on Public Health. **2013**.

9. WHO, World Health Organization. International Agency for Research on Cancer. Outdoor Air Pollution a Leading Environmental Cause of Cancer Deaths. *International Agency for Research on Cancer: Diesel Engine Exhaust Carcinogenic* **2013**.

10. WHO, World Health Organization. 7 million premature deaths annually linked to air pollution. *World Health Organization* **2014**.

11. Auffan, M., et al., Towards a definition of inorganic nanoparticles from an environmental, health and safety perspective. *Nature nanotechnology* **2009,** *4* (10), 634-641.

12. Buseck, P. R.; Adachi, K., Nanoparticles in the Atmosphere. *Elements* **2008,** *4* (6), 389-394.

13. Dibb, J. E., Overview of field data on the deposition of aerosol-associated species to the surface snow of polar glaciers, particularly recent work in Greenland. In *Chemical exchange between the atmosphere and Polar snow*, Springer: 1996; pp 249-274.

14. Seinfeld, J. H.; Pandis, S. N., *Atmospheric chemistry and physics: from air pollution to climate change*. John Wiley & Sons: 2012.

15. Simmel, M.; Heinrich, H.; Diehl, K., Ice Initiation for Various Ice Nuclei Types and its Infl uence on Precipitation Formation in Convective Clouds. In *Nucleation and Atmospheric Aerosols*, O'Dowd, C.; Wagner, P., Eds. Springer Netherlands: 2007; pp 427-431.

16. Morris, C.; Georgakopoulos, D.; Sands, D. In *Ice nucleation active bacteria and their potential role in precipitation*, Journal de Physique IV (Proceedings), EDP sciences: 2004; pp 87-103.

17. Flossmann, A.; Hall, W.; Pruppacher, H., A theoretical study of the wet removal of atmospheric pollutants. Part I: The redistribution of aerosol particles captured through nucleation and impaction scavenging by growing cloud drops. *Journal of the atmospheric sciences* **1985,** *42* (6), 583-606.

18. Flossmann, A.; Pruppacher, H., A theoretical study of the wet removal of atmospheric pollutants. Part III: The uptake, redistribution, and deposition of (NH4) 2SO4 particles by a convective cloud using a two-dimensional cloud dynamics model. *Journal of the atmospheric sciences* **1988,** *45* (13), 1857-1871.

19. Koop, T., et al., Water activity as the determinant for homogeneous ice nucleation in aqueous solutions. *Nature* **2000,** *406* (6796), 611-614.

20. Finlayson-Pitts, B. J.; Pitts Jr, J. N., *Chemistry of the upper and lower atmosphere: theory, experiments, and applications*. Academic press: 1999.

21. Hoose, C.; Möhler, O., Heterogeneous ice nucleation on atmospheric aerosols: a review of results from laboratory experiments. *Atmospheric Chemistry and Physics* **2012,** *12* (20), 9817-9854.

22. Keller, B. O., Li, L., Water activity as the determinant for homogeneous ice nucleation in aqueous solutions. *J. Am. Soc. Mass Spectrom.* **2000,** *11* (1), 88-93.

23. Ariya, P. A.; Sun, J.; Eltouny, N. A.; Hudson, E. D.; Hayes, C. T.; Kos, G., Physical and chemical characterization of bioaerosols – Implications for nucleation processes. *International Reviews in Physical Chemistry* **2009,** *28* (1), 1-32.

24. Archuleta, C. M.; DeMott, P.; Kreidenweis, S., Ice nucleation by surrogates for atmospheric mineral dust and mineral dust/sulfate particles at cirrus temperatures. *Atmospheric Chemistry and Physics* **2005,** *5* (10), 2617-2634.

25. Welti, A.; Lüönd, F.; Stetzer, O.; Lohmann, U., Influence of particle size on the ice nucleating ability of mineral dusts. *Atmospheric Chemistry and Physics* **2009,** *9* (18), 6705-6715.

26. Lüönd, F., et al., Experimental study on the ice nucleation ability of size-selected kaolinite particles in the immersion mode. *J. Geophys. Res.* **2010,** *115* (D14).

27. Rogers, D. C.; DeMott, P. J.; Kreidenweis, S. M., Airborne measurements of tropospheric ice-nucleating aerosol particles in the Arctic spring. *Journal of Geophysical Research* **2001,** *106* (D14), 15053.

28. Schnell, R.; Vali, G., Biogenic ice nuclei: Part I. Terrestrial and marine sources. *Journal of the Atmospheric Sciences* **1976,** *33* (8), 1554-1564.

29. Fröhlich-Nowoisky, J.; Hill, T. C. J.; Pummer, B. G.; Yordanova, P.; Franc, G. D.; Pöschl, U., Ice nucleation activity in the widespread soil fungus <i>Mortierella alpina</i>. *Biogeosciences* **2015,** *12* (4), 1057-1071.

30. Georgakopoulos, D. G., et al., Microbiology and atmospheric processes: biological, physical and chemical characterization of aerosol particles. *Biogeosciences* **2009,** *6* (1), 721–737.

31. Möhler, O., et al., Microbiology and atmospheric processes: the role of biological particles in cloud physics. *Biogeosciences* **2007,** *4* (1), 1059–1071.

32. Bigg, E. K.; Leck, C., Cloud-active particles over the central Arctic Ocean. *Journal of Geophysical Research: Atmospheres (1984–2012)* **2001,** *106* (D23), 32155-32166.

33. Leck, C.; Bigg, E. K., Biogenic particles in the surface microlayer and overlaying atmosphere in the central Arctic Ocean during summer. *Tellus B* **2005,** *57* (4), 305-316.

34. Biskos, G.; Paulsen, D.; Russell, L.; Buseck, P.; Martin, S., Prompt deliquescence and efflorescence of aerosol nanoparticles. *Atmospheric Chemistry and Physics* **2006,** *6* (12), 4633-4642.

35. Cheng, Y.; Su, H.; Koop, T.; Mikhailov, E.; Pöschl, U., Size dependence of phase transitions in aerosol nanoparticles. *Nature communications* **2015,** *6*.

36. Kos, G., Ariya, P. A., Volatile organic compounds in snow in the Quebec-Windsor Corridor. *J. Geophys. Res.* **2010,** *115* (D1).

37. Kos, G., Ariya, P. A., Determination of a wide range of volatile and semivolatile organic compounds in snow by use of solid-phase micro-extraction (SPME). *Anal. Bioanal. Chem.* **2006,** *385* (1), 57-66.

38. Kim, K.; Choi, W.; Hoffmann, M. R.; Yoon, H.-I.; Park, B.-K., Photoreductive dissolution of iron oxides trapped in ice and its environmental implications. *Environ. Sci. Technol.* **2010,** *44* (11), 4142-4148.

39. Hinds, W. C., *Aerosol technology: properties, behavior, and measurement of airborne particles*. 2, illustrated ed.; John Wiley & Sons, Inc.: New York, NY, 1999; p 483.

40. Tuch, T. M.; Haudek, A.; Müller, T.; Nowak, A.; Wex, H.; Wiedensohler, A., Design and performance of an automatic regenerating adsorption aerosol dryer for continuous operation at monitoring sites. *Atmospheric Measurement Techniques* **2009,** *2* (2), 417-422.
41. Caprioli, R. M., et al., Molecular Imaging of Biological Samples: Localization of Peptides and Proteins Using MALDI-TOF MS. *Anal. Chem.* **1997,** *69*, 4751-4760.
42. Vali, G., Quantitative evaluation of experimental results on the heterogeneous freezing nucleation of supercooled liquids. *Journal of the atmospheric sciences* **1971,** *28*, 402-409.
43. Gagnon, C.; Bessette, C.; Boulet, D.; Garneau, Y.; Paquette, P.; Mallet, R., Air Quality in Montréal. 2007 Annual Report, City of Montréal, Service des infrastructures, transport et environnement, Direction de l'environnement et du développement durable, Division de la planification et du suivi environnemental, RSQA, 12p. **2007**.
44. Nazarenko, Y.; Lioy, P. J.; Mainelis, G., Nanomaterial Inhalation Exposure from Nanotechnology-Based Consumer Products. In *Inhal. Toxicol.*, 3rd ed.; Salem, H.; Katz, S. A., Eds. CRC Press: 2014; p 623.
45. Nazarenko, Y.; Han, T. W.; Lioy, P. J.; Mainelis, G., Potential for exposure to engineered nanoparticles from nanotechnology-based consumer spray products. *J. Exp. Sci. Env. Epid.* **2011,** *21*, 515–528.
46. Pant, V.; Deshpande, C. G.; Kamra, A. K., The concentration and number size distribution measurements of the Marine Boundary Layer aerosols over the Indian Ocean. *Atmospheric Research* **2009,** *92* (4), 381-393.
47. Grannas, A. M.; Shepson, P. B.; Filley, T. R., Photochemistry and nature of organic matter in Arctic and Antarctic snow. *Global Biogeochemical Cycles* **2004,** *18* (1), n/a-n/a.
48. Voisin, D.; Jaffrezo, J.-L.; Houdier, S.; Barret, M.; Cozic, J.; King, M. D.; France, J. L.; Reay, H. J.; Grannas, A.; Kos, G.; Ariya, P. A.; Beine, H. J.; Domine, F., Carbonaceous species and humic like substances (HULIS) in Arctic snowpack during OASIS field campaign in Barrow. *Journal of Geophysical Research* **2012,** *117*.
49. Hagler, G. S. W.; Bergin, M. H.; Smith, E. A.; Dibb, J. E.; Anderson, C.; Steig, E. J., Particulate and water-soluble carbon measured in recent snow at Summit, Greenland. *Geophysical Research Letters* **2007,** *34* (16), n/a-n/a.
50. Wesdemiotis, C.; Solak, N.; Polce, M. J.; Dabney, D. E.; Chaicharoen, K.; Katzenmeyer, B. C., Fragmentation pathways of polymer ions. *Mass Spectrom. Rev.* **2011,** *30* (4), 523-559.
51. Yol, A. M.; Dabney, D. E.; Wang, S. F.; Laurent, B. A.; Foster, M. D.; Quirk, R. P.; Grayson, S. M.; Wesdemiotis, C., Differentiation of linear and cyclic polymer architectures by MALDI tandem mass spectrometry (MALDI-MS2). *J Am Soc Mass Spectrom* **2013,** *24* (1), 74-82.
52. Jaenicke, R., Abundance of cellular material and proteins in the atmosphere. *Science* **2005,** *308* (5718), 73-73.
53. Gelencsér, A., *Carbonaceous aerosol*. Springer Science & Business Media: 2004; Vol. 30.
54. Antony, R.; Grannas, A. M.; Willoughby, A. S.; Sleighter, R. L.; Thamban, M.; Hatcher, P. G., Origin and sources of dissolved organic matter in snow on the East Antarctic ice sheet. *Environ Sci Technol* **2014,** *48* (11), 6151-9.
55. Domine, F.; Gallet, J.-C.; Barret, M.; Houdier, S.; Voisin, D.; Douglas, T. A.; Blum, J. D.; Beine, H. J.; Anastasio, C.; Bréon, F.-M., The specific surface area and chemical composition of diamond dust near Barrow, Alaska. *Journal of Geophysical Research* **2011,** *116*.
56. Jones, J. H., *Amino Acids Peptides and Proteins*. Royal society of chemistry: 1984; Vol. 15.

57. Watson, M. L., Staining of tissue sections for electron microscopy with heavy metals. *The Journal of Biophysical and Biochemical Cytology* **1958,** *4* (4), 475-478.

58. Hayat, M. A.; Miller, S. E., *Negative staining*. McGraw-Hill: 1990.

59. Baustian, K. J.; Cziczo, D. J.; Wise, M. E.; Pratt, K. A.; Kulkarni, G.; Hallar, A. G.; Tolbert, M. A., Importance of aerosol composition, mixing state, and morphology for heterogeneous ice nucleation: A combined field and laboratory approach. *Journal of Geophysical Research* **2012,** *117* (D6).

60. Krueger, B. J.; Grassian, V. H.; Cowin, J. P.; Laskin, A., Heterogeneous chemistry of individual mineral dust particles from different dust source regions: the importance of particle mineralogy. *Atmospheric Environment* **2004,** *38* (36), 6253-6261.

61. Kos, G.; Kanthasami, V.; Adechina, N.; Ariya, P. A., Volatile organic compounds in Arctic snow: concentrations and implications for atmospheric processes. *Environ Sci Process Impacts* **2014,** *16* (11), 2592-603.

62. Hudson, E. D.; Ariya, P. A.; Gélinas, Y., A method for the simultaneous quantification of 23 C1–C9 trace aldehydes and ketones in seawater. *Environmental Chemistry* **2011,** *8* (4), 441-449.

63. Peterson, B. W.; Sharma, P. K.; van der Mei, H. C.; Busscher, H. J., Bacterial cell surface damage due to centrifugal compaction. *Appl. Environ. Microbiol.* **2012,** *78* (1), 120-125.

64. Baustian, K. J., et al., Depositional ice nucleation on solid ammonium sulfate and glutaric acid particles. *Atmos. Chem. Phys.* **2010,** *10*, 2307–2317.

65. Wise, M. E. e. a., Internally mixed sulfate and organic particles as potential ice nuclei in the tropical tropopause region. *Proc. Natl. Acad. Sci. U S A* **2010,** *107* (15), 6693-8.

66. Steinke, I., et al., Ice nucleation properties of fine ash particles from the Eyjafjallajokull eruption in April 2010. *Atmospheric Chemistry and Physics* **2011,** *11* (24), 12945-12958.

67. Möhler, O.; Field, P.; Connolly, P.; Benz, S.; Saathoff, H.; Schnaiter, M.; Wagner, R.; Cotton, R.; Krämer, M.; Mangold, A., Efficiency of the deposition mode ice nucleation on mineral dust particles. *Atmospheric Chemistry and Physics* **2006,** *6* (10), 3007-3021.

68. Mortazavi, R.; Attiya, S.; Ariya, P. A., Arctic microbial and next-generation sequencing approach for bacteria in snow and frost flowers: selected identification, abundance and freezing nucleation. *Atmospheric Chemistry and Physics* **2015,** *15* (11), 6183-6204.

69. Wilkinson, K. J.; Balnois, E.; Leppard, G. G.; Buffle, J., Characteristic features of the major components of freshwater colloidal organic matter revealed by transmission electron and atomic force microscopy. *Colloids and Surfaces A: Physicochemical and Engineering Aspects* **1999,** *155* (2), 287-310.

70. Pummer, B.; Budke, C.; Augustin-Bauditz, S.; Niedermeier, D.; Felgitsch, L.; Kampf, C.; Huber, R.; Liedl, K.; Loerting, T.; Moschen, T., Ice nucleation by water-soluble macromolecules. *Atmospheric Chemistry and Physics Discussions* **2014,** *14* (17), 24273-24309.

71. Junge, K., Swanson, B.D., High-resolution ice nucleation spectra of sea-ice bacteria: implications for cloud formation and life in frozen environments. *Biogeosciences* **2008,** *5*, 865–873.

72. Leberman, R., Use of Uranyl Formate as a Negative Stain. *J. Mol. Biol.* **1965,** *13* (2), 606.

73. Markham, R., et al., Methods for the enhancement of image detail and accentuation of structure in electron microscopy. *Virology* **1963,** *20*, 88-102.

74. Chen, J.-P., et al., Parameterizing ice nucleation rates using contact angle and activation energy derived from laboratory data. *Atmos. Chem. Phys.* **2008,** *8*, 7431–7449.

75. Matsumoto, M., et al., Molecular dynamics simulation of the ice nucleation and growth process leading to water freezing. *Nature* **2002,** *416*, 409-413.

76. Marcolli, C., Deposition nucleation viewed as homogeneous or immersion freezing in pores and cavities. *Atmos. Chem. Phys. Discuss.* **2013,** *13* (6), 16367-16456.

77. Algara-Siller, G.; Lehtinen, O.; Wang, F. C.; Nair, R. R.; Kaiser, U.; Wu, H. A.; Geim, A. K.; Grigorieva, I. V., Square ice in graphene nanocapillaries. *Nature* **2015,** *519* (7544), 443-5.

78. Vali, G., Sizes of atmospheric ice nuclei. *Nature* **1966,** *212*, 384-385.

79. Vali, G., Freezing nucleus content of hail and rain in NE Colorado. *Am. Meteorol. Soc. Monogr* **1978,** *38*, 93-105.

Chapter 4

4. Athabasca Oil Sand Snow Contains Efficient Ice Nucleating Particles

My contributions to this paper were the following:

Just as in Chapter 3, I used the technique outlined in Chapter 2 to obtain the particle size distributions of the snow samples. Because the nucleation ability of particles from contaminated snow was very high, I compared the results with samples previously used in the study of Chapter 3. My analysis of the results revealed that particles < 200 nm from contaminated snow were more efficient than particles > 200 nm from cleaner snow.

In the second part of the paper, I performed nucleation experiments with common mineral dust particle components (clays and iron oxides) in the presence of mercury(II) halides. I performed surface studies (BET and XRD) of the mineral/mercury particles to try to understand why particles in highly contaminated areas, are highly efficient ice nucleating particles. Jane Kirk, Vincent St. Laurent and Chelsea Willis did the sampling at the AOSR and provided valuable comments on the paper. Most of the writing was done by myself. Marc Amyot and Dominic Belanger did the metal analysis by ICP-MS.

This last chapter complements the study of the physical and chemical characteristics of particles in snow studied in the previous chapter. We further expand on the study of the impact of environmental contaminants on the ice nucleation of snow-borne particles.

Manuscript submitted to Environmental Science & Technology

Athabasca Oil Sand Snow Contains Efficient Ice Nucleating Particles

Rodrigo B. Rangel-Alvarado[1], Jane L. Kirk[3], Vincent L. St. Louis[4], Chelsea E. Willis[5], Marc Amyot[6], Dominic Bélanger[6], and Parisa A. Ariya[*1,2]

[1] Department of Chemistry and [2] Department of Atmospheric & Oceanic Sciences, McGill University, Montréal, QC, H3A 2K6, Canada

[3]Aquatic Contaminants Research Division, Environment and Climate Change Canada, Burlington, ON L7S 1A1, Canada

[4]Department of Biological Sciences, University of Alberta, Edmonton, AB T6G 2E9, Canada

[5]Environmental Protection Branch, Environment and Climate Change Canada, Gatineau, QC J8Y 3Z5, Canada

[6]Département de Sciences Biologiques, Université de Montréal, Montréal, QC H3T 1J4, Canada

*Corresponding author: Parisa A. Ariya

Abstract. The Athabasca Oil Sands Region (AOSR) in Alberta, Canada, is an important source of atmospheric pollutants, such as aerosols, having repercussions on climate and health. We show that the mean freezing temperature of snow-borne particles from AOSR was elevated (-7.1 ± 1.8 °C), higher than mineral dust which freezes at ~ -15 °C and is recognized as the most relevant ice nuclei globally, and significantly higher than snow-borne particles from downtown Montreal snow (used as a control; -13.4 ± 2.1 °C). AOSR snow had a higher concentration (~2 orders of magnitude) of >100 nm particles than Montreal. Triple quadrupole ICP-(QQQ)-MS/MS analysis of AOSR snow showed concentrations of 34.1, 34.1, 16.6, 5.8, 0.3, 0.1, and 9.4 µg/L for Cr, Ni, Cu, As, Se, Cd, and Pb respectively, in contrast to concentrations of 1.3, 0.3, 2.0, <0.03, 0.1, 0.03, and 1.2 µg/L in Montreal snow. HR-TEM/STEM imaging provided evidence for various anthropogenic nanostructures, such as carbon nanotubes, in AOSR snow up to 7-25 km away from oil sands upgrading facilities. To decipher potential mechanistic pathways of nucleation microphysics, we performed nucleation experiments on model particles, in the presence of $HgCl_2$ and $HgBr_2$. BET and XRD studies provided evidence for surface physicochemical alterations upon the addition of Hg(II), which explained the impact on nucleation. We discuss the potential impact of AOSR emissions on atmospheric and microphysical processes locally and regionally.

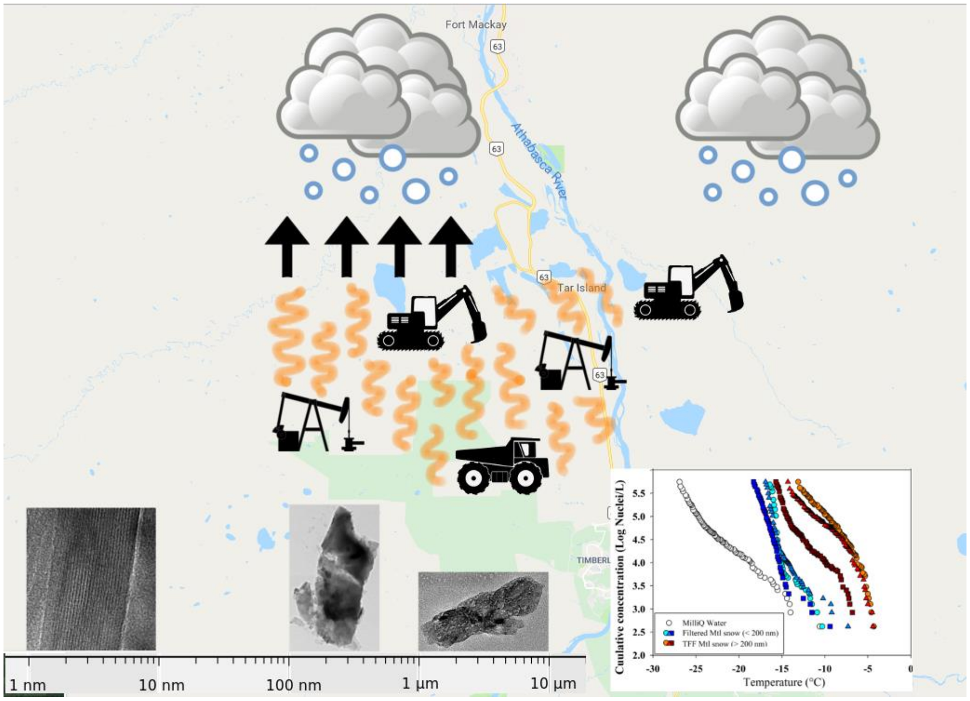

4.1. Introduction

Aerosols are widely considered to be critical in the formation of clouds and precipitation, and at dictating the energy budget of Earth by absorbing and scattering radiation.[1-6] The presence of aerosols is essential in the formation of ice at sub-zero temperatures and at low water vapour supersaturations.[2] These particles can be inorganic, organic, and biological in origin and come from natural and anthropogenic sources.[7] Aerosol-cloud interactions are the utmost uncertainty identified by the International Panel for climate change and radiative forcing predictions. A major component of this uncertainty is ice nucleation, which depends on the physical and chemical properties of the aerosols, such as size, chemical composition, contact angle, photochemical reactions, and surface properties.[8-9]

Inorganic aerosols containing metals are ubiquitous in atmospheric mineral dust.[10] Mineral dust particles contain various types of metals and metal oxides and are known to include a wide range of trace metals.[11] Many of these inorganic aerosols are considered efficient ice nucleating particles (INP) on a global scale,[10, 12-13] while several organic compounds are also known to be important in ice nucleation in polluted and remote environments.[14]

The Athabasca Oil Sands Region (AOSR) is now recognized as an anthropogenic pollution emission site,[15] with impacts on human and environmental health and on the local climate.[16-17] For example, snow from AOSR has been shown to contain elevated concentrations of several metals considered to be priority pollutants elements under the US Environmental Protection Agency's Clean Water Act, along with high concentrations of other contaminants, including particles and particulate-bound metals during wintertime.[18] Yet, there is no study examining the effect of such pollutants on ice nucleation, which is important because these pollutants can interact with aerosols in clouds and modify their cloud formation properties. This can result in redistribution of these same pollutants in nearby ecosystems.

Falling snow can contain a snapshot of ongoing atmospheric aerosol processes. Aerosols of various sizes can be taken up by falling snow as well as the landscape, while being subjected to gravitational settling. Previous research has shown that falling and settled snow on ground can serve as an efficient scavenger of atmospheric pollutants and aerosols.[14, 19] Analyses of these snow-borne particles can provide valuable insight on the composition and surface properties of pollutants, as well as their cloud and ice nucleating properties.

Several metals have been observed in snow from Northern locations,[20-23] including AOSR.[24] Of these metals, mercury (Hg) is among the most toxic known to be associated with mineral dust aerosols.[25-26] Particulate forms of Hg have been detected in atmospheric waters such as fog, clouds and mixed-phase clouds[27] where immersion freezing is arguably the dominant mechanism of ice nucleation.[27] Nevertheless, the ice nucleation properties of particulate inorganic Hg(II), or Hg associated with mineral dust particles, remain largely unknown. Recent research has shown that a series of metal contaminants including those composed of Hg halides, can indeed be very efficient for ice nucleation.[11]

The focus of this study was to explore whether snow-borne particle microphysical properties are affected by AOSR industrial activities. We performed complementary particle surface distribution and chemical composition studies, and ice nucleation experiments with snow collected in AOSR and Montreal (used as an urban site control). By using high resolution scanning transmission electron microscopy (HR-STEM), Brunauer–Emmett–Teller (BET) surface area, inductively couple plasma triple quadrupole mass spectrometer (ICP-(QQQ)-MS/MS) and X-ray powder diffraction (XRD) analyses of key metal and mineral dust particles, we explored the links between ice nucleation and the surface properties of snow-borne particles as well as dust particles with and without Hg halides coating. We discuss the implications of AOSR activities on the atmospheric chemistry and microphysics of snow-borne particles on regional scales.

4.2. Experimental section

4.2.1. Sample collection and storage

Snow samples were collected in AOSR at a site located <1 km from two of the largest upgrading facilities in the area (referred herein as the 0 km site) and two others located 7 km southeast and 25 km north of the 0 km site (Figure S1) between 4-14 March 2015. Locations were accessed by helicopter, and samples collected 50-100 m upwind of the landing location. Samples in Montreal were collected in a public park, away from pedestrian, vehicular, and pet traffic after a heavy snowfall in 2014, 2015 and 2017. Snow was collected into 950-mL pre-cleaned amber glass jars with PTFE-lined lids (Daniels Scientific, Charleston, SC, USA) by dragging the jars across the top 5 cm of the snowpack. Details on the sampling locations and procedures for Montreal and AOSR can be found elsewhere.[24, 28] After transport to the laboratory, samples were immediately transferred to a −35 °C freezer and stored until use. Samples were thawed at room temperature before analysis.

4.2.2. Particle Size Distributions

Melted snow samples were aerosolized with a d C-Flow 700d PFA Nebulizer (Savillex Corporation, Minnetonka, MN, USA). Particle size distributions of aerosolized melted snow as electrical mobility and aerodynamic diameter were obtained using a NanoScan™ Scanning Mobility Particle Sizer (SMPS) model 3910 (TSI Inc.) and an Optical Particle Sizer (OPS) model 3330 (TSI Inc.), respectively. The particle sizes measured by the instruments were from 10 nm to 10 μm (assuming particles are spherical with densities of 1.0 g/cm^3 for simplification). The detailed procedure is describe elsewhere.[24, 29]

4.2.3. High-resolution scanning transmission electron microscopy with energy dispersive X-ray spectroscopy (HR-STEM-EDS) and Scanning Electron Microscopy (SEM)

HR-STEM-EDS was used to study the morphology and size of particles in snow samples and at the same time obtain their elemental composition. SEM provided information regarding topography of particles in snow. Sample preparation consisted of depositing 5 μL aliquots of melted snow on glow discharged carbon film coated copper electron microscopy grids. The droplets were kept on the grids for one minute, followed by blotting off of the excess liquid with the edge of a piece of filter paper. Samples were imaged using a FEI Quanta 450 Environmental Scanning Electron Microscope (FE-ESEM) and a FEI Tecnai G^2 F20 200 kV Cryo-STEM (FEI Electron Optics) equipped with a tungsten filament, at 120 kV. Images were acquired using a Gatan Ultrascan 4000 4k x 4k CCD Camera System Model 895. EDS analysis was performed with an EDAX Octane T Ultra W /Apollo XLT2 SDD and TEAM EDS Analysis System.

4.2.4. Analysis of metal concentrations by ICP-(QQQ)-MS/MS

Metal concentrations in snow samples were quantified by ICP-(QQQ)-MS/MS. We used an 8900 Agilent equipped with an SPS 4 auto-sampler, a quartz spray chamber, and a glass concentric nebulizer with a Nickel (Ni) interface cone for the analysis of metals. Data acquisition was carried out using Agilent ICP-(QQQ)-MS/MS MassHunter software. Instrument parameters were present with the "Low matrix" plasma condition, and lens voltage was auto-tuned before each run. Metals were analyzed in He mode and rare earth elements (REE) in O_2 mode. Multi-element standards (metals: 10 µg/mL, Agilent #8500-6940; REE: 10 µg/mL, High-Purity Standards ICP-(QQQ)-MS/MS-B) were calibrated in a 2.0% HNO_3 matrix (grade Omnitrace Ultra, EMD) with the range of 0.0-50 µg/L (metals) and 0.0-10 µg/L (REE). Manual dilution of samples was carried out if concentrations exceeded calibration ranges.

Snow samples were analyzed for total Hg (THg) generally following method 1631 of the U.S.E.P.A.[30] A sub-sample was reacted overnight with BrCl (0.5% v/v). The excess of BrCl was neutralized by hydroxylamine. Stannous chloride (60 µl of $SnCl_2$ 20% w/v) was added and the sample was analyzed by in-vial purge, double gold trap amalgamation coupled to a cold vapour atomic fluorescence spectrometer (CVAFS, Tekran 2600, Tekran, Toronto, Canada). The laboratory recently participated to CALA proficiency testing for THg in water resulting in over 95% recovery on 4 blind samples.

4.2.5. Brunauer–Emmett–Teller Specific surface area of particles

The Brunauer–Emmett–Teller (BET) specific surface area of Fe_3O_4 with and without $HgCl_2$ and $HgBr_2$ was measured to determine how Hg halides changed the surface of Fe_3O_4. Fe_3O_4 suspensions with $HgCl_2$ and $HgBr_2$ were prepared by mixing 0.01 g of each solid in 10 mL of Milli-Q water. The mixture was sonicated for 15 min and then centrifuged. The precipitate was separated and washed three times with Milli-Q water. Surface areas were calculated by nitrogen adsorption on a TriStar 3000 V6.07 surface area analyzer at 77 K. Fe_3O_4 and α-Fe_2O_3 were purchased from Alfa Aesar. Kaolinite, montmorillonite, $HgCl_2$ and $HgBr_2$ were purchased from Sigma-Aldrich. These materials were used without further modification.

4.2.6. X-ray Powder Diffraction (XRD) patterns of particles

X-ray diffraction patterns of Fe_3O_4 were obtained using a Siemens D500 diffractometer with a Co Kα radiation source at a wavelength of 1.5418 Å. All analyses were carried out at $10\ ° \leq 2\theta \leq 80\ °$ in intervals of 0.02 °. Samples were prepared for analyses by adding equal parts of Fe_3O_4 and $HgCl_2$ or $HgBr_2$ to water. Fe_3O_4 was separated by decantation and washed with Milli-Q water to remove excess $HgCl_2$ or $HgBr_2$. The final product was dried in a vacuum oven.

4.2.7. Ice nucleation experiments on snow-borne particles

Cumulative concentrations of active ice nuclei at specific temperatures were obtained by doing drop freezing assays of melted snow. These experiments were performed as described by Vali(1971)[31] using an in-house made copper cooling plate. In each experiment, 240 10 μL droplets of suspension were placed on a cooling plate. The temperature was decreased at a rate of 0.1 °C/min. Freezing temperatures of each droplet were recorded.[32] Data was processed to plot the cumulative nucleus concentration as a function of temperature.[31] These experiments were performed with melted snow and filtered melted snow. Filtration was performed using an Agilent Captive PES syringe filter with 0.2 μm pore size to remove particles >0.2 μm and with Tangential Flow Filtration to remove particles <0.2 μm. Centrifugation was also used to separate smaller particles from large ones and prevent deformation of the larger particles. Statistical analysis for both tangential flow filtration and centrifugation techniques provided identical results within experimental uncertainties (p = 0.82). Centrifugation was carried out at 14000 rpm in a 14-cm diameter centrifuge. Only the bottom 0.5 mL of a 1.5 mL Eppendorf tube were used.

4.3. Results and Discussion

4.3.1. Snow-borne particle composition, size and morphology: AORS vs. Urban Montreal

4.3.1.1. Carbon Nanotubes

High resolution electron microscopy images of AOSR snow revealed particles from ~100 nm to >1 micron. EDS analysis revealed that the particles are mostly composed of C, Si, Al, and Fe, which are common components of soot and mineral dust. These elements can also be of lithogenic source originating from the mining and land clearing activities near the sampled areas.[24] The areas on the particles with higher electron contrast were composed of Si, Al, Fe, and other metals (Figure 4.1E) while the areas with lower electron contrast were composed mainly of organic carbon (Figure 4.1F) showing that these particles can have diverse chemical composition.

Selected particles >200 nm are shown in Figure 4.1A. Inspection of these particles revealed the presence of structures that resemble nanotubes (Figure 4.1B).[33] This type of particle is anthropogenic in origin and probably from AOSR sites.[34] This is not surprising since industrial activities in AOSR generate a substantial number of particles, some of which are inorganic elements and heavy metals, as well as carbon.[35] Other types of particles of similar size resembled agglomerates of smaller nanoparticles (Figure 4.1D). It is possible these agglomerates nucleate ice more efficiently than nanoparticles by themselves. Self-assembly of nanoparticles and carbon nanotubes have been previously demonstrated.[36] They can provide a larger surface area for nucleation, as even the cavities formed between nanoparticles can serve as active nucleating sites.[37]

4.3.1.2. Identification of metals in melted snow using ICP-(QQQ)-MS/MS, and complementary HR-STEM with EDS

Analyses of the elemental composition of melted snow by ICP-(QQQ)-MS/MS revealed that the concentration of all detected metals was higher in AOSR than in Montreal (Table 4.1) including metals such as Cr, Ni, Cu, As, Se, Cd and Pb which are on the World Health Organisation as well as US Environmental Protection Agency Priority Pollutant list.[38]

Concentrations of Al, Mn, and Fe in AOSR samples were as high as 38.9, 1.1, and 72.3 mg/L respectively, while in Montreal the concentrations did not exceed 0.3 mg/L. Elements such as Cr, Ni, and Ba had concentrations of 64.3, 50, and 367 μg/L respectively in AOSR samples, which is > 25 times higher than the Montreal samples. Other elements (Co, Cu, As, Se, Sr, Cd, and Pb) had concentrations of ~10 μg/L in AOSR samples, or ~ <10 times higher than those from Montreal.

Samples taken at the 7 and 25 km sites were not all aligned on the same trajectory (Figure S1). As such, the 7 and 25 km sampling sites did not have identical air masses trajectories (shown in the back-trajectory analysis given in the supplementary material Figure S2). Basically, they were subjected to different micrometeorological conditions, which lead to distinct metal concentrations and could have repercussions on the intensity of precipitation events. As shown in Table 4.1, samples from the 7 km site were consistently higher than other locations in AOSR, and much higher than Montreal data.

EDS analysis also revealed the existence of metals among the nanoparticles (Figures 1A, B, and D). Analysis of filtered samples by ICP-(QQQ)-MS/MS suggested that a large part of the metals in the snow samples were in particulate form (particles >200 nm) as the concentration of filtered samples were lower than the unfiltered ones. There is still a substantial amount of various metals in filtered snow (Table 4.1), possibly in nano-sized particles (Figure 4.1).

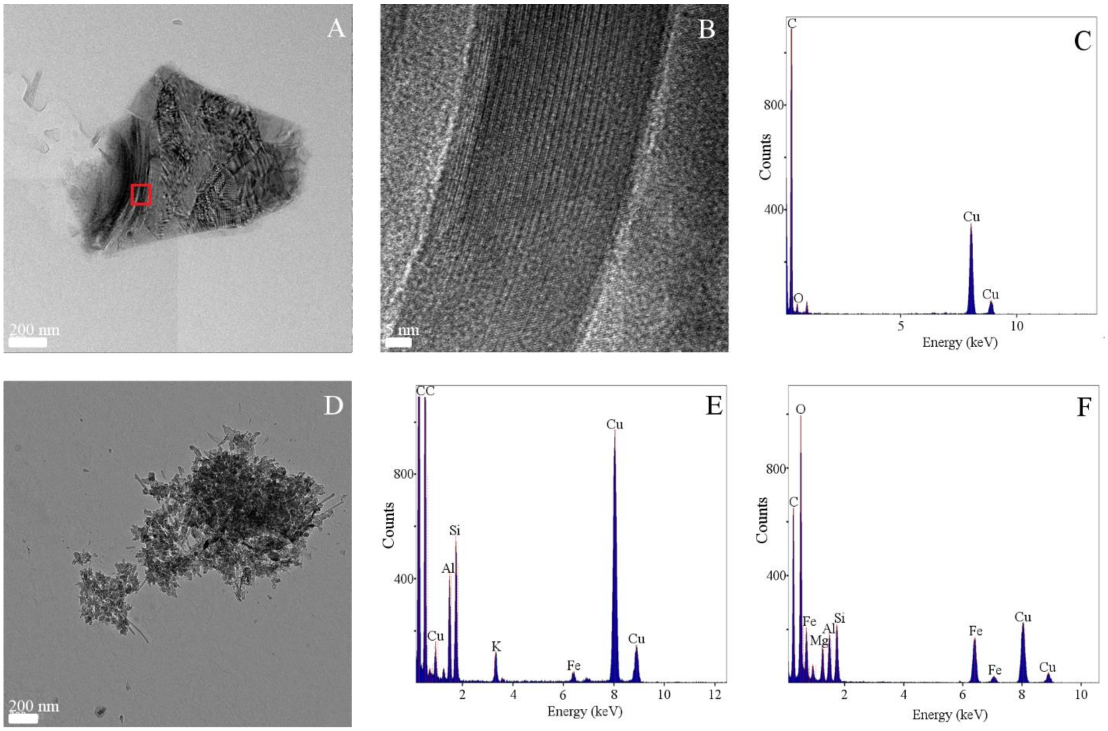

Figure 4.1 Electron microscopy images of particles found in snow from AOSR: (A) particles containing anthropogenic structures, (B) close-up of A showing a nanotube structure, (C) EDS analysis of A, (D) cluster of nanoparticles, (E-F) EDS analysis of (D).

Anthropogenic activities dominate the release of metals and organic particles into the atmosphere. It is possible that the elements found by EDS and ICP-(QQQ)-MS/MS come from sources in AOSR. Important sources of organic pollutants include upgraders, tailings ponds, and pet coke piles.[39] Sources of metals include upgraders,[24] landscape clearing[40], open pit mining[41], and haul emissions[40] as well as fugitive dust generated from oil sand and processed material, tailing sand, combustion processes, limestone, and haul road.[42-43]

Table 4.1 Elemental concentrations in melted snow from Montreal and AOSR. ND signifies non-detectable, and DL the detection limit. An (F) next to the element symbol means that the sample was filtered using a 0.2 µm filter. Montreal samples are denoted as MTL followed by the year they were sampled (2014, 2015, and 2017).

Element	Units	MTL14	MTL15	MTL17	0 km	7 km	25 km	DL
Al	mg/L	0.07	0.34	0.03	8.92	38.9	11.1	12.0×10^{-6}
AL (F)		6.0×10^{-3}	6.8×10^{-3}	0.05	0.40	0.79	0.27	
Cr	µg/L	0.84	1.30	1.76	15.7	64.3	22.3	21.0×10^{-3}
Cr (F)		0.06	0.06	0.62	0.02	0.04	0.04	
Mn	mg/L	0.01	0.01	0.5×10^{-3}	0.22	1.13	0.22	24.0×10^{-6}
Mn (F)		4.9×10^{-3}	5.0×10^{-3}	0.4×10^{-3}	1.5×10^{-3}	2.8×10^{-3}	4.4×10^{-3}	
Fe	mg/L	0.07	0.30	0.02	13.7	72.3	12.2	67.0×10^{-6}
Fe (F)		3.4×10^{-3}	4.1×10^{-3}	4.4×10^{-3}	0.01	0.02	7.3×10^{-3}	
Co	µg/L	ND	ND	ND	4.19	20.9	4.41	12.0×10^{-3}
Co (F)		ND	ND	ND	0.03	0.05	0.04	
Ni	µg/L	0.07	0.66	0.05	39.3	50.0	13.0	21.0×10^{-3}
Ni (F)		0.13	0.14	0.19	0.12	0.27	0.27	
Cu	µg/L	1.34	3.73	0.89	8.54	31.3	9.86	11.0×10^{-3}
Cu (F)		0.80	1.08	2.90	0.24	0.37	0.73	
As	µg/L	ND	ND	ND	2.57	12.3	2.66	31.0×10^{-3}
As (F)		ND	ND	ND	0.10	0.12	0.12	
Se	µg/L	ND	0.10	ND	0.17	0.60	0.16	76.0×10^{-3}
Se (F)		ND	0.04	ND	0.02	0.03	0.01	
Sr	µg/L	0.52	6.4	0.49	29.0	174	31.1	38.0×10^{-3}
Sr (F)		0.69	7.19	1.32	4.18	9.15	5.01	
Cd	µg/L	0.03	0.06	0.01	0.07	0.22	0.08	13.0×10^{-3}
Cd(F)		0.05	0.06	0.01	0.02	0.02	0.02	
Ba	µg/L	2.15	6.59	1.27	87.2	367	85.9	53.0×10^{-3}
Ba (F)		0.82	2.85	0.54	2.30	5.67	2.46	
Pb	µg/L	0.28	2.99	0.2	4.97	17.4	5.75	9.00×10^{-3}
Pb (F)		0.15	0.22	0.27	0.01	ND	0.01	
U	µg/L	0.01	0.02	0.01	0.35	ND	0.43	10.0×10^{-3}
U (F)		0.01	0.01	0.01	0.01	0.02	0.01	
Hg	ng/L	5.10	3.35	2.61	5.93	3.04	8.08	4.00×10^{-3}
Hg (F)		4.27	2.91	1.50	4.07	6.44	7.88	

Large particles >2.5 µm were also detected in AOSR snow samples (Figure S3). It has been reported that 83% of particulate matter >10 µm (PM_{10}) in AOSR originates from industry related emissions, so it is likely that these particles come from the sources mentioned above.[43] Larger particles have less negative health effects than smaller particles,[44-45] however, large particles can have different effects on selected climate-driven processes. For example, larger particles are better INP than smaller particles of the same composition.[46-47] However, there is increasing evidence showing the importance of nano-sized particles (<200 nm), particularly clusters, in atmospheric ice nucleation.[28, 48] Montreal and AOSR snow samples contained similar nanoparticle concentrations (10-100 nm), within experimental errors (Figure 4.2). However, concentrations of particle size fractions larger than 100 nm were higher in AOSR than in Montreal snow.

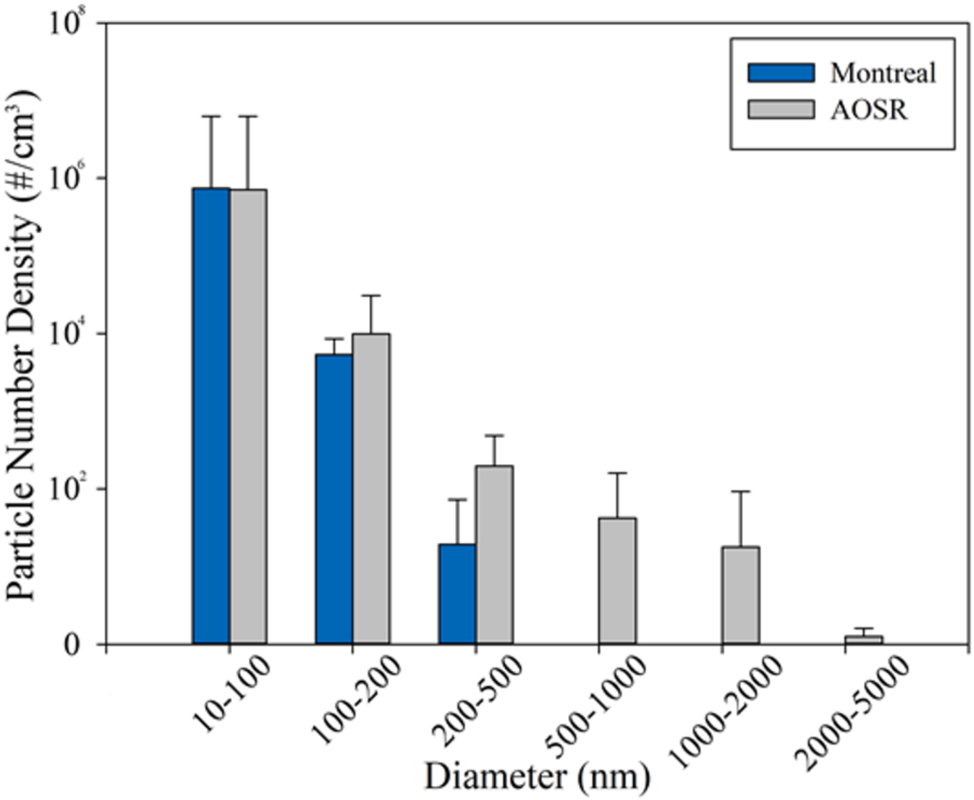

Figure 4.2 Particle number density of aerosolized melted snow from Montreal and near AOSR as electrical mobility diameter (EMD) in the size range of 10 – 100, 100-200, 200-500, 500-1000, 1000-2000, and 2000-5000.

4.3.2. Comparison of ice nucleation efficiency between AOSR and Montreal snow-borne particles

AOSR snow samples presented nucleation at higher than normal temperatures (-7.13 ± 1.79 °C), significantly warmer than Montreal snow samples (-13.36 ± 2.06 °C, $p = 0.003$) (Figure 4.3). The more efficient nature of the nucleation activity of AOSR particles could be due to, but not limited to, differences in particle size. In AOSR samples relative to those from Montreal, higher number density of large particles and clusters of nanoparticles were observed (Figure 4.1D), along with higher concentrations of metals (Table 4.1).

4.3.3. Relationship between snow-borne particle size and ice nucleation efficiency

As noted above, AOSR snow-borne particles of all sizes are indeed very efficient INP, considerably more so than what is currently known of airborne mineral dust particles.[2] To evaluate the relationship between particle size and ice nucleation, we performed nucleation experiments with two different particle size fractions: <200 nm and >200 nm.

For AOSR samples, particles >200 nm (clusters of nanoparticles and single large particles) nucleated ice at relatively warm temperatures (-6.3 ± 1.0 °C), while particles <200 nm nucleated ice at lower temperatures (-11.6 ± 2.0 °C, Figure 4.3B). Particles <200 nm from AOSR were still very efficient INP, even better than mineral dust, which nucleates ice ~ -15 °C.[10] Our results indicate that clusters >200 nm and micron-sized particles were the most efficient INP in AOSR snow, yet smaller particles <200 nm were still excellent INP.

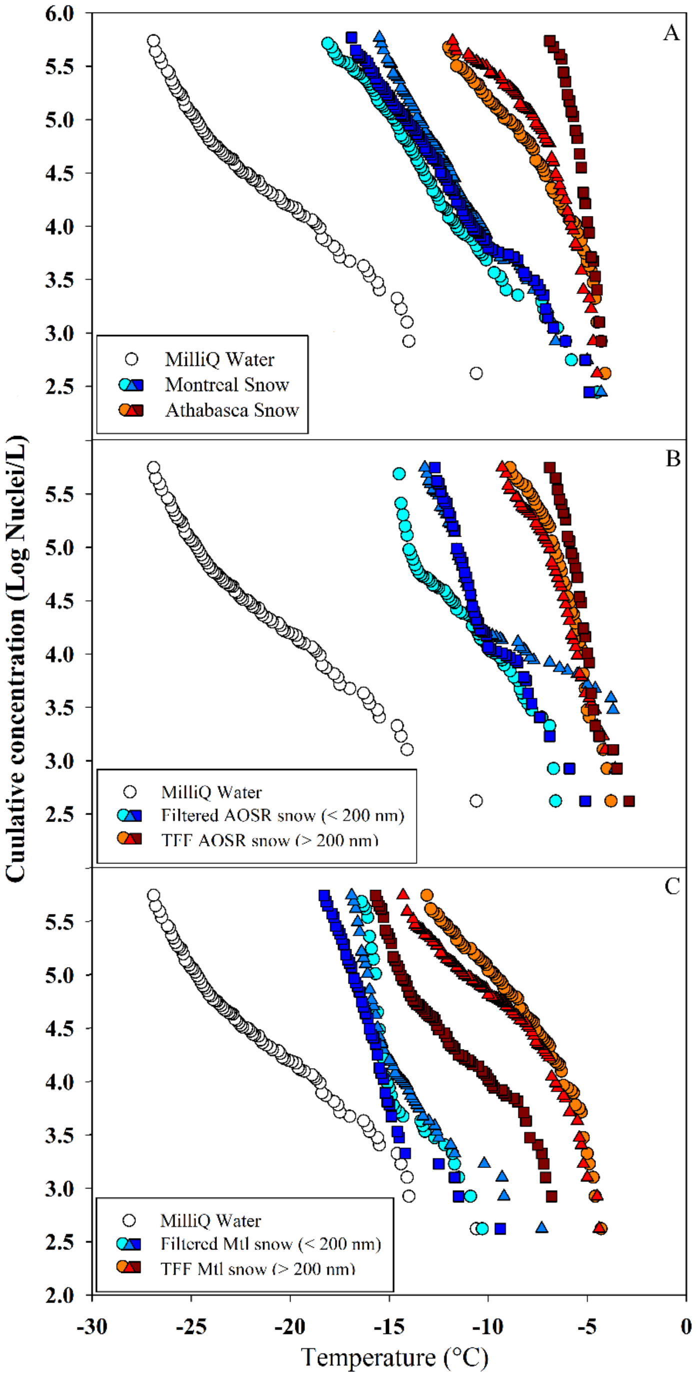

Figure 4.3 Cumulative INP concentration of: (A) snow collected near AOSR compared to snow collected at Mont Royal park, Montreal, (B) filtered AOSR snow containing particles <200 nm compared to particles >200 nm, and (C) filtered Montreal snow containing mostly particles <200 nm compared to particles >200 nm. For Montreal data, different symbols represent samples from different years: ▲ 2014, ■ 2015, and ● 2017. For AOSR data different symbols represent the different sampling sites: ▲ (0 km), ■ (7 km), and ● (25 km).

Figure 4.3 also illustrates that aerosols of all sizes in snow samples taken at AOSR (filtered, centrifuged and unfiltered; Figure S4), exhibited more efficient ice nucleation in comparison to Montreal samples. This observation suggests that the ice nucleating ability of particles produced through AOSR activities might affect the aerosol-cloud interactions in the region.[49]

4.3.4. The effect of Hg halide coverage on the ice nucleation on model mineral particles

4.3.4.1. Hg halides as proxy for oxidized Hg in snow

Hg has been a major focus of research in AOSR due to concerns about its effects on health and the environment.[24] Hg is also known to be associated with particulate matter in the atmosphere.[50-52] Recent laboratory results have even shown that some Hg halide composites can indeed be very efficient INP.[11] Since we also observed halides in snow samples, we decided to focus on Hg halides and explore their effect on ice nucleation. We performed nucleation experiments with common components of mineral dust (kaolin, montmorillonite α-Fe_2O_3 and Fe_3O_4) and Hg halides.

High resolution electron microscopy coupled to EDS, allowed us to demonstrate that the composition of particles is complex and that multiple elements exist in similar particles. Since ice nucleation is a function of several factors including surface coverage and contact angle, we opted to further explore the impact of Hg halides ($HgCl_2$ and $HgBr_2$) on Fe oxide particles. Air borne mineral dust particles ubiquitously contain various Fe.[10, 53] Halides have been shown in snow to generate reactive $Cl^{\bullet}$ and $Br^{\bullet}$ radicals at snow-air interfaces,[54-55] and upon reaction with elemental Hg, they readily generate $HgCl_2$ and $HgBr_2$.[56] As such, we performed targeted experiments with iron oxides (α-Fe_2O_3 and Fe_3O_4) and clays (kaolinite and montmorillonite) as the core of a particle, and used various concentrations of $HgCl_2$ and $HgBr_2$ as coverage over the core.

4.3.4.2. Effect of HgX_2 coverage on iron oxides particles

We found that the average freezing temperatures differed somewhat between the different tested suspensions (Figure 4.4). α-Fe_2O_3 particles nucleated ice at -16.3 ± 2.7 °C. Adding $HgCl_2$ to the α-Fe_2O_3 suspension resulted in ice nucleation temperature to decrease to -18.5 ± 2.3 °C ($p = 0.217$). The addition of $HgBr_2$ to α-Fe_2O_3 particles decreased the nucleating temperature of the α-Fe_2O_3 particles to -18.8 ± 1.7 °C ($p = 0.087$). On the other hand, the average freezing temperature of Fe_3O_4 nanoparticles was -14.9 ± 2.0 °C. Addition of $HgCl_2$ to Fe_3O_4 did not significantly decreased the freezing temperature of Fe_3O_4 to -15.7 ± 2.3 ($p = 0.0065$). The addition of $HgBr_2$ also did not significantly decreased the freezing temperature of Fe_3O_4 to -18.2 ± 2.3 °C ($p = 0.0127$).

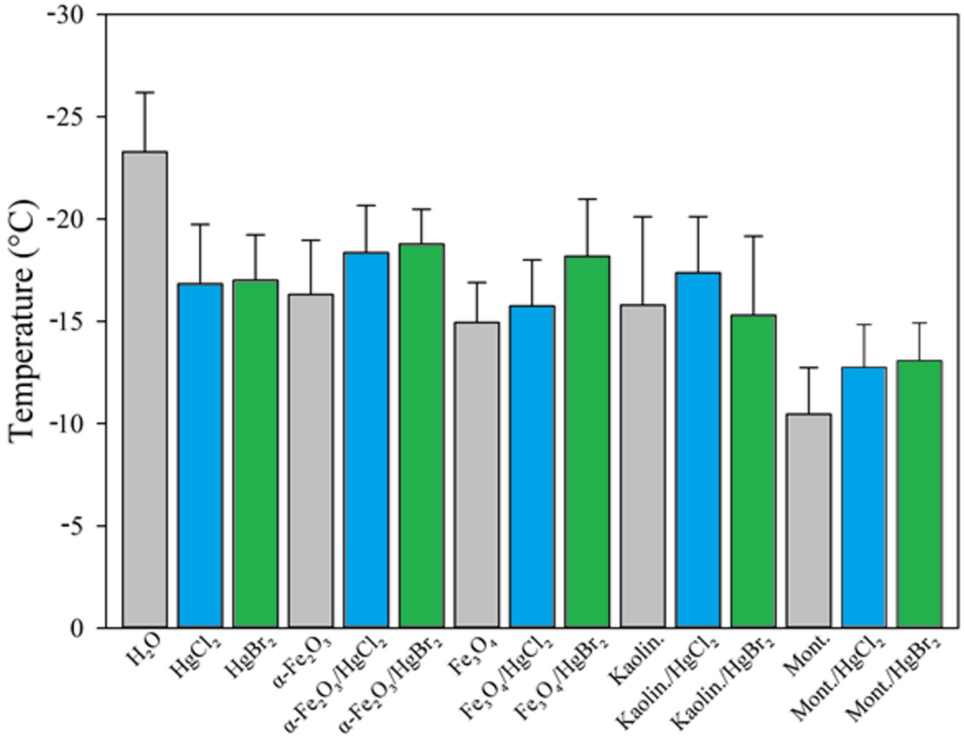

Figure 4.4 Freezing average temperatures of $HgCl_2$ and $HgBr_2$ compared to α-Fe_2O_3, Fe_3O_4, kaolinite, montmorillonite, and their respective mixtures with Hg halides.

4.3.4.3. Effect of Hg halides coverage on clay minerals

Upon addition of $HgCl_2$ to kaolinite, the average freezing temperature dropped from -15.8 ± 4.3 °C to -17.4 ± 2.7 °C (Figure 4.4). It is possible that $HgCl_2$ had coated (partially or totally) kaolinite particles, supressing its nucleating abilities. We also found that the average freezing temperature of the kaolinite/$HgBr_2$ mix (-15.3 ± 3.9 °C) matched that of kaolinite alone. In this case, it appears that $HgBr_2$ did not coat the kaolinite particles.

Montmorillonite particles nucleated ice at average temperatures of -10.5 ± 2.3 °C, which was more efficient than kaolinite (Figure 4.4). The freezing temperatures of the montmorillonite in the presence of $HgCl_2$ and $HgBr_2$ were -12.7 ± 2.1°C and 13.1 ± 1.8 °C, respectively.

The studied particles with Hg halides were efficient INP within the temperature range of atmospheric mineral dust particles.[10] Yet, AOSR snow-borne particles were more efficient than all aforementioned INP. The elevated freezing temperatures of the oil sands samples are likely due to a significantly higher concentration of larger particles.

4.3.5. Surface studies of iron oxide (BET & XRD): Hg halides alter iron oxide surfaces

We observed that upon addition of Hg halide salts, the nucleating properties of the mineral particles changed, possibly due to a change in surface properties. To evaluate this hypothesis, we performed Brunauer–Emmett–Teller surface analysis of Fe_3O_4, which revealed a surface area of 72.06 m^2/g. This value was reduced by 77 % when $HgCl_2$ was added to the solution, demonstrating that $HgCl_2$ coverage reduces the availability of surfaces per g of Fe_3O_4 particles under our experimental conditions.

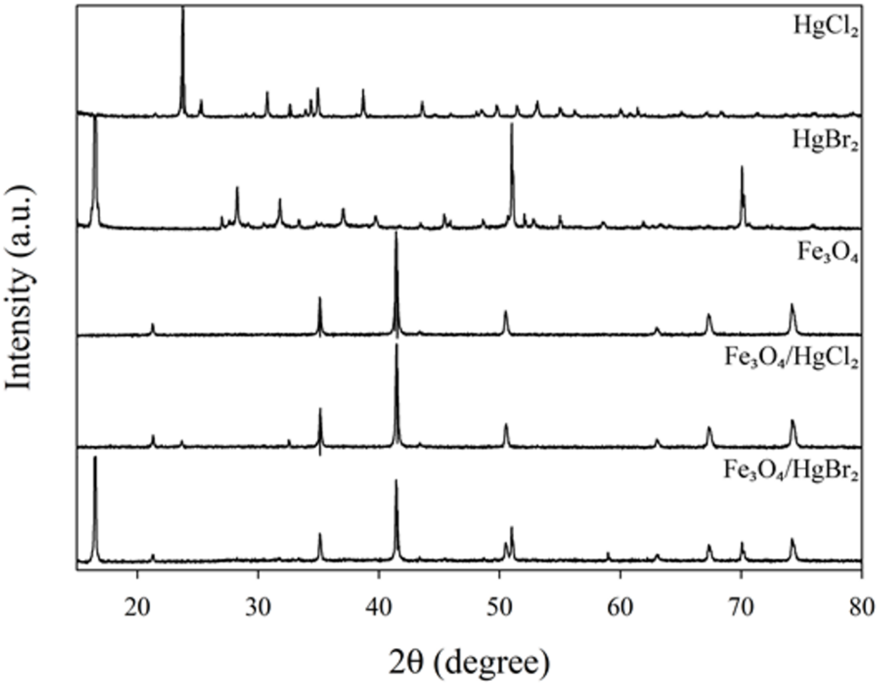

Figure 4.5 X-ray powder diffraction patterns of Fe_3O_4 in the presence of $HgCl_2$ and $HgBr_2$.

The XRD patterns of Fe_3O_4 in the presence of $HgCl_2$ and $HgBr_2$ (Figure 4.5) showed peaks that seemed to match the diffraction patterns of the $HgCl_2$ and $HgBr_2$ references.[57] Although we expected to remove most of the $HgCl_2$ and $HgBr_2$ during the washing process before analysis, we could still see the presence of these species regardless of their high solubility. The XRD pattern of Fe_3O_4 with $HgCl_2$ did not have sharp diffraction peaks belonging to $HgCl_2$. This could be because $HgCl_2$ was not in a crystalline state, but rather in a glassy state. Glassy coatings can modify the ice nucleating properties of the aerosols they are coating.[58] This would explain why the sample with $HgCl_2$ was slightly more efficient at ice nucleation than the sample with $HgBr_2$. Another possibility is that $HgCl_2$ reacted with the surface of Fe_3O_4 and formed a coating of Hg(II) oxide.[59] The same analysis could not be done with α-Fe_2O_3 in the presence of $HgCl_2$ and $HgBr_2$ because the XRD patterns of α-Fe_2O_3 did not depict sharp signals.

The BET and XRD experiments together indicate that the surface coverage, structure, composition, and surface properties of Fe oxides were altered by the surface coverage of Hg halides. Further experimental research is recommended to determine the impact of heterogeneity of particle surfaces on ice nucleation properties. Previous research has indicated that Hg can alter the water-surface interactions creating a small crystallographic lattice mismatch which is pivotal for an increased ice nucleation efficiency of particles.[11]

In this study, we demonstrated that ice nucleation by snow-borne particles from the highly polluted AORS happens at -7.1 ± 1.8 °C, and that particles <200 nm are more efficient at ice nucleation than any particle of all-sizes, from downtown Montreal. These elevated freezing temperatures are even more efficient than mineral dust particles, which are considered the most relevant global INP. We observed several anthropogenic particles, including those similar in shape to nanostructures, specifically carbon nanotubes, which are known to be used in various oil industry activities and combustion.[34, 60] AOSR snow samples had a higher concentration of metal contaminants in snow in comparison to downtown Montreal. Targeted surface studies suggested that the presence of Hg(II) alters the surface properties of particles, thus affecting ice nucleation. Since Hg halides are herein shown to affect ice nucleation, we encourage further studies of major oxidized Hg sources, including coal-operated power plants. Further research is recommended to determine whether anthropogenic AOSR activities lead to other unknown efficient INP that are generated directly or via secondary reactions. The presence of efficient INP in the atmosphere may signify increase precipitation in nearby areas, shortening the lifetimes of pollutants in the atmosphere. This is of concern because particles and other pollutants may enter regional water bodies as snow melts.

Acknowledgements

We thank Sahana Selladurai and Christine deWolf from the Department of Chemistry and Biochemistry, Concordia University. We are grateful to NSERC, Environment and Climate Change Canada, the Joint Oil Sands Monitoring (JOSM) program, NSERC-CREATE Mine of Knowledge, the Canadian Foundation for Innovation and Canada Research Chairs Program for financial support.

References

1. Guido, V., Fundamentals of physics and chemistry of the atmosphere. Springer, Berlin: 2001.
2. Pruppacher, H. R.; Klett, J. D.; Wang, P. K., Microphysics of clouds and precipitation. **1998**.
3. Solomon, S.; Qin, D.; Manning, M.; Chen, Z.; Marquis, M.; Averyt, K.; Tignor, M.; Miller, H., Contribution of working group I to the fourth assessment report of the intergovernmental panel on climate change, 2007. Cambridge University Press, Cambridge: 2007.
4. Stocker, T. F.; Qin, D.; Plattner, G.-K.; Tignor, M.; Allen, S. K.; Boschung, J.; Nauels, A.; Xia, Y.; Bex, V.; Midgley, P. M., Climate change 2013: The physical science basis. Cambridge University Press Cambridge, UK, and New York: 2014.
5. Platt, C. M. R., Temperature dependence of cirrus extinction: Implications for climate feedback. *Journal of Geophysical Research: Atmospheres* **1988,** *93* (D9), 11051-11058.
6. Chylek, P.; Wong, J., Effect of absorbing aerosols on global radiation budget. *Geophysical research letters* **1995,** *22* (8), 929-931.
7. Ariya, P.; Sun, J.; Eltouny, N.; Hudson, E.; Hayes, C.; Kos, G., Physical and chemical characterization of bioaerosols–Implications for nucleation processes. *International Reviews in Physical Chemistry* **2009,** *28* (1), 1-32.
8. DeMott, P. J.; Prenni, A. J.; Liu, X.; Kreidenweis, S. M.; Petters, M. D.; Twohy, C. H.; Richardson, M.; Eidhammer, T.; Rogers, D., Predicting global atmospheric ice nuclei distributions and their impacts on climate. *Proceedings of the National Academy of Sciences* **2010,** *107* (25), 11217-11222.
9. Hoose, C.; Kristjánsson, J.; Burrows, S., How important is biological ice nucleation in clouds on a global scale? *Environmental Research Letters* **2010,** *5* (2), 024009.
10. Archuleta, C. M.; DeMott, P.; Kreidenweis, S., Ice nucleation by surrogates for atmospheric mineral dust and mineral dust/sulfate particles at cirrus temperatures. *Atmospheric Chemistry and Physics* **2005,** *5* (10), 2617-2634.
11. M. Ganguly, S. D., P. Ariya, The Purely Inorganic Highly Efficient Ice Nucleating Particle. *ACS Omega* **2018**.
12. Atkinson, J. D.; Murray, B. J.; Woodhouse, M. T.; Whale, T. F.; Baustian, K. J.; Carslaw, K. S.; Dobbie, S.; O'Sullivan, D.; Malkin, T. L., The importance of feldspar for ice nucleation by mineral dust in mixed-phase clouds. *Nature* **2013,** *498* (7454), 355.

13. Möhler, O.; Benz, S.; Saathoff, H.; Schnaiter, M.; Wagner, R.; Schneider, J.; Walter, S.; Ebert, V.; Wagner, S., The effect of organic coating on the heterogeneous ice nucleation efficiency of mineral dust aerosols. *Environmental Research Letters* **2008,** *3* (2), 025007.

14. Nazarenko, Y.; Fournier, S.; Kurien, U.; Rangel-Alvarado, R. B.; Nepotchatykh, O.; Seers, P.; Ariya, P. A., Role of snow in the fate of gaseous and particulate exhaust pollutants from gasoline-powered vehicles. *Environmental Pollution* **2017,** *223*, 665-675.

15. Liggio, J.; Li, S.-M.; Hayden, K.; Taha, Y. M.; Stroud, C.; Darlington, A.; Drollette, B. D.; Gordon, M.; Lee, P.; Liu, P., Oil sands operations as a large source of secondary organic aerosols. *Nature* **2016,** *534* (7605), 91-94.

16. Parajulee, A.; Wania, F., Evaluating officially reported polycyclic aromatic hydrocarbon emissions in the Athabasca oil sands region with a multimedia fate model. *Proceedings of the National Academy of Sciences* **2014,** *111* (9), 3344-3349.

17. Kurek, J.; Kirk, J. L.; Muir, D. C.; Wang, X.; Evans, M. S.; Smol, J. P., Legacy of a half century of Athabasca oil sands development recorded by lake ecosystems. *Proceedings of the National Academy of Sciences* **2013,** *110* (5), 1761-1766.

18. Kirk, J. L.; Muir, D. C.; Gleason, A.; Wang, X.; Lawson, G.; Frank, R. A.; Lehnherr, I.; Wrona, F., Atmospheric deposition of mercury and methylmercury to landscapes and waterbodies of the Athabasca oil sands region. *Environmental science & technology* **2014,** *48* (13), 7374-7383.

19. Zhang, L.; Wang, X.; Moran, M.; Feng, J., Review and uncertainty assessment of size-resolved scavenging coefficient formulations for below-cloud snow scavenging of atmospheric aerosols. *Atmospheric Chemistry and Physics* **2013,** *13* (19), 10005-10025.

20. Boutron, C. F.; Candelone, J.-P.; Hong, S., Greenland snow and ice cores: unique archives of large-scale pollution of the troposphere of the Northern Hemisphere by lead and other heavy metals. *Science of the total environment* **1995,** *160*, 233-241.

21. Candelone, J. P.; Hong, S.; Pellone, C.; Boutron, C. F., Post-Industrial Revolution changes in large-scale atmospheric pollution of the northern hemisphere by heavy metals as documented in central Greenland snow and ice. *Journal of Geophysical Research: Atmospheres* **1995,** *100* (D8), 16605-16616.

22. Steffen, A.; Douglas, T.; Amyot, M.; Ariya, P.; Aspmo, K.; Berg, T.; Bottenheim, J.; Brooks, S.; Cobbett, F.; Dastoor, A., A synthesis of atmospheric mercury depletion event chemistry in the atmosphere and snow. *Atmospheric Chemistry and Physics* **2008,** *8* (6), 1445-1482.

23. Lalonde, J. D.; Poulain, A. J.; Amyot, M., The role of mercury redox reactions in snow on snow-to-air mercury transfer. *Environmental science & technology* **2002,** *36* (2), 174-178.

24. Willis, C. E.; Kirk, J. L.; St. Louis, V. L.; Lehnherr, I.; Ariya, P. A.; Rangel-Alvarado, R. B., Sources of methylmercury to snowpacks of the Alberta Oil Sands Region: A study of in situ methylation and particulates. *Environmental science & technology* **2017**.

25. Subir, M.; Ariya, P. A.; Dastoor, A. P., A review of uncertainties in atmospheric modeling of mercury chemistry I. Uncertainties in existing kinetic parameters–Fundamental limitations and the importance of heterogeneous chemistry. *Atmospheric environment* **2011,** *45* (32), 5664-5676.

26. Subir, M.; Ariya, P. A.; Dastoor, A. P., A review of the sources of uncertainties in atmospheric mercury modeling II. Mercury surface and heterogeneous chemistry–A missing link. *Atmospheric environment* **2012,** *46*, 1-10.

27. Murray, B.; O'sullivan, D.; Atkinson, J.; Webb, M., Ice nucleation by particles immersed in supercooled cloud droplets. *Chemical Society Reviews* **2012,** *41* (19), 6519-6554.

28. Rangel-Alvarado, R. B.; Nazarenko, Y.; Ariya, P. A., Snow-borne nanosized particles: Abundance, distribution, composition, and significance in ice nucleation processes. *Journal of Geophysical Research: Atmospheres* **2015**.
29. Hinds, W. C., Aerosol Technology: Properties. *Behavior, and Measurement of airborne Particles (2nd* **1999**.
30. U.S.EPA, Specifications and guidance for contaminant-free sample containers. *Office of Solid Waste and Emergency Response, Washington, DC* **1992**.
31. Vali, G., Quantitative evaluation of experimental results an the heterogeneous freezing nucleation of supercooled liquids. *Journal of the Atmospheric Sciences* **1971,** *28* (3), 402-409.
32. Mortazavi, R.; Hayes, C. T.; Ariya, P. A., Ice nucleation activity of bacteria isolated from snow compared with organic and inorganic substrates. *Environmental Chemistry* **2008,** *5* (6), 373-381.
33. Wang, M.; Golberg, D.; Bando, Y., In situ TEM investigations of the interface behavior between carbon nanotubes and metals. *Mass Transport of Nanocarriers* **2016**, 345.
34. Kim, E.-S.; Liu, Y.; El-Din, M. G., An in-situ integrated system of carbon nanotubes nanocomposite membrane for oil sands process-affected water treatment. *Journal of membrane science* **2013,** *429*, 418-427.
35. Bari, M.; Kindzierski, W.; Cho, S., A wintertime investigation of atmospheric deposition of metals and polycyclic aromatic hydrocarbons in the Athabasca Oil Sands Region, Canada. *Science of the Total Environment* **2014,** *485*, 180-192.
36. Li, J.; Tang, S.; Lu, L.; Zeng, H. C., Preparation of nanocomposites of metals, metal oxides, and carbon nanotubes via self-assembly. *Journal of the American Chemical Society* **2007,** *129* (30), 9401-9409.
37. Marcolli, C., Deposition nucleation viewed as homogeneous or immersion freezing in pores and cavities. *Atmospheric Chemistry and Physics* **2014,** *14* (4), 2071-2104.
38. U.S. Environmental Protection Agency. Toxic and Priority Pollutants. http://pubs.usgs.gov/circ/1953/0285/report.pdf.
39. Manzano, C. A.; Marvin, C.; Muir, D.; Harner, T.; Martin, J.; Zhang, Y., Heterocyclic aromatics in petroleum coke, snow, lake sediments, and air samples from the Athabasca oil sands region. *Environmental Science & Technology* **2017,** *51* (10), 5445-5453.
40. Lynam, M.; Dvonch, J. T.; Barres, J.; Percy, K., Atmospheric wet deposition of mercury to the Athabasca Oil Sands Region, Alberta, Canada. *Air Quality, Atmosphere & Health* **2017**, 1-11.
41. Cooke, C. A.; Kirk, J. L.; Muir, D. C.; Wiklund, J. A.; Wang, X.; Gleason, A.; Evans, M. S., Spatial and temporal patterns in trace element deposition to lakes in the Athabasca oil sands region (Alberta, Canada). *Environmental Research Letters* **2017,** *12* (12), 124001.
42. Landis, M.; Pancras, J.; Graney, J.; Stevens, R.; Percy, K.; Krupa, S., Receptor modeling of epiphytic lichens to elucidate the sources and spatial distribution of inorganic air pollution in the Athabasca Oil Sands Region. In *Developments in Environmental Science*, Elsevier: 2012; Vol. 11, pp 427-467.
43. Landis, M. S.; Pancras, J. P.; Graney, J. R.; White, E. M.; Edgerton, E. S.; Legge, A.; Percy, K. E., Source apportionment of ambient fine and coarse particulate matter at the Fort McKay community site, in the Athabasca Oil Sands Region, Alberta, Canada. *Science of the Total Environment* **2017,** *584*, 105-117.
44. Organization, W. H., Outdoor air pollution a leading environmental cause of cancer deaths. *Press release* **2013,** *221*.

45. Organization, W. H., 7 million premature deaths annually linked to air pollution. *World Health Organization, Geneva, Switzerland* **2014**.

46. Lüönd, F.; Stetzer, O.; Welti, A.; Lohmann, U., Experimental study on the ice nucleation ability of size-selected kaolinite particles in the immersion mode. *Journal of Geophysical Research: Atmospheres* **2010,** *115* (D14).

47. Welti, A.; Lüönd, F.; Stetzer, O.; Lohmann, U., Influence of particle size on the ice nucleating ability of mineral dusts. *Atmospheric Chemistry and Physics* **2009,** *9* (18), 6705-6715.

48. O'Sullivan, D.; Murray, B. J.; Ross, J. F.; Webb, M. E., The adsorption of fungal ice-nucleating proteins on mineral dusts: a terrestrial reservoir of atmospheric ice-nucleating particles. *Atmospheric Chemistry and Physics* **2016,** *16* (12), 7879-7887.

49. Ariya, P.; Domine, F.; Kos, G.; Amyot, M.; Côté, V.; Vali, H.; Lauzier, T.; Kuhs, W.; Techmer, K.; Heinrichs, T., Snow–a photobiochemical exchange platform for volatile and semi-volatile organic compounds with the atmosphere. *Environmental Chemistry* **2011,** *8* (1), 62-73.

50. Keeler, G.; Glinsorn, G.; Pirrone, N., Particulate mercury in the atmosphere: its significance, transport, transformation and sources. *Water, Air, & Soil Pollution* **1995,** *80* (1), 159-168.

51. Sakata, M.; Marumoto, K., Formation of atmospheric particulate mercury in the Tokyo metropolitan area. *Atmospheric Environment* **2002,** *36* (2), 239-246.

52. Schleicher, N.; Schäfer, J.; Blanc, G.; Chen, Y.; Chai, F.; Cen, K.; Norra, S., Atmospheric particulate mercury in the megacity Beijing: Spatio-temporal variations and source apportionment. *Atmospheric Environment* **2015,** *109*, 251-261.

53. Lafon, S.; Sokolik, I. N.; Rajot, J. L.; Caquineau, S.; Gaudichet, A., Characterization of iron oxides in mineral dust aerosols: Implications for light absorption. *Journal of Geophysical Research: Atmospheres* **2006,** *111* (D21).

54. Ariya, P. A.; Niki, H.; Harris, G. W.; Anlauf, K. G.; Worthy, D. E., Polar sunrise experiment 1995: hydrocarbon measurements and tropospheric Cl and Br-atoms chemistry. *Atmospheric Environment* **1999,** *33* (6), 931-938.

55. Ariya, P. A.; Hopper, J. F.; Harris, G. W., C2-C7 hydrocarbon concentrations in Arctic snowpack interstitial air: Potential presence of active Br within the snowpack. *Journal of atmospheric chemistry* **1999,** *34* (1), 55-64.

56. Kos, G.; Ryzhkov, A.; Dastoor, A.; Narayan, J.; Steffen, A.; Ariya, P.; Zhang, L., Evaluation of discrepancy between measured and modelled oxidized mercury species. *Atmospheric Chemistry and Physics* **2013,** *13* (9), 4839-4863.

57. Swanson, H. E.; Tatge, E., Standard X-ray diffraction patterns. *Journal of Research of the National Bureau of Standards* **1951,** *46* (4), 318.

58. Schill, G.; Tolbert, M., Heterogeneous ice nucleation on phase-separated organic-sulfate particles: effect of liquid vs. glassy coatings. *Atmospheric Chemistry and Physics* **2013,** *13* (9), 4681-4695.

59. Eltouny, N.; Ariya, P. A., Enhanced reactivity toward oxidation by water vapor: interactions of toluene and NO2 on hydrated magnetite nanoparticles. *The Journal of Physical Chemistry C* **2014,** *118* (41), 23654-23663.

60. Mansurov, Z., Soot formation in combustion processes. *Combustion, Explosion and Shock Waves* **2005,** *41* (6), 727.

Chapter 5

5. Conclusions and Future Work

5.1. Summary

In this work the particulate content in different types of snow was studied. Snow samples from remote, arctic locations (Alert, NU, Canada and Barrow, AK, USA) as well as from urban areas (Montreal, QC and the Athabasca Oils Sands Region in Alberta, Canada) were used. Snow samples were used because they can provide an easy and affordable snapshot of atmospheric processes in cold environments specifically ice nucleation. Due to challenges arising from the processing of the samples a method to study the particulate content with minimal perturbation of the original particle size distribution was developed. This method consisted of aerosolization of melted snow followed by drying and sizing of the aerosol in real time to prevent aggregation of particles. Concentration of aerosols in an air stream could be measure in the size range of 10 nm to 10 µm. Additional to particle size distribution, collection of particles on electron microscopy grids was possible for further characterization of particles. Nanosized particles (< 200 nm) were the more abundant that larger particles in samples from Alert, Barrow and Montreal with 15 nm being the most abundant.

After finding that nanosized particles dominated the particle size distribution on the studied samples, we studied their ice nucleation abilities. Arctic nanosized particles presented a mean freezing temperature of -17 °C while Montreal was -15 °C. These results are similar to those of micronsized mineral dust particles meaning that despite being small they can nucleate ice at relatively warm sub-zero temperatures. Having molecular masses of more than 1000 Dalton, it seems these particles are biological in nature like small proteins or subcellular structures or even composite particles of biological and inorganic nature.

Following the study of nanosized particles from clean snow we studied nanosized particles from snow near oil sands regions. The concentration of nanosized particles the AOSR was similar to Montreal. AOSR nanosized particles presented a mean freezing temperature of -12 ℃. Larger particles presented an even larger freezing temperature (-7 ℃). These samples also contained a high concertation of metals and heavy metals. Experiments with mineral dust particles with mercury halides suggested these contaminants modify the surface properties of particles and in turn their ice nucleation efficiency.

5.2. Original Contribution to Knowledge

- The development of a technique, which allows the study of particles in liquid samples with low concentrations.
- Systematic study of the particulate content in a wide variety of northern locations.
- Nanosized particles are the most abundant particle sizes in northern snow and that they nucleate ice at warm temperatures (~ -15 ℃).
- Nanosized particles from highly polluted environments nucleate ice at very warm sub-zero temperatures, even warmer than large particles (> 200 nm) from less polluted areas.

5.3. Future Work

A missing aspect in this work was the study the ice nucleation of specific size segregated particles. This was just somewhat done in the last part of the work to separate particles < 200 nm and > 200 nm. Separating particles by their different particle sizes and performing nucleation studies on each group. This can be achieved by using a step by step Tangential Flow Filtration using different membranes. Alternatively, the particles can be sorted by using particle electrostatic classifiers which can generate monodispersed aerosol. This way we can see how the ice nucleation changes with size and relate to the concentration is a sample. This is important because a very efficient INP is not considered as relevant if their concentrations are not elevated. This can help decide which particles are the most relevant for nucleation in a specific location.

In this work we only investigated the effect of mercury(II) on the ice nucleation of mineral dust components. However, in places such as the AOSR a large diversity of pollutants is generated. A large portion of these components are organic compounds. In previous studies, the effect on ice nucleation of coatings of organic compounds on mineral dust have been investigated, even coatings of secondary organic aerosols where the organic coating is oxidized on the surface of particles. It would be interesting to identify relevant organic pollutants coating that make particles from the oil sands region so efficient at ice nucleation. Additionally, we could not confirm if metals were present in the nanoparticulate fraction. We know that a large part of the metals were associated with particles > 200 nm. Future studies could focus of the effect of inorganic coatings on the properties and ice nucleation of nanoparticles.

Finally, to complement this work, it would be necessary to study the cloud condensation properties of nanosized aerosols. Unlike the experiments performed here, it would be necessary to include other variables, such as saturation vapor pressure. In our case, we already had the particles immersed in a liquid (melted water), but for the study of CCN particles, it would be necessary to make particles airborne. The system we developed and used, can be employed for this purpose. Once airborne, particles would need to be introduced into a chamber where temperature and water vapour pressure can be controlled. This way we could know how efficient the particles in our samples can be as CCN and IN.

Appendix A

A. Chapter 2 Supplementary Information

A.1. Supplementary Methods

A.1.1. Analysis of Total Organic Carbon in Melted Snow

Unprocessed and filtered melted snow samples were poured into sterile Falcon™ 50 mL conical centrifuge tubes (Corning Life Sciences, Inc., Tewksbury MA, USA) to a minimum level of 40 mL of liquid for each sample. Samples were not diluted before analysis with an Aurora 1030W TOC Analyzer (O.I. Corp., College Station, TX) using the persulfate oxidation method (Nollet and De Gelder, 2013). In the reaction process, 5 ml of water was subsampled from each sample. For detection of total inorganic carbon, 0.5 mL of 5 % phosphoric acid was added to the subsample, which was then combusted at 700 °C. For detection of organic carbon, 2 mL of 10 % sodium persulfate was added and combusted at 980 °C. A nondispersive infrared sensor (NDIR) was used to detect separately the CO2 produced from the two combustion reactions. To ensure the consistency of results between analyses, external standards (0 and 5 ppm) were added to each batch of samples. All samples were processed in triplicate. The machine was calibrated using 0.0, 1.1, 2.0, 5.0, and 10 mg/L (ppm) standards. This calibration curve and the purity of the reagents allowed detection down to 0.1 mg/L TOC.

A.1.2. Ion Chromatography Analysis of Melted Snow

Unprocessed and dialyzed melted snow samples were analyzed for soluble inorganic content using a Dionex ICS-500 ion chromatograph with an IonPac AS 14 and IonPac CS 12 separation columns for anions and cations, respectively. A 3.5 mM Na2CO3/1.0 mM NaHCO3 solution was used as mobile phase to separate anions using a flow rate of 0.30 mL/min. A 20 nM methanesulfonic acid solution was used as a mobile phase to separate cations with a flow rate of 0.25 mL/min. Suppressed conductivity detection was used for both anions and cations using an Anion Self-Regenerating ASRS 300 2mm and a Cation Self-Regenerating CSRS Ultra II 2mm suppressors. All analyses were performed at room temperature (18 – 22 °C) using 10 μL of analyte solution. Each sample was processed in triplicate under the same conditions. The detection limit of all ions was 0.1 ppm.

A.2. Supplementary Figures

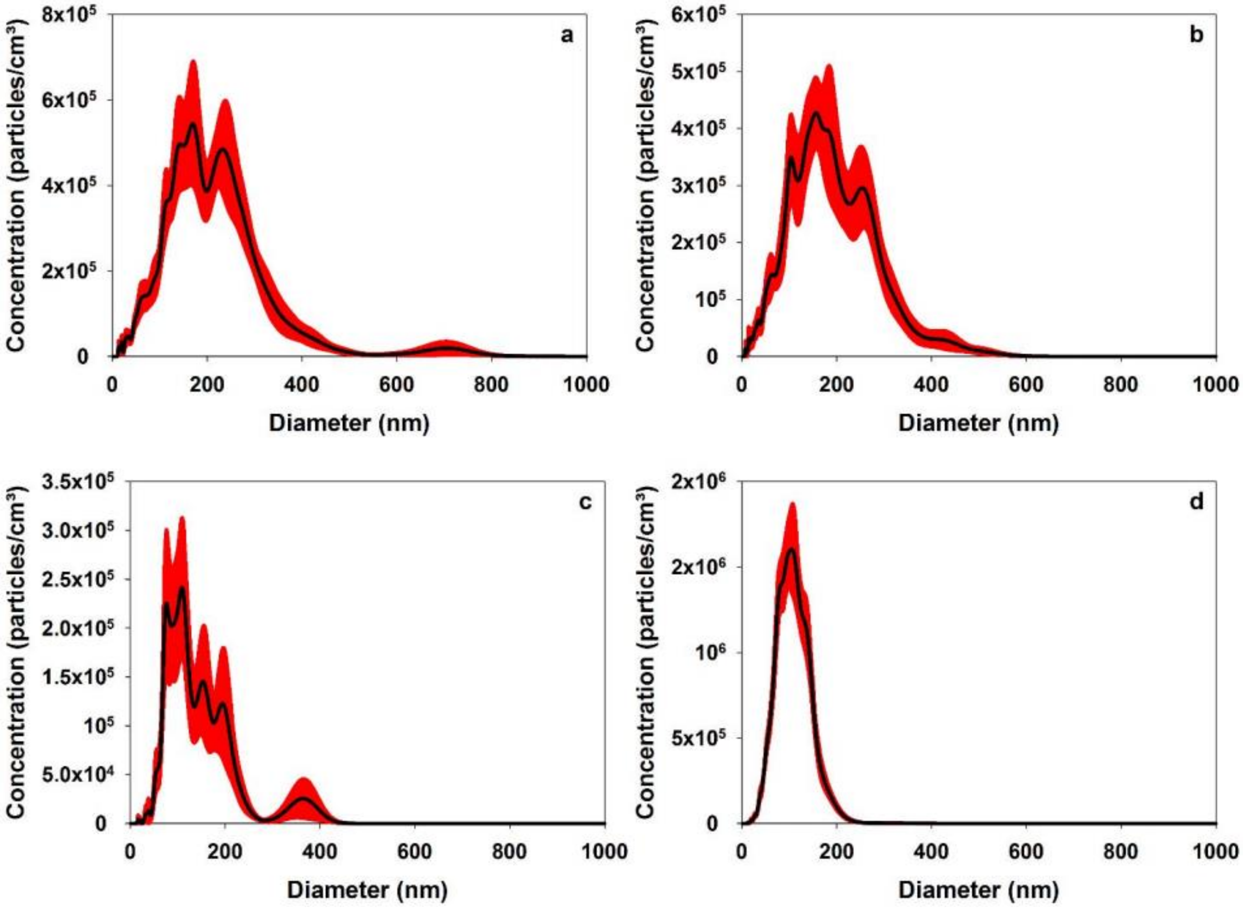

Figure A.1 Particle size distribution of samples from Alert: (a) unprocessed; (b) dialyzed; (c) filtered; and (d) filtered and dialyzed.

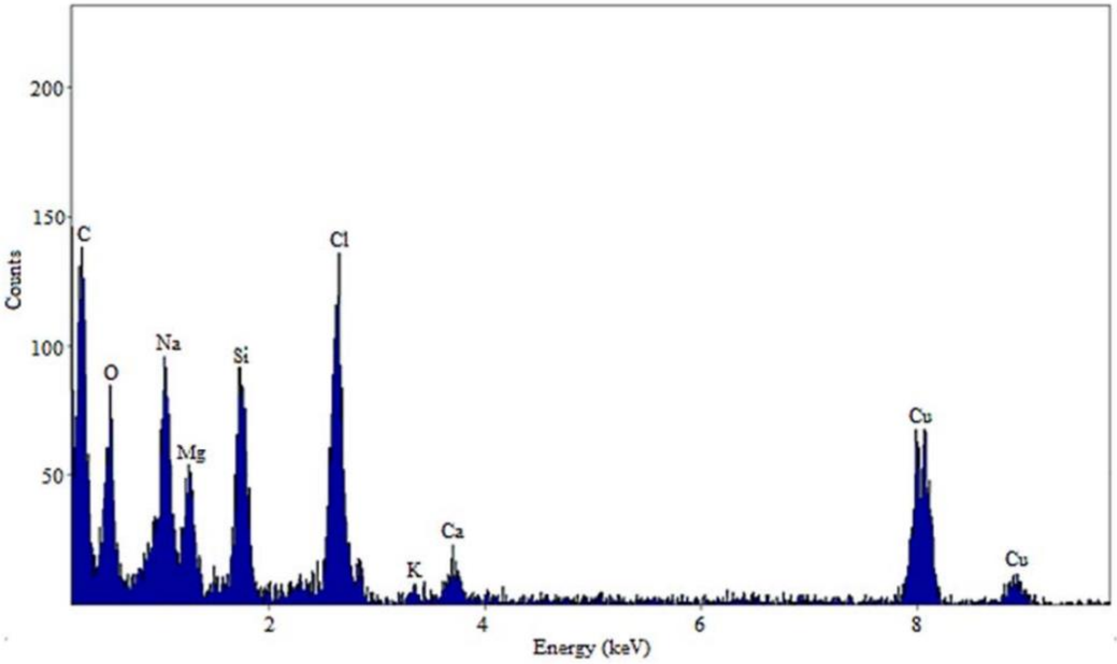

Figure A.2 EDS Spectrum of a particle in snow from Montreal, Quebec, collected in 2006. Peaks for Cu around 8 and 9 keV are caused by copper in the sample substrate (TEM-grids).

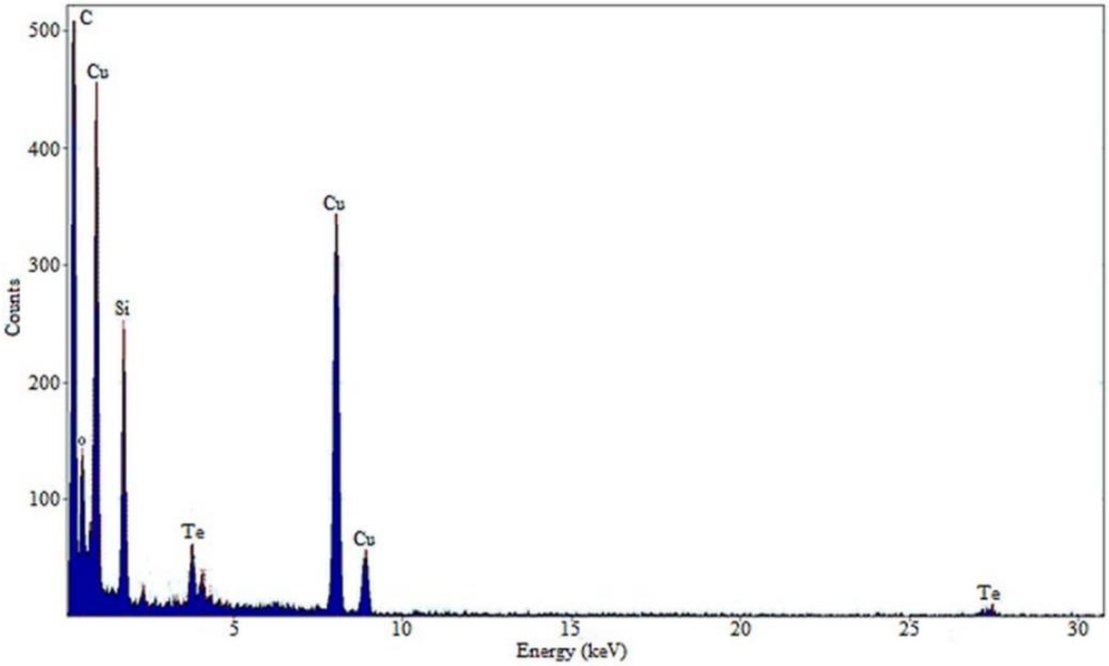

Figure A.3 EDS Spectrum of a particle in snow from Alert, Nunavut. Peaks for Cu around 8 and 9 keV are caused by copper in the sample substrate (TEM-grids).

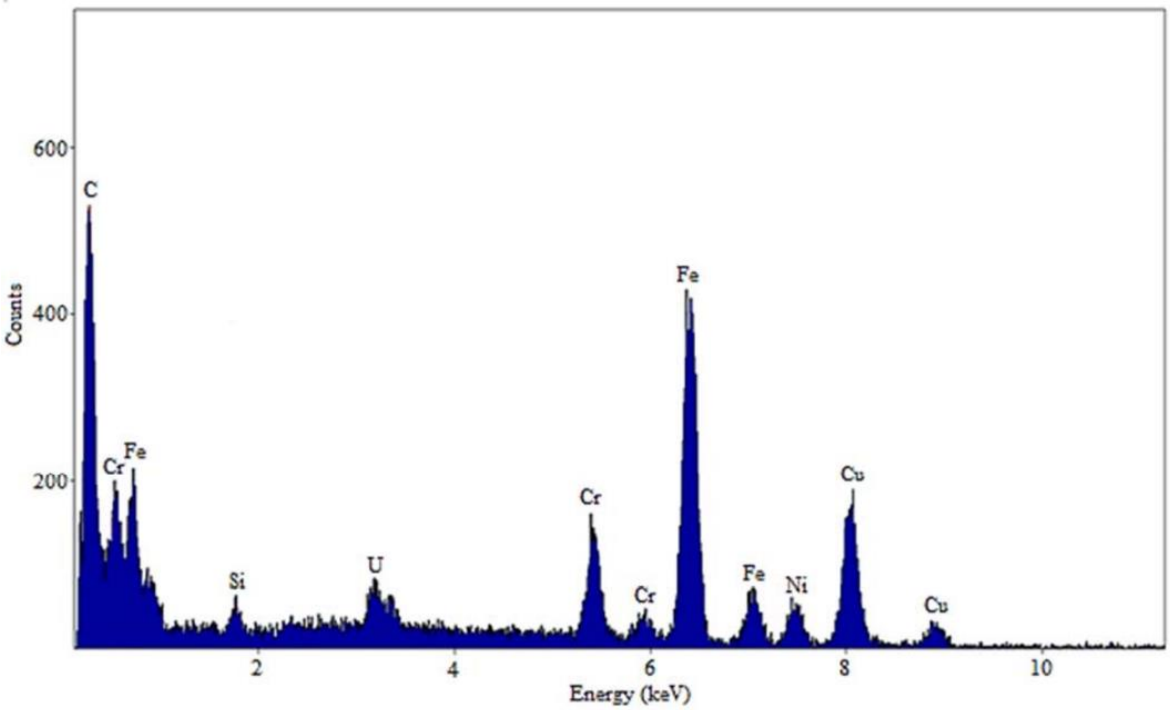

Figure A.4 EDS Spectrum of a particle in snow from Barrow, Alaska. Peaks for Cu around 8 and 9 keV are cause by copper in the sample substrate (TEM-grids).

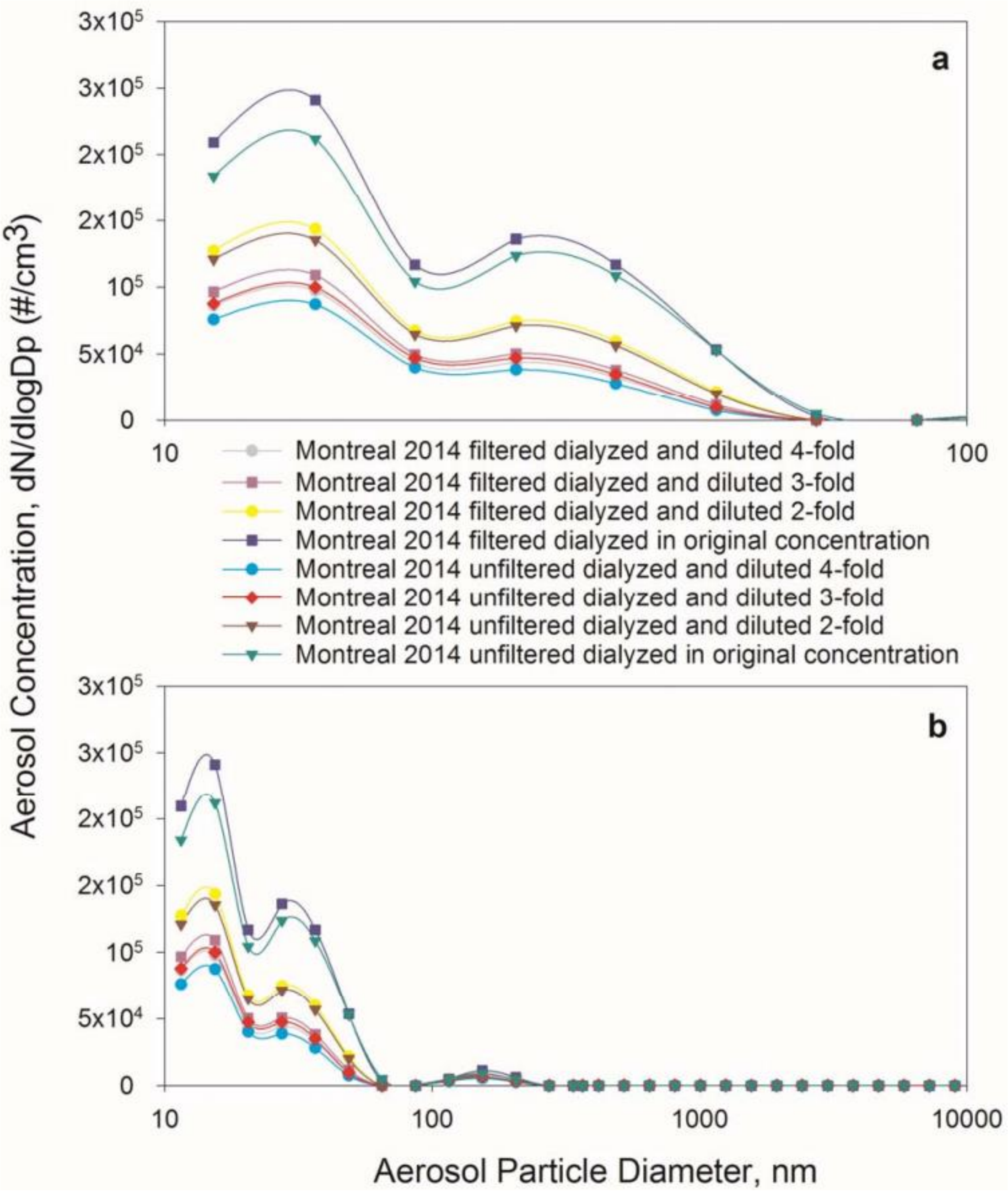

Figure A.5 Effect of dilution of select melted snow samples on aerosol size distribution: high resolution for the 10 – 100 nm region and complete for the total measured region of 10 – 10,000 nm.

Appendix B

B. Chapter 3 Supplementary Information

In this section we present supplementary figures. Figure B.1 represents the particle size distribution of samples from Alert, Barrow and Montreal. For these distributions, each sample was tested 5 times, and the average concentrations were plotted. The weighed standard deviations were used to plot the red error bars displayed in each graph. Data from Figure B.2 depicts the mass spectrum of the matrix used for MALDI-TOF analysis. The matrix used was α-cyano-4-hydroxycinnamic acid. The procedure for the blank was the same as the one mentioned in the main manuscript, but with no analytes.

B.1. Supplementary Figures

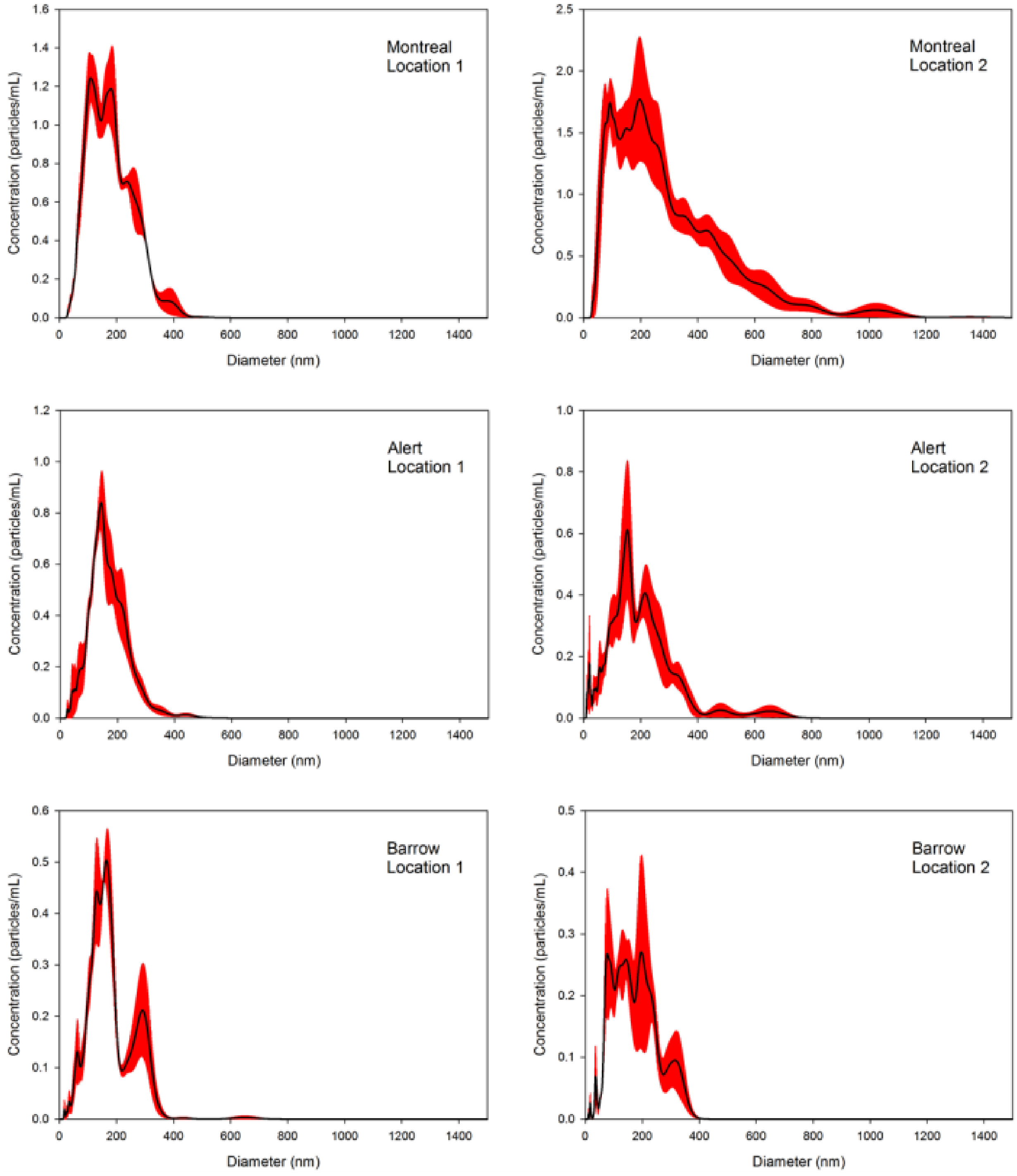

Figure B.1 Particle size distributions as a function of hydrodynamic diameter. Particle size distributions of individual samples (black line). Each sample was tested 5 times. The red bars represent the weighed standard deviation of the 5 runs at each single diameter.

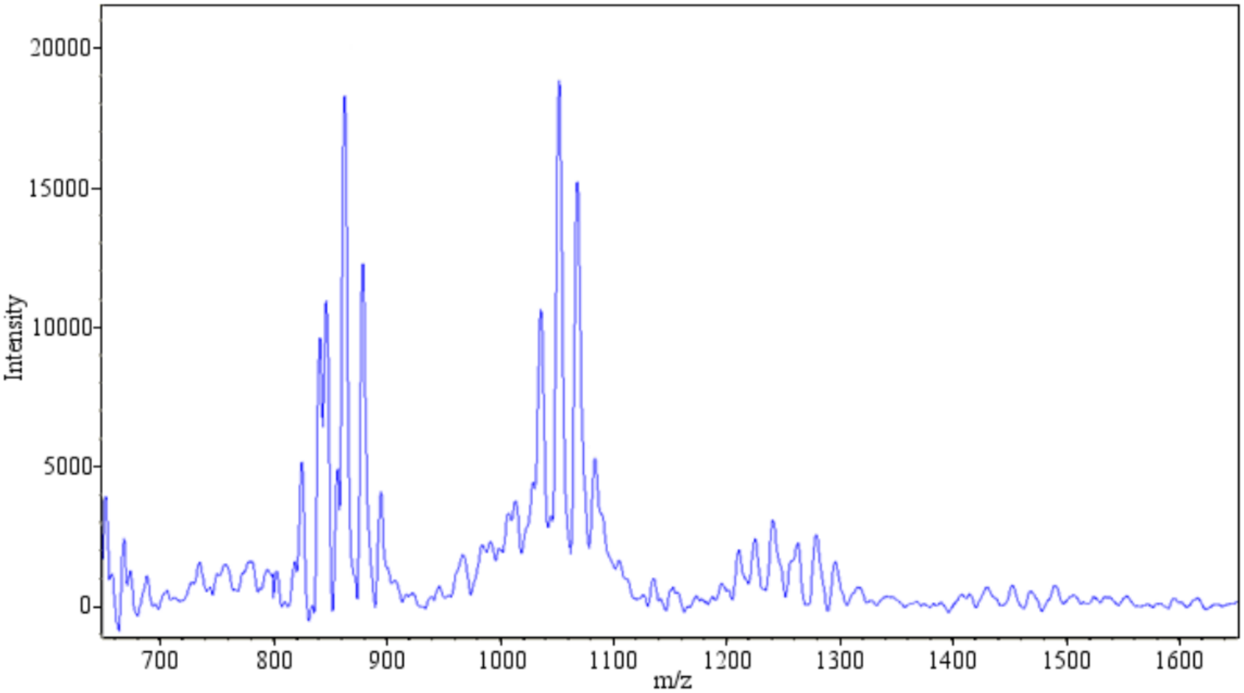

Figure B.2 MALDI- TOF spectrum of the blank. This spectrum shows the contamination (if any) of the matrix used for the analysis of snow samples. The peaks in this figure do not match the peaks of the sample shown in the main text.

Appendix C

C. Chapter 3 Supplementary Information

In this section we present supplementary figures. Figure C.1 represents the sampling locations in the AOSR between Fort Mackay and Fort McMurray. Location A is a centralized area < 1 Km from two major bitumen upgrading facilities. Locations B and C are 7 and 25 Km from location A respectively. Figure C.2 depicts the back-trajectory analysis for sampling location A from the 4th to the 14th of March 2015. Figure C.3 shows course particles > 2.5 μm demonstrating that large particles are also present in the AOSR samples. Figure C.4 is similar to Figure 4.3. It shows the different ice nucleation by particles < 200 nm and larger particles. The difference is that the results in Figure C.4 were obtained using centrifugation to separate particles. This is just an approximation because centrifugation separates particles by density, not size, if we assume that the INP have similar densities, then the centrifugation can separate particles by size.

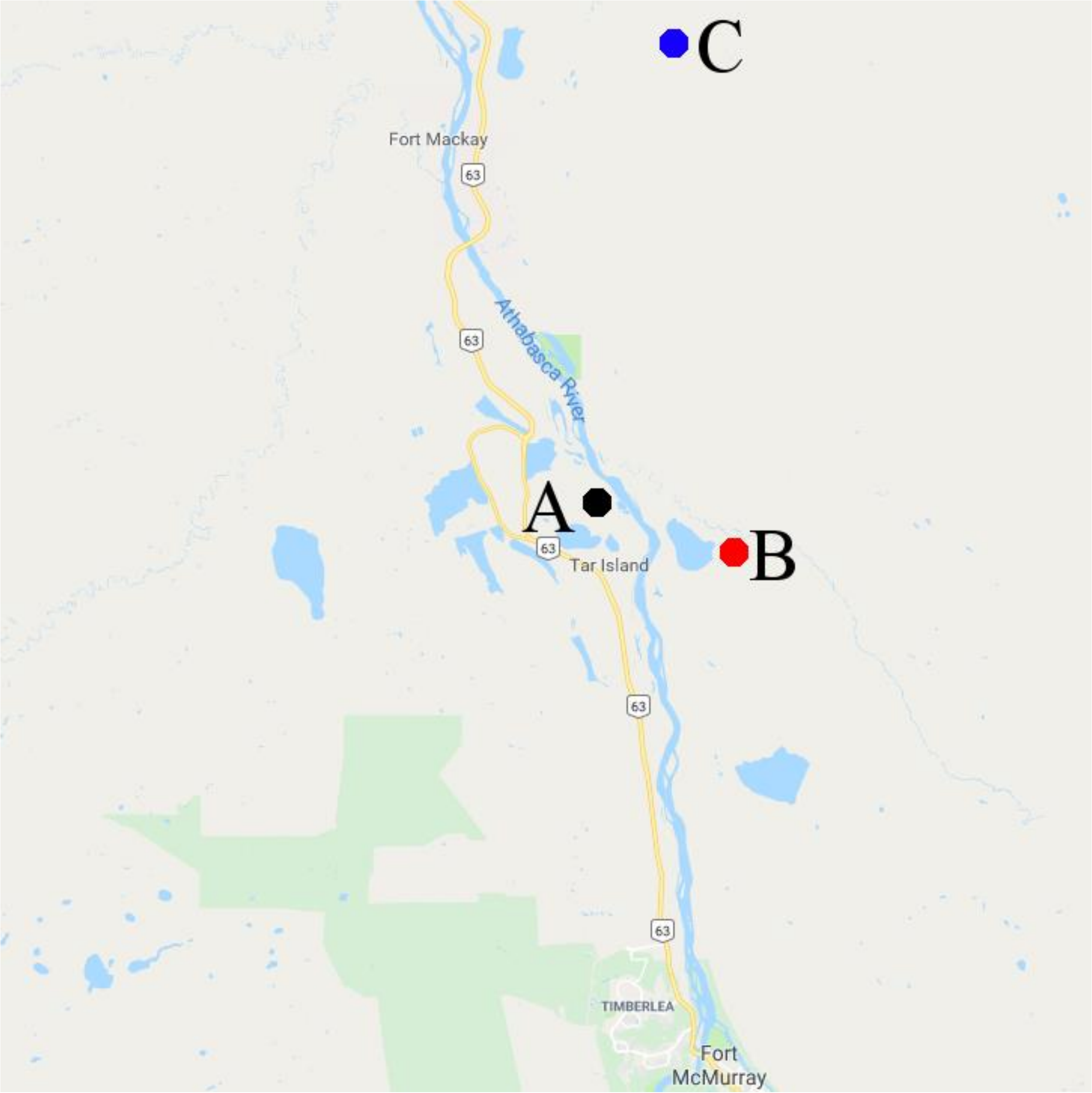

Figure C.1 Sampling sites in the AOSR. Sampling location (A) is located < 1 Km from the two of the largest upgrading facilities. Sampling location (B) is 7 Km southeast from location (A), and sampling location (C) is 25 Km ways from location (A).

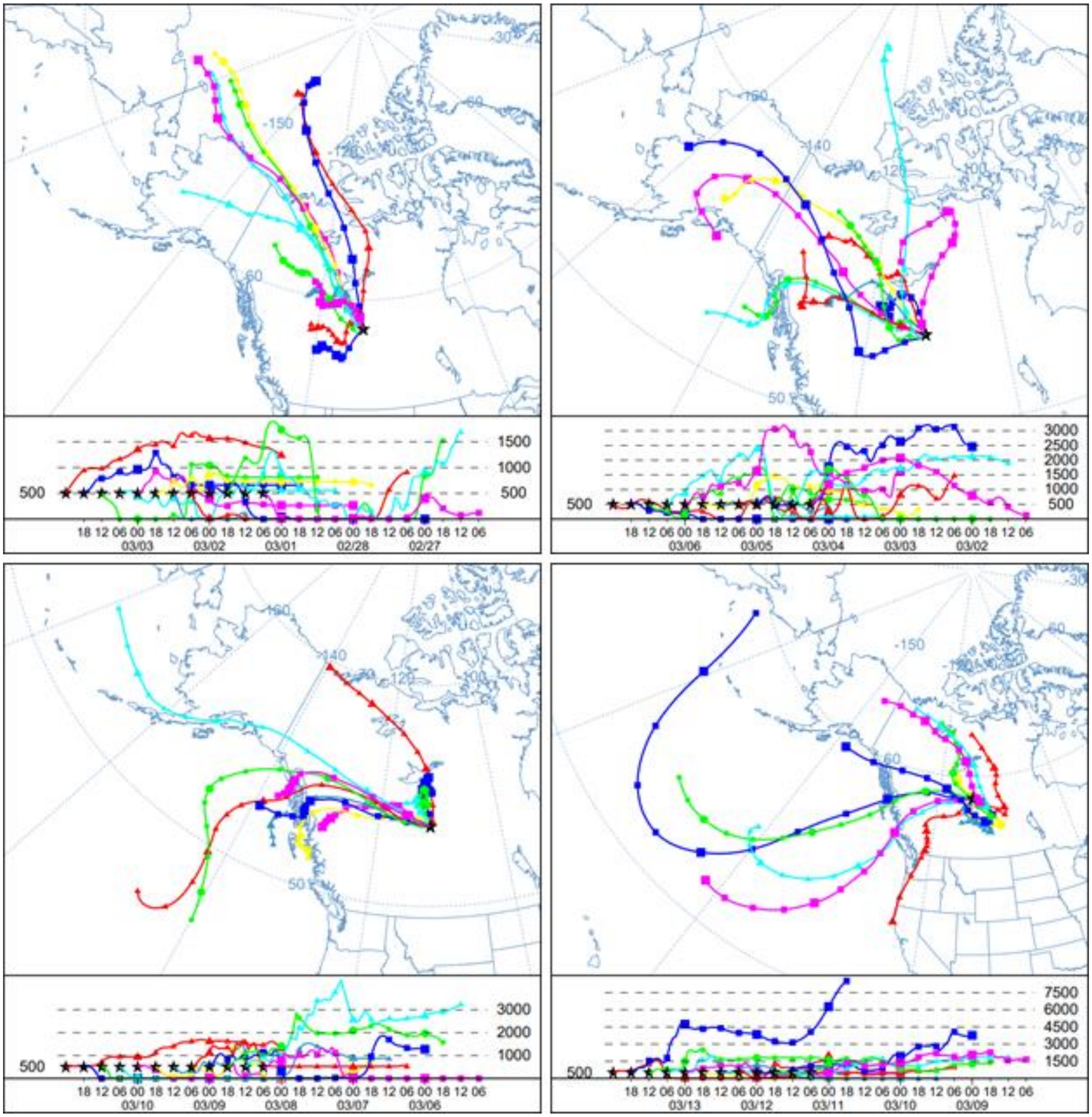

Figure C.2 Back-trajectory analysis for the 4th, 7th, 11th, and 14th of March 2015 calculated for the 0 km site. Calculations were done for 72 hours every 6 hours with 12 trajectories each. Most trajectories show that air masses come from the north.

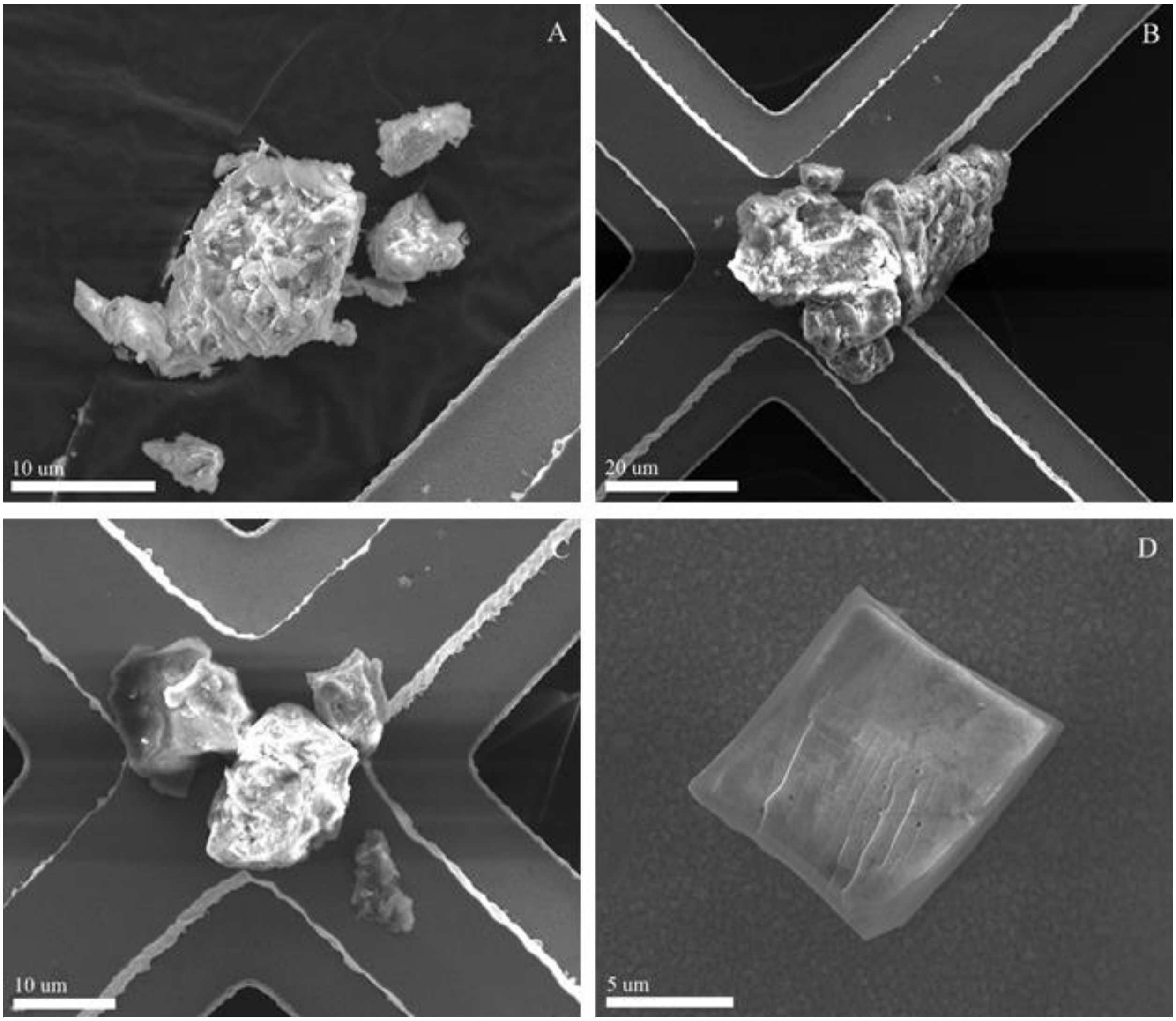

Figure C.3 Electron microscopy images of particles > 2.5 micron.

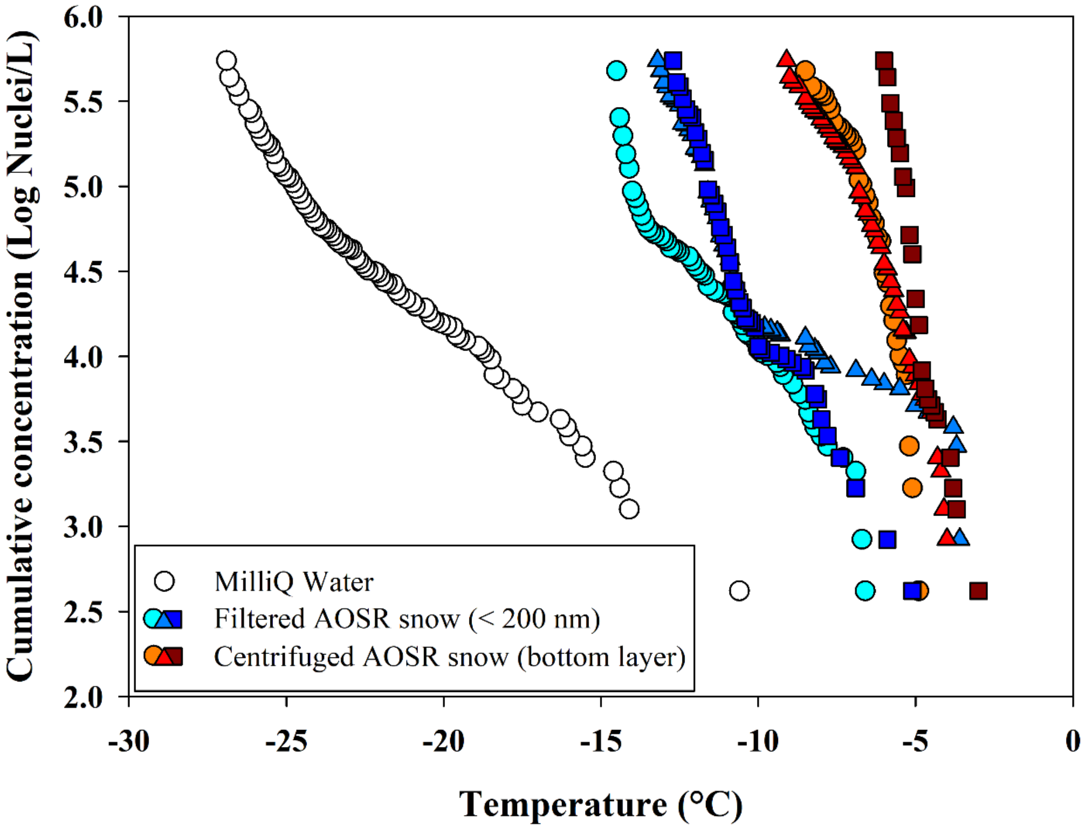

Figure C.4 Cumulative ice nucleating particle concentration of particles separated by centrifugation. Different symbols represent the different sampling sites: ▲ (0 Km), ■ (7 Km), and ● (25 Km).